This is a preprint of: "Global Analysis of Riccati Quadratic Differential Systems", Joan Carles Artés, Jaume Llibre, Dana Schlomiuk, Nicolae Vulpe, *Internat. J. Bifur. Chaos Appl. Sci. Engrg.*, vol. 34(1), 2450004, 2024.
DOI: [10.1142/S0218127424500044]

GLOBAL ANALYSIS OF RICCATI QUADRATIC DIFFERENTIAL SYSTEMS

JOAN C. ARTÉS[1] AND JAUME LLIBRE[2]
Departament de Matemàtiques, Universitat Autònoma de Barcelona,
08193 Bellaterra, Barcelona, Catalonia, Spain
E–mail: [1]*joancarles.artes@uab.cat,* [2]*jaume.llibre@uab.cat*
DANA SCHLOMIUK
Département de Mathématiques et de Statistiques
Université de Montréal, Canada,
E–mail: dasch@DMS.UMontreal.CA
NICOLAE VULPE
Vladimir Andrunakievichi Institute of Mathematics
and Computer Science, Moldova,
E–mail: nvulpe@gmail.com

In this article we study the family of quadratic Riccati differential systems. Our goal is to obtain the complete topological classification of this family on the Poincaré disk compactification of the plane. The family was partially studied before but never from a truly global viewpoint. Our approach is global and we use geometry to achive our goal. The geometric analysis we perform is via the presence of two invariant parallel straight lines in any generic Riccati system. We obtain a total of 119 topologically distinct phase portraits for this family. Furthermore we give the complete bifurcation diagram in the 12-dimensional space of parameters of this family in terms of invariant polynomials, that means it is independent of the normal forms in which the systems may be presented. This bifurcation diagram provides an algorithm to decide for any given quadratic system in any form it may be presented, whether it is a Riccati system or not, and in case it is to provide its phase portrait.

1. Introduction and the statement of the main theorem

We consider here polynomial differential systems

$$\frac{dx}{dt} = P(x, y), \qquad \frac{dy}{dt} = Q(x, y), \tag{1}$$

where $P, Q \in \mathbb{R}[x, y]$ i.e. P, Q are polynomials in x, y with real coefficients. We call *degree* of a system (1) the number $\widetilde{m} = \max(\deg(P), \deg(Q))$. Among the planar polynomial differential systems the simplest are the quadratic ones, i.e. $\widetilde{m} = 2$ and they are of the form:

$$\begin{aligned} \frac{dx}{dt} &= a + cx + dy + gx^2 + 2hxy + ky^2, \\ \frac{dy}{dt} &= b + ex + fy + lx^2 + 2mxy + ny^2. \end{aligned} \tag{2}$$

We call *cubic* a system (1) with $\widetilde{m} = 3$.

Studies on some quadratic systems are old as it is the case with the Riccati systems. They go back over 300 years (see [Jungers, 2017] for their history).

Definition 1.1. The quadratic Riccati systems are of the form:

$$\begin{aligned}\frac{dx}{dt} =& a + cx + gx^2,\\ \frac{dy}{dt} =& b + ex + fy + lx^2 + 2mxy + ny^2.\end{aligned} \tag{3}$$

Notation 1.1. *We denote the family of quadratic Riccati differential systems by the symbol* $\boldsymbol{QS}_{Ric}$.

As indicated in [Jungers, 2017] the first time that Riccati equations occurred in the literature was in 1694 in a paper of Johann I. Bernoulli. They are however called after Jacopo F. Riccati who first mentioned them in 1718 in a letter to Giovanni Poleni, where the Riccati equations were not necessarily quadratic. Apart from Johann I. Bernoulli, several members of the Bernoulli family had contributions on this subject. Initially the problem was to solve the equations, at least in some particular cases, using separation of variables. Seeing that for the higher degree equations the generic case was hard to treat, Riccati proposed to consider the particular quadratic case. This case proved to be useful in areas of applied mathematics, for example in control theory. For more applications consult [Llibre *et al.*, 2021].

In [Llibre *et al.*, 2021] the authors say in their abstract that they "give the complete description of the phase portraits in the Poincaré disk (i.e. in the compactification of $\mathbb{R}^2$ adding the circle $\mathbb{S}^1$ of the infinity) modulo topological equivalence" of the Riccati systems with $n(b^2 + e^2 + l^2) \neq 0$. The motivation for this exclusion was firstly that for $n = 0$ the systems are Liénard and secondly that in case $b = e = l = 0$ the systems are Bernoulli equations. We point out however that any Bernoulli system can be transformed by only using a translation $y \to y + \alpha$, $\alpha \neq 0$ into a Riccati system with new coefficients $a, c, g, b', e', f', l', m', n'$ such that $b'^2 + c'^2 + l'^2 \neq 0$ and hence it is useless to add this restriction. The authors provided five normal forms covering the whole parameter space, each one with fewer parameters and obtained by classical methods 74 phase portraits none of them with limit cycles.. It turns out that they missed some phase portraits.

The problem of classifying topologically any quadratic family of equations is global in the parameter space as we want phase portraits on the Poincaré disk for *all* values of the parameters of the equations. In particular the Riccati family depends on nine parameters (modulo rescaling only eight) and clearly we expect to have many phase portraits. It is therefore convenient to split the family into smaller ones where we have fewer phase portraits and hence we have a better control not to miss any.

The authors did not rely on the geometry of the systems. In the generic case each system in this family has two parallel invariant lines. The notion of Configuration of invariant algebraic curves of a polynomial differential system is a powerful affine invariant. Using it in this paper allows us to apply to the Ricatti family results already obtained about systems with configurations of invariant lines (see Definition 1.2 for configuration of invariant lines on next page).

At the beginning of this century global geometric tools began to be used see for example [Llibre & Schlomiuk, 2004, Schlomiuk & Vulpe, 2004]. Furthermore using these tools together with polynomial invariants a number of families of quadratic or cubic differential systems were topologically classified.

An interesting case is the study of all Lotka-Volterra differential systems, well known for their many applications. We recall that a Lotka-Volterra differential system is defined to be a quadratic system (1) with $P(x, y) = x(ax+by+c)$ and $Q(x, y) = y(dx + ey + f)$, with $a, \ldots, f \in \mathbb{R}$.

As in the Riccati family the phase portraits of the Lotka-Volterra family were studied first by using only the classical methods and three papers were written in this way, none of them complete and each of them with repeated phase portraits and

some with errors.

The Lotka-Volterra systems have an algebraic geometric property, namely they possess two distinct real invariant lines ($x = 0, y = 0$) intersecting in the finite plane (at $(0, 0)$). This geometric property actually defines them as any quadratic system possessing two real invariant lines intersecting at a finite point can be brought via an affine transformation to one of this form. To obtain the global topological classification the authors of [Schlomiuk & Vulpe, 2012] used this algebraic geometric property valid for *all* Lotka-Volterra systems and the notion of *configuration of invariant lines* introduced by them in [Schlomiuk & Vulpe, 2004].

Definition 1.2. We call configuration of invariant lines (or simply configuration) of a system (1) the set of all its invariant lines (real or complex), each endowed with its own multiplicity and together with all the real singular points of the system located on these lines, each one endowed with its own multiplicity.

The notion of multiplicity of an invariant line was introduced in [Schlomiuk & Vulpe, 2004].

Definition 1.3. We say that an invariant straight line $L(x, y) = ux + vy + w = 0$, $(u, v) \neq (0, 0)$, $(u, v, w) \in \mathbb{C}^3$ for a real polynomial differential system (S) has multiplicity m if there exists a sequence of real polynomial systems (S_k) $k \geq 1$ converging to (S), such that each (S_k) has m distinct (complex) invariant straight lines $L_k^j = u_k^j x + v_k^j y + w_k^j = 0$, $j = 0, \ldots m$, converging to $L = 0$ as $k \to \infty$, i.e. $[u_k^j : v_k^j : w_k^j] \to [u : v : w]$ as $k \to \infty$ in $\mathbf{P}_2(\mathbb{C})$ and this does not occur for $m + 1$.

An analogous definition of multiplicity of the line at infinity was also introduced in [Schlomiuk & Vulpe, 2004].

Definition 1.4. We say that the line at infinity is an invariant line of multiplicity m for a system (S) of the form (1) if and only if there exists a sequence of systems (S_i) of the form (1) tending to (S) when $i \to \infty$ and (S_i) have $m-1$ distinct invariant affine lines $L_i^j = u_i^j x + v_i^j y + w_i^j = 0$ $(u_i^j, v_i^j) \neq (0, 0)$, $(u_i^j, v_i^j, w_i^j) \in \mathbb{C}^3$, $(j = 1, \ldots, m-1)$ such that for every j, $(u_i^j, v_i^j, w_i^j) \to (0, 0, 1)$ and they do not have m invariant such lines L_j^i $j = 1, ..., m$ holding the above mentioned conditions.

Note that in the previous definition the multiplicity is m because apart from the $m - 1$ lines we must also take into account the line at infinity that is invariant.

In the above definitions the convergence of the systems means convergence of the coefficients of the systems in the $(N - 1)$-dimensional sphere $\mathbb{S}^{N-1}$ after time rescaling by the square root of the sum of the squares of the $N = (m+1)(m+2)$ coefficients of the systems involved where $m = \deg(S)$.

Definition 1.5. We call total multiplicity of invariant lines of a polynomial system (1) the sum of multiplicities of all its invariant lines including the multiplicity of the line at infinity.

A quadratic system (1) is *non-degenerate* if the polynomials P, Q have no common real factors other than constants.

Proposition 1.6. (Corollary 5 [Artés *et al.*, 1998]) *A non-degenerate quadratic system could have invariant lines, including the line at infinity, of total multiplicity at most six.*

Notation 1.2. *We denote by* $\mathbf{QSL}_{\geq n}$*, the family of non-degenerate quadratic systems possessing invariant lines of total multiplicity at least n, (*$1 \leq n \leq 6$*).*

Like in the case of the Lotka-Volterra differential systems the quadratic Riccati systems have invariant lines so we can use this geometric property in order to first find their possible configurations of invariant lines and classify the whole family in subfamilies of systems according to their configurations.

We note that the presence of an invariant line does not affect the topological equivalence relation as it can be deformed by a homeomorphism. How-

ever, the presence of invariant lines is very useful as the affine transformations conserve them and they also preserve the topological equivalence class Any polynomial system (1) has singularities, but the condition to possess invariant lines is a substantial restriction that turns out to be valuable for handling the large number of phase portraits. Furthermore although a configuration of invariant lines is not a phase portrait it is at least part of one and occasionally this information even leads to a single phase portrait.

The above observations show that whenever the systems have some algebraic geometric property, it is useful to pay attention and use it for the topological classifications. In particular, the family $\mathbf{QSL}_{\geq 2}$ is an interesting object to study and this provides us with additional motivation for this work as $\mathbf{QS}_{Ric} \subset \mathbf{QSL}_{\geq 3} \subset \mathbf{QSL}_{\geq 2}$.

Our topological classification of $\mathbf{QS}_{Ric}$ was the only piece so far lacking in the global topological classification of $\mathbf{QSL}_{\geq 3}$. Indeed, the case when we have two affine invariant lines intersecting in the finite space is solved (if the lines are real this is the Lotka-Volterra case and if they are complex this problem was solved in [Schlomiuk & Zhang, 2018]). The Riccati systems cover the case of two parallel lines, real or complex that intersect at infinity and their limiting cases.

All that remains to do in order to obtain the topological classification of $\mathbf{QSL}_{\geq 2}$ is to construct all phase portraits of quadratic systems having exactly two invariant lines, both simple, i.e. a real simple affine line and the line at infinity simple, or no affine invariant line and the infinite line double.

Knowing the configuration of invariant lines of a system gives a part of the information on the phase portrait that can then be completed by adding what else is missing, for example the proof of absence of limit cycles as it is the case for the quadratic Riccati family, or the proof of presence of limit cycles a fact occurring in other families such as for example the family of quadratic systems possessing two complex invariant lines intersecting at a finite point (see [Schlomiuk & Zhang, 2018]).

Our goal in this paper is to obtain the classification of the phase portraitsof the Ricatti family in the Poincaré disk according to topological equivalence relation. To do this we rely on the geometric lemma:

Lemma 1.7. *If a real quadratic system* (1) *possesses two distinct parallel invariant affine lines (real or complex) this system could be brought via a real affine transformation to a quadratic Riccati system (3).*

We denote by $\mathbf{QSL^{2p}}$ the class of non-degenerate quadratic systems which via an affine transformation could be brought to the canonical form (3). The notation $\mathbf{QSL^{2p}}$ brings into focus the principal property of Riccati systems, i.e. that generically they have two parallel invariant lines.

In [Bujac *et al.*, 2022] the author's obtained configurations of invariant lines (real or complex) for the family $\mathbf{QSL^{2p}}$. Except for seven configurations heir list is complete. In this paper we provide the complete list of configurations of this family by adding the seven missing configurations in [Bujac *et al.*, 2022]. We also give the bifurcation diagram of these configurations in the 12-dimensional space of coefficients of systems in this family was obtained in terms of invariant polynomials. To reach our goal of obtaining the topological classification all that remains to be done is to obtain the phase portraits for each one of the configurations.

We have $\mathbf{QS}_{Ric} \subset \mathbf{QSL^{2p}}$ and any system in $\mathbf{QSL^{2p}}$ is affinely equivalent to one in $\mathbf{QS}_{Ric}$. Clearly the two families $\mathbf{QS}_{Ric}$ and $\mathbf{QSL^{2p}}$ thus have the same set of phase portraits. Our goal now is to find all phase portraits of $\mathbf{QSL^{2p}}$.

When in the systems of the Lemma 1.7 we have $c^2-4ag \neq 0$ then $a+cx+gx^2$ splits into two distinct factors giving two invariant straight lines intersecting at infinity, parallel to the y-axis. But the family $\mathbf{QSL^{2p}}$ contains also the limit cases, i.e. when $c^2 - 4ag = 0$. If $g = 0$ and $c \neq 0$ (or $g = c = 0$), systems (3) possess only one (respectively do not possess any) invariant straight line in the direction $x = 0$. If $a = c = 0$ the y-axis $x = 0$ is a double affine line.

Theorem 1.8 ([Bujac *et al.*, 2022]). *Assume that a quadratic non-degenerate system (S) belongs to* $\mathbf{QSL^{2p}}$*, then (S) possesses one of the distinct configurations of invariant straight lines presented in Figures 1–4.*

We need to specify when two configurations are to be considered as distinct or equivalently. We first introduce some notions.

Suppose we have an invariant straight line $l = ax+by+c = 0$, with $a, b, c \in \mathbb{R}$. Let $L = aX+bY+cZ = 0$ be its projective completion in the complex projective plane $\mathbb{P}_2(\mathbb{C})$.

Definition 1.9. We call total curve $F(X, Y, Z) = 0$ of a configuration C of invariant straight lines with projective invariant straight lines $L_i = 0$, where $F = \prod L_i^{m_i} \prod Z^m$, m_i is the multiplicity of $L_i = 0$ and m is the multiplicity of $Z = 0$.

Definition 1.10. We say that two configurations C_1 and C_2 of invariant straight lines are equivalent if the following conditions hold:
1) we have a bijection f from the set of invariant straight lines of C_1 to the set of invariant straight lines of C_2;
2) for each straight line L of C_1 we have a bijection r of the set of real singularities (finite and infinite) of L to the set of real singularities of $f(L)$, sending a finite (respectively infinite) singularity to a finite (respectively infinite) singularity and preserving their multiplicities;
3) each such map r conserves the multiplicity of the real singular points considered as simple or multiple singular points of the total curve $F = 0$.

Our goals in this paper are:

- to find all phase portraits of the family $\mathbf{QSL^{2p}}$;
- this classification should be done in the twelve parameters space $\mathbb{R}^{12}$ independently of the normal forms the systems may be presented;
- to determine the bifurcation diagram of the phase portraits in the same space $\mathbb{R}^{12}$ of the coefficients of systems.

Our main result in this paper is the following theorem:

Main Theorem. *The following statements hold:*

(i) The family $\mathbf{QSL^{2p}}$ *(as well as the family* $\mathbf{QS}_{Ric}$*) possesses a total of 118 Configurations of invariant straight lines given in Figures 5 to 6 and a total of 119 phase topologically distinct phase portraits given in Figures 5 and 6 all of them without limit cycles.*

(ii) The topological classification is done using algebraic invariants and hence it is independent of the normal forms in which the systems may be presented.

(iii) The bifurcation diagram of the phase portraits of systems in the family $\mathbf{QSL^{2p}}$ *is done in the twelve-dimensional parameter space $\mathbb{R}^{12}$ and it is presented in Diagrams j for $j \in \{5, 6, 7, 8\}$. These diagrams give an algorithm to determine for any given system if it belongs or not to the family* $\mathbf{QSL^{2p}}$ *and in case it belongs to this family, it gives the specific phase portrait.*

Remark 1.11. Phase portraits for the quadratic Riccati family were given before in [Llibre *et al.*, 2021]. However this is the first time that a complete topological classification of this family was achieved. This family has numerous phase portraits and to be able to obtain a complete list of them we not only relied on the classical methods but also used modern ones, practically all methods for topologically classifying large families of quadratic systems available to us today. We gave in the Appendix of preprint [Artés *et al.*, 2023] a critical review of [Llibre *et al.*, 2021] that also sums up all the methods we used in this work.

The main tool we used for obtaining the global topological classification of this family was the geometry of the non-degenerate systems expressed in their 118 distinct configurations of invariant straight lines. In constructing the phase portraits

this splitting of the family into 118 smaller subfamilies, each one having the same configuration is very helpful for handling the mass of phase portraits as we pursue with our study of the phase portraits within each one of the subfamilies of systems having the same configuration. Furthermore we can then use the bifurcation diagram in intrinsic form in terms of invariant polynomials given in [Bujac *et al.*, 2022] to obtain an intrinsic bifurcation diagram of the phase portraits of the whole Ricatti family in terms of polynomial invariants in the 12-dimensional space

The main idea of the proof of our main theorem is first to pick a specific configuration and then follow the bifurcation diagram calculating the invariants that lead to the chosen configuration, and then calculating its resulting normal form. Once we have this normal form we calculate the phase portraits for that specific configuration by the usual classical method. Thus the splitting of the family into normal forms is done here not only by the group action but also by using the geometry of the systems. It is only afterwards that the computation of all the phase portraits for each one of the 118 configurations is done, by usual classical methods .

The bifurcation diagram, done in terms of algebraic invariants is also an algorithm for deciding for any system given in any normal form if it is or not a Riccati system, and if it is then to provide with its phase portrait.

Both geometric and algebraic tools were used. But for some configurations more tools were needed. In the cases where there exist several potential phase portraits we needed to rely on papers (on structurally stable [Artés *et al.*, 1998], codimension 1 systems [Artés *et al.*, 2018b] and a paper on codimension 2 systems [Artés *et al.*, 2020b]) that have studied the realizability of those potential phase portraits. We also had to check if these phase portraits were compatible or not with the geometric property expressed in the presence of invariant straight lines as in Riccati systems. This geometric property of the Riccati systems was instrumental in eliminating some of the potential phase portraits.

This paper thus relies on most of the diverse available techniques (geometric, algebraic, analytical and topological) in the *global* topological classifications of families of planar polynomial vector fields.

Our article is organized as follows: In Section 2 we exhibit the main affine invariant polynomials that intervene in this classification. In Section 3 we present some preliminary results involving the use of invariant polynomials, in particular we present the bifurcation diagram in the 12-dimensional space of the parameters, in terms of invariant polynomials of the configurations of the family $\mathbf{QSL^{2p}}$ obtained in [Bujac *et al.*, 2022]. The actual construction of the phase portraits of the Riccati systems is done in Section 4 where the statement (i) of Theorem 4.1 (corresponding to the case $\eta > 0$) is completely proved). The rest on the proof of Theorem 4.1 comes from preprint [Artés *et al.*, 2023]. The proof of our Main Theorem follows from the classification given in Theorem 4.1.

2. The main invariant polynomials associated to the class $\mathbf{QS}_{Ric}$

Consider quadratic systems of the form (2). It is known that on the set **QS** acts the group $Aff(2,\mathbb{R})$ of affine transformations on the plane (cf. [Schlomiuk & Vulpe, 2005]). For every subgroup $G \subseteq Aff(2,\mathbb{R})$ we have an induced action of G on **QS**. We can identify the set **QS** of systems (2) with a subset of $\mathbb{R}^{12}$ via the map $\mathbf{QS} \longrightarrow \mathbb{R}^{12}$ which associates to each system (2) the 12–tuple $\tilde{a} = (a, c, d, g, h, k, b, e, f, l, m, n)$ of its coefficients. We associate to this group action polynomials in x, y and parameters which behave well with respect to this action, the GL–comitants (GL–invariants), the T–comitants (affine invariants) and the CT–comitants. For their definitions as well as their detailed constructions we refer the reader to the paper [Schlomiuk & Vulpe, 2005] (see also [Artés *et al.*, 2021]).

Next we define the following 40 invariant poly-

nomials needed for the class $\mathbf{QS}_{Ric}$:

$$\Big\{\mu_0,\ldots,\mu_4,\ \mathbf{D},\ \mathbf{R},\ \mathbf{U},\ \eta,\ B_1,\ B_2,\ B_3,\ \widetilde{M},\ C_2,\ \theta,\ \theta_3,\ \theta_5,\ \widetilde{K},\ \widetilde{N},\ \widetilde{D},\ H_1,\ H_3,\ldots,H_{12},\ H_{15},\ H_{16},\ D_1,\ N_1,\ N_2,\ N_5,\ N_6,\ \mathcal{G}_2,\mathcal{G}_3\Big\}. \tag{4}$$

According to [Artés *et al.*, 2021] (see also [Baltag & Vulpe, 1997]) we apply the differential operator $\mathcal{L} = x\cdot\mathbf{L}_2 - y\cdot\mathbf{L}_1$ acting on $\mathbb{R}[\tilde{a},x,y]$ with

$$\begin{aligned}\mathbf{L}_1 =& 2a\frac{\partial}{\partial c} + c\frac{\partial}{\partial g} + \frac{1}{2}d\frac{\partial}{\partial h} + 2b\frac{\partial}{\partial e} + e\frac{\partial}{\partial l} + \frac{1}{2}f\frac{\partial}{\partial m},\\ \mathbf{L}_2 =& 2a\frac{\partial}{\partial d} + d\frac{\partial}{\partial k} + \frac{1}{2}c\frac{\partial}{\partial h} + 2b\frac{\partial}{\partial f} + f\frac{\partial}{\partial n} + \frac{1}{2}e\frac{\partial}{\partial m},\end{aligned}$$

to construct several invariant polynomials from the set (4). More precisely using this operator and the affine invariant $\mu_0 = \operatorname{Res}_x\big(p_2(\tilde{a},x,y), q_2(\tilde{a},x,y)\big)/y^4$ we construct the following polynomials

$$\begin{aligned}&\mu_i(\tilde{a},x,y) = \frac{1}{i!}\mathcal{L}^{(i)}(\mu_0),\ i=1,..,4,\\ &\text{where}\ \ \mathcal{L}^{(i)}(\mu_0) = \mathcal{L}(\mathcal{L}^{(i-1)}(\mu_0)).\end{aligned}$$

Using these polynomial invariants we define some new ones, which according to [Artés *et al.*, 2021] are responsible for the number and multiplicities of the finite singular points of (2):

$$\begin{aligned}\mathbf{D} =& \Big[3\big((\mu_3,\mu_3)^{(2)},\ \mu_2\big)^{(2)} - \\ &\big(6\mu_0\mu_4 - 3\mu_1\mu_3 + \mu_2^2,\ \mu_4\big)^{(4)}\Big]/48,\\ \mathbf{P} =& 12\mu_0\mu_4 - 3\mu_1\mu_3 + \mu_2^2,\\ \mathbf{R} =& 3\mu_1^2 - 8\mu_0\mu_2,\\ \mathbf{S} =& \mathbf{R}^2 - 16\mu_0^2\mathbf{P},\\ \mathbf{T} =& 18\mu_0^2(3\mu_3^2 - 8\mu_2\mu_4) + 2\mu_0(2\mu_2^3 - \\ &9\mu_1\mu_2\mu_3 + 27\mu_1^2\mu_4) - \mathbf{PR},\\ \mathbf{U} =& \mu_3^2 - 4\mu_2\mu_4.\end{aligned}$$

In what follows we also need the so-called *transvectant of order k* (see [Grace & Young, 1941], [Olver, 1999]) of two polynomials $f,\ g\in\mathbb{R}[\tilde{a},x,y]$

$$(f,g)^{(k)} = \sum_{h=0}^{k}(-1)^h\binom{k}{h}\frac{\partial^k f}{\partial x^{k-h}\partial y^h}\ \frac{\partial^k g}{\partial x^h\partial y^{k-h}}.$$

In order to construct the remaining invariant polynomials contained in the set (4) we first need to define some elemental bricks which help us to construct these elements of the set.

We remark that the following polynomials in $\mathbb{R}[\tilde{a},x,y]$ are the simplest invariant polynomials of degree one with respect to the coefficients of the differential systems (2) which are GL-comitants:

$$\begin{aligned}C_i(x,y) &= yp_i(x,y) - xq_i(x,y),\ i=0,1,2;\\ D_i(x,y) &= \frac{\partial}{\partial x}p_i(x,y) + \frac{\partial}{\partial y}q_i(x,y),\ i=1,2.\end{aligned}$$

Apart from these simple invariant polynomials we shall also make use of the following nine GL-invariant polynomials:

$$\begin{aligned}&T_1 = (C_0,C_1)^{(1)}, \quad T_2 = (C_0,C_2)^{(1)},\\ &T_3 = (C_0,D_2)^{(1)}, \quad T_4 = (C_1,C_1)^{(2)},\\ &T_5 = (C_1,C_2)^{(1)}, \quad T_6 = (C_1,C_2)^{(2)},\\ &T_7 = (C_1,D_2)^{(1)}, \quad T_8 = (C_2,C_2)^{(2)},\\ &T_9 = (C_2,D_2)^{(1)}.\end{aligned}$$

These are of degree two with respect to the coefficients of systems (2).

We next define a list of T-comitants:

$$\begin{aligned}\hat{A}(\tilde{a}) =& (C_1, T_8 - 2T_9 + D_2^2)^{(2)}/144,\\ \widehat{D}(\tilde{a},x,y) =& \big[2C_0(T_8 - 8T_9 - 2D_2^2) + C_1(6T_7 - T_6) - \\ &(C_1,T_5)^{(1)} - 9D_1^2C_2 + 6D_1(C_1D_2 - T_5)\big]/36,\\ \widehat{E}(\tilde{a},x,y) =& \big[D_1(2T_9 - T_8) - 3(C_1,T_9)^{(1)} - \\ &D_2(3T_7 + D_1D_2)\big]/72,\\ \widehat{K}(\tilde{a},x,y) =& (T_8 + 4T_9 + 4D_2^2)/72,\\ \widehat{H}(\tilde{a},x,y) =& (-T_8 + 8T_9 + 2D_2^2)/72,\end{aligned}$$

$$\begin{aligned}
\widehat{B}(\tilde{a},x,y) =&\Big\{16D_1(D_2,T_8)^{(1)}(3C_1D_1-2C_0D_2+\\
&4T_2)+32C_0(D_2,T_9)^{(1)}(3D_1D_2-5T_6+\\
&9T_7)+2(D_2,T_9)^{(1)}\big(27C_1T_4-18C_1D_1^2-\\
&32D_1T_2+32(C_0,T_5)^{(1)}\big)+6(D_2,T_7)^{(1)}\times\\
&\big[8C_0(T_8-12T_9)-12C_1(D_1D_2+T_7)+\\
&D_1(26C_2D_1+32T_5)+C_2(9T_4+96T_3)\big]+\\
&6(D_2,T_6)^{(1)}\big[32C_0T_9-C_1(12T_7+\\
&52D_1D_2)-32C_2D_1^2\big]+48D_2(D_2,T_1)^{(1)}\times\\
&(2D_2^2-T_8)+6D_1D_2T_4(T_8-7D_2^2-42T_9)-\\
&32D_1T_8(D_2,T_2)^{(1)}+9D_2^2T_4(T_6-2T_7)-\\
&16D_1(C_2,T_8)^{(1)}(D_1^2+4T_3)+\\
&12D_1(C_1,T_8)^{(2)}(C_1D_2-2C_2D_1)+\\
&12D_1(C_1,T_8)^{(1)}(T_7+2D_1D_2)+96D_2^2\times\\
&\big[D_1(C_1,T_6t)^{(1)}+D_2(C_0,T_6)^{(1)}\big]-\\
&4D_1^3D_2(D_2^2+3T_8+6T_9)-16D_1D_2T_3\times\\
&(2D_2^2+3T_8)+6D_1^2D_2^2(7T_6+2T_7)-\\
&252D_1D_2T_4T_9\Big\}/(2^8 3^3),\\
\widehat{F}(\tilde{a},x,y) =&\big[6D_1^2(D_2^2-4T_9)+4D_1D_2(T_6+6T_7)+\\
&48C_0(D_2,T_9)^{(1)}-9D_2^2T_4+288D_1\widehat{E}-\\
&24(C_2,\widehat{D})^{(2)}+120(D_2,\widehat{D})^{(1)}-36C_1\times\\
&(D_2,T_7)^{(1)}+8D_1(D_2,T_5)^{(1)}\big]/144,
\end{aligned}$$

as well as the needed bricks:

$$\begin{aligned}
A_2(\tilde{a}) =&(C_2,\widehat{D})^{(3)}/12,\\
A_8(\tilde{a}) =&\big((\widehat{D},\widehat{H})^{(2)},D_2\big)^{(1)}/8,\\
A_{11}(\tilde{a}) =&(\widehat{F},\widehat{K})^{(2)}/4,\\
A_{20}(\tilde{a}) =&\big((C_2,\widehat{D})^{(2)},\widehat{F}\big)^{(2)}/16,\\
A_{21}(\tilde{a}) =&\big((\widehat{D},\widehat{D})^{(2)},\widehat{K}\big)^{(2)}/16,\\
A_{39}(\tilde{a}) =&\big(((\widehat{D},\widehat{D})^{(2)},\widehat{F}\big)^{(1)},\widehat{H}\big)^{(2)}/64,\\
A_{42}(\tilde{a}) =&\big(((\widehat{D},\widehat{F})^{(2)},\widehat{F}\big)^{(1)},D_2\big)^{(1)}/16.
\end{aligned}$$

Now we can define the remaining invariant polynomials of the set (4):

$$\begin{aligned}
\widetilde{K}(\tilde{a},x,y) =&4\widehat{K}\equiv\text{Jacob}\left(p_2(\tilde{a},x,y),q_2(\tilde{a},x,y)\right),\\
\widetilde{M}(\tilde{a},x,y) =&(C_2,C_2)^{(2)}\equiv 2\text{Hess}\left(C_2(\tilde{a},x,y)\right),\\
\widetilde{N}(\tilde{a},x,y) =&\widetilde{K}-4\widehat{H},\\
\eta(\tilde{a}) =&(\widetilde{M},\widetilde{M})^{(2)}/384\equiv\text{Discrim}\left(C_2(\tilde{a},x,y)\right),\\
\theta(\tilde{a}) =&-(\widetilde{N},\widetilde{N})^{(2)}/2\equiv\text{Discrim}\left(\widetilde{N}(\tilde{a},x,y)\right);\\
\theta_3(\tilde{a}) =&A_8+A_{11},\\
B_1(\tilde{a}) =&\text{Res}_x\left(C_2,\widetilde{D}\right)/y^9=-2^{-9}3^{-8}\left(B_2,B_3\right)^{(4)},\\
B_2(\tilde{a},x,y) =&(B_3,B_3)^{(2)}-6B_3(C_2,\widetilde{D})^{(3)},\\
B_3(\tilde{a},x,y) =&(C_2,\widetilde{D})^{(1)}\equiv\text{Jacob}\left(C_2,\widetilde{D}\right),\\
H_1(\tilde{a}) =&-\left((C_2,C_2)^{(2)},C_2)^{(1)},D\right)^{(3)},\\
H_3(\tilde{a},x,y) =&(C_2,D)^{(2)},\\
H_4(\tilde{a}) =&\big((C_2,D)^{(2)},(C_2,D_2)^{(1)}\big)^{(2)},\\
H_5(\tilde{a}) =&\big((C_2,C_2)^{(2)},(D,D)^{(2)}\big)^{(2)}+\\
&8\big((C_2,D)^{(2)},(D,D_2)^{(1)}\big)^{(2)},\\
H_6(\tilde{a},x,y) =&16N^2(C_2,D)^{(2)}+H_2^2(C_2,C_2)^{(2)},\\
H_7(\tilde{a}) =&(\widetilde{N},C_1)^{(2)},\\
H_8(\tilde{a}) =&9\big((C_2,D)^{(2)},(D,D_2)^{(1)}\big)^{(2)}+\\
&2\Big[(C_2,D)^{(3)}\Big]^2,\\
H_9(\tilde{a}) =&-\left(\left((\widetilde{D},\widetilde{D})^{(2)},\widetilde{D},\right)^{(1)},\widetilde{D}\right)^{(3)},\\
H_{10}(\tilde{a}) =&\big((\widetilde{N},\widetilde{D})^{(2)},\ D_2\big)^{(1)},\\
H_{11}(\tilde{a},x,y) =&8\widehat{H}\big[(C_2,\widetilde{D})^{(2)}+8(\widetilde{D},D_2)^{(1)}\big]+\\
&3\big[(C_1,\,2\widehat{H}-\widetilde{N})^{(1)}-2D_1\widetilde{N}\big]^2,\\
H_{12}(\tilde{a},x,y) =&(\widetilde{D},\widetilde{D})^{(2)}\equiv\text{Hessian}(\widetilde{D}),\\
H_{15}(\tilde{a}) =&\big((\widetilde{D},\widetilde{D})^{(2)},\ -4\widehat{H}\big)^{(2)},\\
H_{16}(\tilde{a}) =&14A_2^4-A_2^2(10A_{20}+33A_{21})-\\
&2A_2(15A_{39}+A_{42}),\\
\mathcal{G}_2(\tilde{a}) =&8H_8-9H_5,\\
\mathcal{G}_3(\tilde{a}) =&(\mu_0-\eta)H_1-6\eta(H_4+12H_{10}).
\end{aligned}$$

We remark that the above invariant polynomials were constructed and used in [Artés *et al.*, 2015, Schlomiuk & Vulpe, 2008d, Schlomiuk & Vulpe, 2008c].

3. Preliminary results involving the use of polynomial invariants

The following two lemmas reveal the geometrical meaning of the invariant polynomials B_1, B_2, B_3, θ and $\widetilde{N}$.

Lemma 3.1 ([Schlomiuk & Vulpe, 2004]). *For the existence of an invariant straight line in one (respectively 2; 3 distinct) directions in the affine plane it is necessary that $B_1 = 0$ (respectively $B_2 = 0$; $B_3 = 0$).*

Lemma 3.2 ([Schlomiuk & Vulpe, 2004]). *A necessary condition for the existence of one couple (respectively, two couples) of parallel invariant straight lines of a system (2) corresponding to $\boldsymbol{a} \in \mathbb{R}^{12}$ is the condition $\theta(\boldsymbol{a}) = 0$ (respectively, $\widetilde{N}(\boldsymbol{a}, x, y) = 0$).*

We remark that the invariant polynomials $\mu_i(\tilde{a}, x, y)$ $(i = 0, 1, \ldots, 4)$ defined earlier are responsible for the total multiplicity of the finite singularities of quadratic systems (2). Moreover they detect whether a quadratic system is degenerate or not. More exactly, according to [Baltag & Vulpe, 1997] (see also [Artés *et al.*, 2021] we have the following lemma.

Lemma 3.3. *Consider a quadratic system (S) with coefficients $\boldsymbol{a} \in \mathbb{R}^{12}$. Then:*

(i) The total multiplicity of the finite singularities of this system is $4 - k$ if and only if for every i such that $0 \le i \le k - 1$ we have $\mu_i(\boldsymbol{a}, x, y) = 0$ in $\mathbb{R}[x, y]$ and $\mu_k(\boldsymbol{a}, x, y) \neq 0$.

(ii) The system (S) is degenerate (i.e. $\gcd(p, q) \neq$ constant) if and only if $\mu_i(\boldsymbol{a}, x, y) = 0$ in $\mathbb{R}[x, y]$ for every $i = 0, 1, 2, 3, 4$.

On the other hand the invariant polynomials η, $\widetilde{M}$ and C_2 govern the number of real and complex infinite singularities. More precisely, according to [Sibirskii, 1998] (see also [Schlomiuk & Vulpe, 2005]) we have the next result.

Lemma 3.4. *The number of infinite singularities (real and complex) of a quadratic system in* **QS** *is determined by the following conditions:*

(i) 3 real if $\eta > 0$;

(ii) 1 real and 2 imaginary if $\eta < 0$;

(iii) 2 real if $\eta = 0$ and $\widetilde{M} \neq 0$;

(iv) 1 real if $\eta = \widetilde{M} = 0$ and $C_2 \neq 0$;

(v) ∞ if $\eta = \widetilde{M} = C_2 = 0$.

Moreover, the quadratic systems (2), for each one of these cases, can be brought via a linear transformation to the corresponding case of the following canonical systems $(\mathbf{S}_I) - (\mathbf{S}_V)$:

$$\begin{cases} \dot{x} = a + cx + dy + gx^2 + (h-1)xy, \\ \dot{y} = b + ex + fy + (g-1)xy + hy^2; \end{cases} \quad (\mathbf{S}_I)$$

$$\begin{cases} \dot{x} = a + cx + dy + gx^2 + (h+1)xy, \\ \dot{y} = b + ex + fy - x^2 + gxy + hy^2; \end{cases} \quad (\mathbf{S}_{II})$$

$$\begin{cases} \dot{x} = a + cx + dy + gx^2 + hxy, \\ \dot{y} = b + ex + fy + (g-1)xy + hy^2; \end{cases} \quad (\mathbf{S}_{III})$$

$$\begin{cases} \dot{x} = a + cx + dy + gx^2 + hxy, \\ \dot{y} = b + ex + fy - x^2 + gxy + hy^2; \end{cases} \quad (\mathbf{S}_{IV})$$

$$\begin{cases} \dot{x} = a + cx + dy + x^2, \\ \dot{y} = b + ex + fy + xy. \end{cases} \quad (\mathbf{S}_V)$$

Now we define the affine comitants which are responsible for the existence of invariant lines for a non-degenerate quadratic system (2).

Let us apply a translation $x = x' + x_0$, $y = y' + y_0$ to the polynomials $p(\tilde{a}, x, y)$ and $q(\tilde{a}, x, y)$. We obtain $\hat{p}(\hat{a}(\tilde{a}, x_0, y_0), x', y') = p(\tilde{a}, x' + x_0, y' + y_0)$, $\hat{q}(\hat{a}(\tilde{a}, x_0, y_0), x', y') = q(\tilde{a}, x' + x_0, y' + y_0)$. Let us construct the following polynomials

$$\begin{aligned} \Gamma_i(\tilde{a}, x_0, y_0) \equiv & \operatorname{Res}_{x'}\Big(C_i\big(\hat{a}(\tilde{a}, x_0, y_0), x', y'\big), \\ & C_0\big(\hat{a}(\tilde{a}, x_0, y_0), x', y'\big)\Big)/(y')^{i+1}, \\ \Gamma_i(\tilde{a}, x_0, y_0) \in & \mathbb{R}[\tilde{a}, x_0, y_0], \ (i = 1, 2). \end{aligned}$$

Notation 3.1.

$$\begin{aligned} & \tilde{\mathcal{E}}_i(\tilde{a}, x, y) = \Gamma_i(\tilde{a}, x_0, y_0)|_{\{x_0 = x,\ y_0 = y\}}, \\ & \tilde{\mathcal{E}}_i(\tilde{a}, x, y) \in \mathbb{R}[\tilde{a}, x, y] \quad (i = 1, 2). \end{aligned} \quad (5)$$

Observation 3.1. *We note that the polynomials $\tilde{\mathcal{E}}_1(\tilde{a}, x, y)$ and $\tilde{\mathcal{E}}_2(\tilde{a}, x, y)$ thus constructed are affine comitants of systems (2) and are homogeneous polynomials in the coefficients $a, \ldots, n$ and non-homogeneous in x, y and*

$$\begin{aligned} \deg_{\tilde{a}} \tilde{\mathcal{E}}_1 = & 3, \ \deg_{(x,y)} \tilde{\mathcal{E}}_1 = 5, \\ \deg_{\tilde{a}} \tilde{\mathcal{E}}_2 = & 4, \ \deg_{(x,y)} \tilde{\mathcal{E}}_2 = 6. \end{aligned}$$

Notation 3.2. *Let $\mathcal{E}_i(\tilde{a}, X, Y, Z)$ $(i = 1, 2)$ be the homogenization of $\tilde{\mathcal{E}}_i(\tilde{a}, x, y)$, i.e.*

$$\mathcal{E}_1(\tilde{a}, X, Y, Z) = Z^5\tilde{\mathcal{E}}_1(\tilde{a}, X/Z, Y/Z),$$
$$\mathcal{E}_2(\tilde{a}, X, Y, Z) = Z^6\tilde{\mathcal{E}}_2(\tilde{a}, X/Z, Y/Z)$$

and

$$\mathcal{H}(\tilde{a}, X, Y, Z) = \gcd\Big(\mathcal{E}_1(\tilde{a}, X, Y, Z),\ \mathcal{E}_2(\tilde{a}, X, Y, Z)\Big)$$

in $\mathbb{R}[\tilde{a}, X, Y, Z]$.

The geometrical meaning of these affine comitants is given by the two following lemmas (see [Schlomiuk & Vulpe, 2004]):

Lemma 3.5. *The straight line $\mathcal{L}(x, y) \equiv ux + vy + w = 0$, $u, v, w \in \mathbb{C}$, $(u, v) \neq (0, 0)$ is an invariant line for a quadratic system (2) if and only if the polynomial $\mathcal{L}(x, y)$ is a common factor of the polynomials $\tilde{\mathcal{E}}_1(\boldsymbol{a}, x, y)$ and $\tilde{\mathcal{E}}_2(\boldsymbol{a}, x, y)$ over $\mathbb{C}$, i.e.*

$$\tilde{\mathcal{E}}_i(\boldsymbol{a}, x, y) = (ux + vy + w)\widetilde{W}_i(x, y) \quad (i = 1, 2),$$

where $\widetilde{W}_i(x, y) \in \mathbb{C}[x, y]$.

Lemma 3.6. *1) If $\mathcal{L}(x, y) \equiv ux + vy + w = 0$, $u, v, w \in \mathbb{C}$, $(u, v) \neq (0, 0)$ is an invariant straight line of multiplicity k for a quadratic system (2) corresponding to a point $\boldsymbol{a} \in \mathbb{R}^{12}$ then $\mathcal{L}(x, y)]^k \mid \gcd(\tilde{\mathcal{E}}_1, \tilde{\mathcal{E}}_2)$ in $\mathbb{C}[x, y]$, i.e. there exist $W_i(\boldsymbol{a}, x, y) \in \mathbb{C}[x, y]$ $(i = 1, 2)$ such that*

$$\tilde{\mathcal{E}}_i(\boldsymbol{a}, x, y) = (ux+vy+w)^k W_i(\boldsymbol{a}, x, y),\ i = 1, 2. \quad (6)$$

2) If the line $l_\infty : Z = 0$ is of multiplicity $k > 1$ then $Z^{k-1} \mid \gcd(\mathcal{E}_1, \mathcal{E}_2)$, in other words we have $Z^{k-1} \mid \mathcal{H}(\boldsymbol{a}, X, Y, Z)$.

In [Bujac *et al.*, 2022] the classification of the family $\mathbf{QSL^{2p}}$ of quadratic differential systems possessing two parallel invariant affine lines according to their configurations of invariant lines is given. Since the family $\mathbf{QS}_{Ric}$ of quadratic Riccati systems is a subfamily of $\mathbf{QSL^{2p}}$ it is clear that this classification is a very useful one in order to classify topologically the family $\mathbf{QS}_{Ric}$.

We mention that in [Bujac *et al.*, 2022, see Theorem 5.1] the authors determined the necessary and sufficient conditions for an arbitrary non-degenerate quadratic system to belong to the family $\mathbf{QSL^{2p}}$. We have the following lemma.

Lemma 3.7. *An arbitrary quadratic system (2) belongs to the class $\boldsymbol{QSL^{2p}}$ if and only if $\theta = B_1 = H_7 = 0$ and one of the following conditions holds:*

- ***(i)*** *If $\eta > 0$ then either $\widetilde{N} \neq 0$, or $\widetilde{N} = 0$, $\theta_3 = 0$.*
- ***(ii)*** *If $\eta < 0$ then $\widetilde{N} \neq 0$.*
- ***(iii)*** *If $\eta = 0$, $\widetilde{M} \neq 0$ then either $\widetilde{N} \neq 0$, or $\widetilde{N} = 0$, $\widetilde{K} \neq 0$, $\theta_3 = 0$, or $\widetilde{N} = \widetilde{K} = 0$, $B_2 \neq 0$, $\theta_5 = 0$, or $\widetilde{N} = \widetilde{K} = B_2 = 0$.*
- ***(iv)*** *If $\eta = \widetilde{M} = 0$, $C_2 \neq 0$ then either $\widetilde{N} \neq 0$, or $\widetilde{N} = B_2 = 0$.*
- ***(v)*** *If $\eta = \widetilde{M} = C_2 = 0$.*

Remark 3.8. We point out that in the statement ***(iv)*** of the above lemma (which is the same as in [Bujac *et al.*, 2022, see Theorem 5.1]) it is claimed that in the case $\widetilde{N} = 0$ the condition $B_2 = 0$ is necessary for a quadratic system to be in the class $\mathbf{QSL^{2p}}$. However this condition was omitted in Diagram 4 of [Bujac *et al.*, 2022]. Here we presented Diagrams 1 to 4 given in [Bujac *et al.*, 2022] but with the correction to Diagram 4 by addition of the corresponding branch.

Based on [Bujac *et al.*, 2022, see Theorem 6.1] the next theorem describes all the configurations which could have systems in $\mathbf{QSL^{2p}}$ as well as the corresponding invariant criteria for their realization.

Theorem 3.9. *If a quadratic non-degenerate system (S) belongs to the class of systems $\boldsymbol{QSL^{2p}}$, then this system possesses one of the configurations of invariant lines indicated below if and only if the corresponding conditions hold respectively:*

- ***(i)*** *For $\eta > 0$ the system (S) possesses one of the configurations given in Figure 1 if and only*

if one of the sets of conditions given in the Diagram 1 holds, correspondingly.

(ii) *For $\eta < 0$ the system (S) possesses one of the configurations given in Figure 2 if and only if the one of the sets of conditions given in the Diagram 2 holds, correspondingly.*

(iii) *For $\eta = 0$ and $\widetilde{M} \neq 0$ the system (S) possesses one of the configurations given in Figure 3 if and only if one of the sets of conditions given in the Diagram 3 holds, correspondingly.*

(iv) *For $\eta = \widetilde{M} = 0$ the system (S) possesses one of the configurations given in Figure 4 if and only if one of the sets of conditions given in the Diagram 4 holds, correspondingly.*

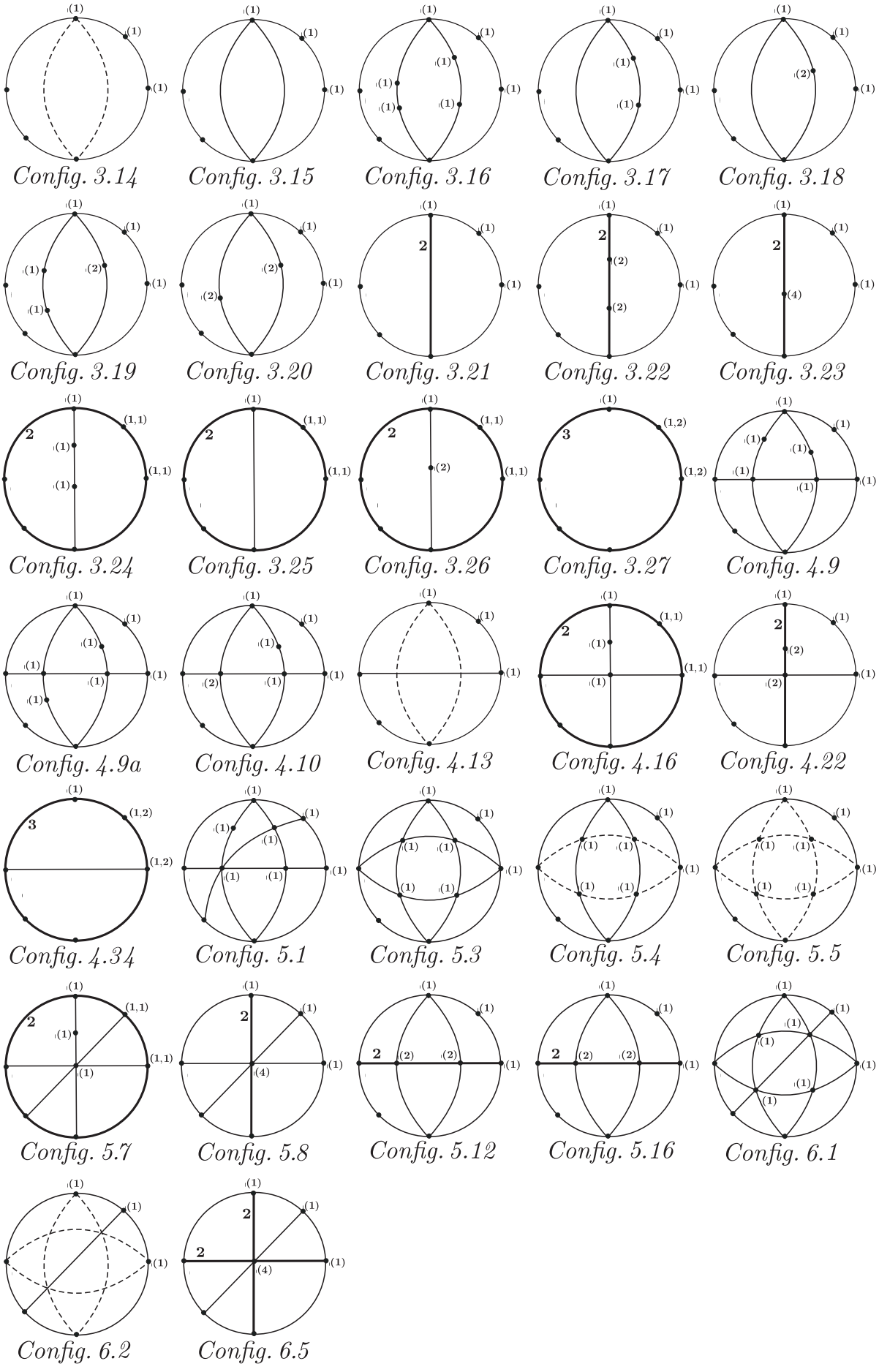

Figure 1. The configurations of quadratic systems in $\mathbf{QSL^{2p}}$ (case $\eta > 0$)

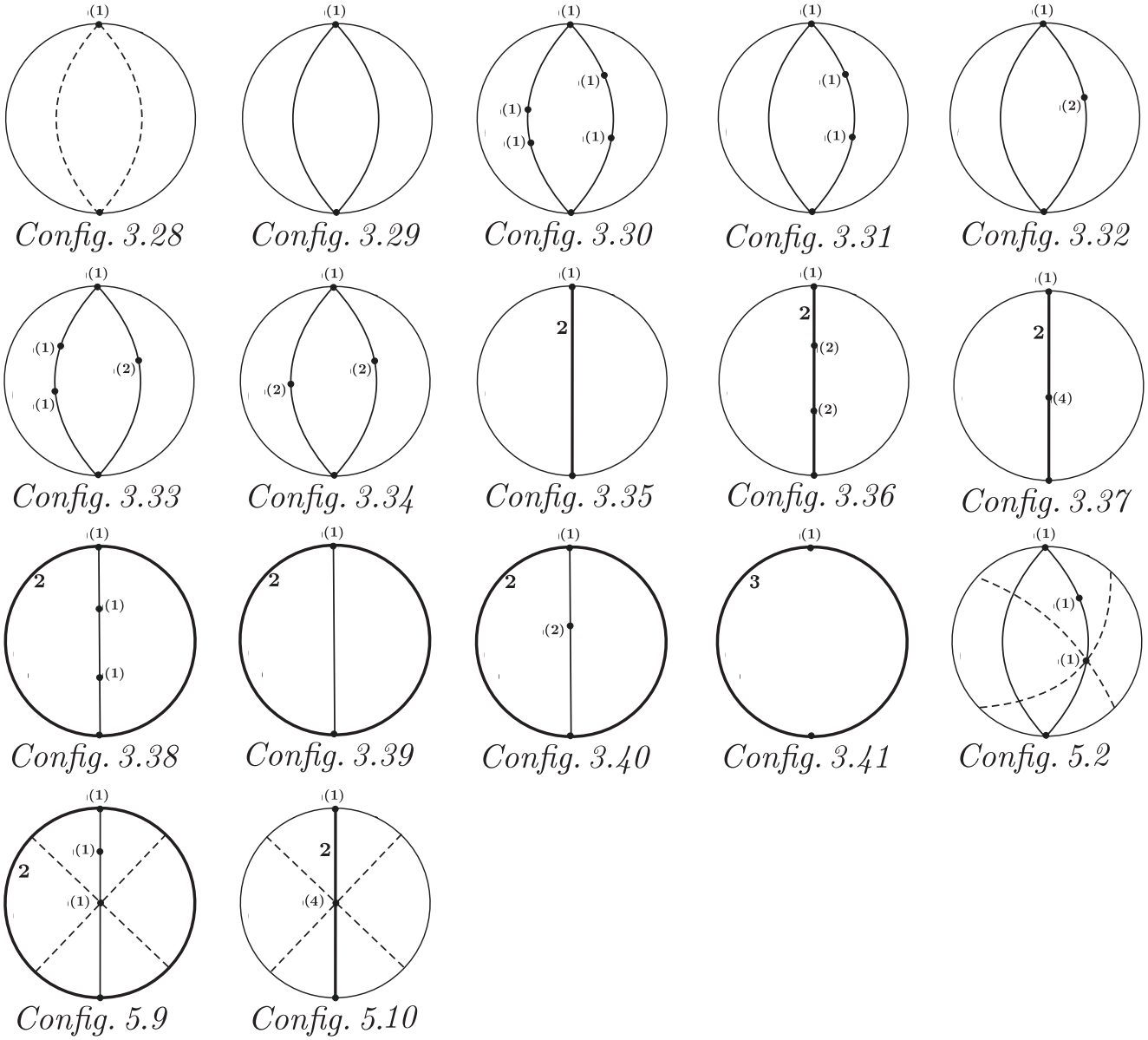

Figure 2. The configurations of quadratic systems in $\mathbf{QSL^{2p}}$ (case $\eta < 0$)

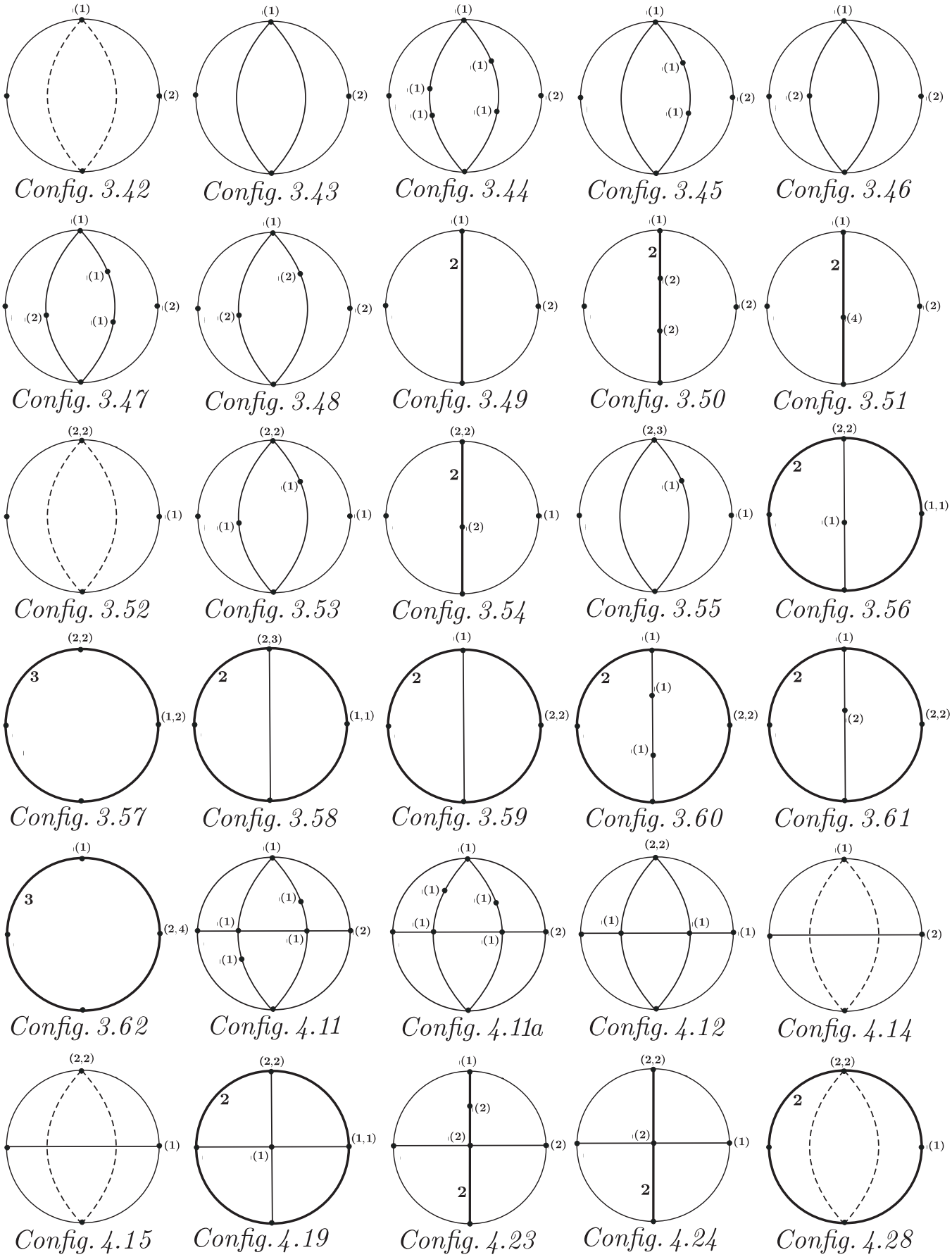

Figure 3. The configurations of quadratic systems in $\mathbf{QSL^{2p}}$ (case $\eta = 0 \neq \widetilde{M}$)

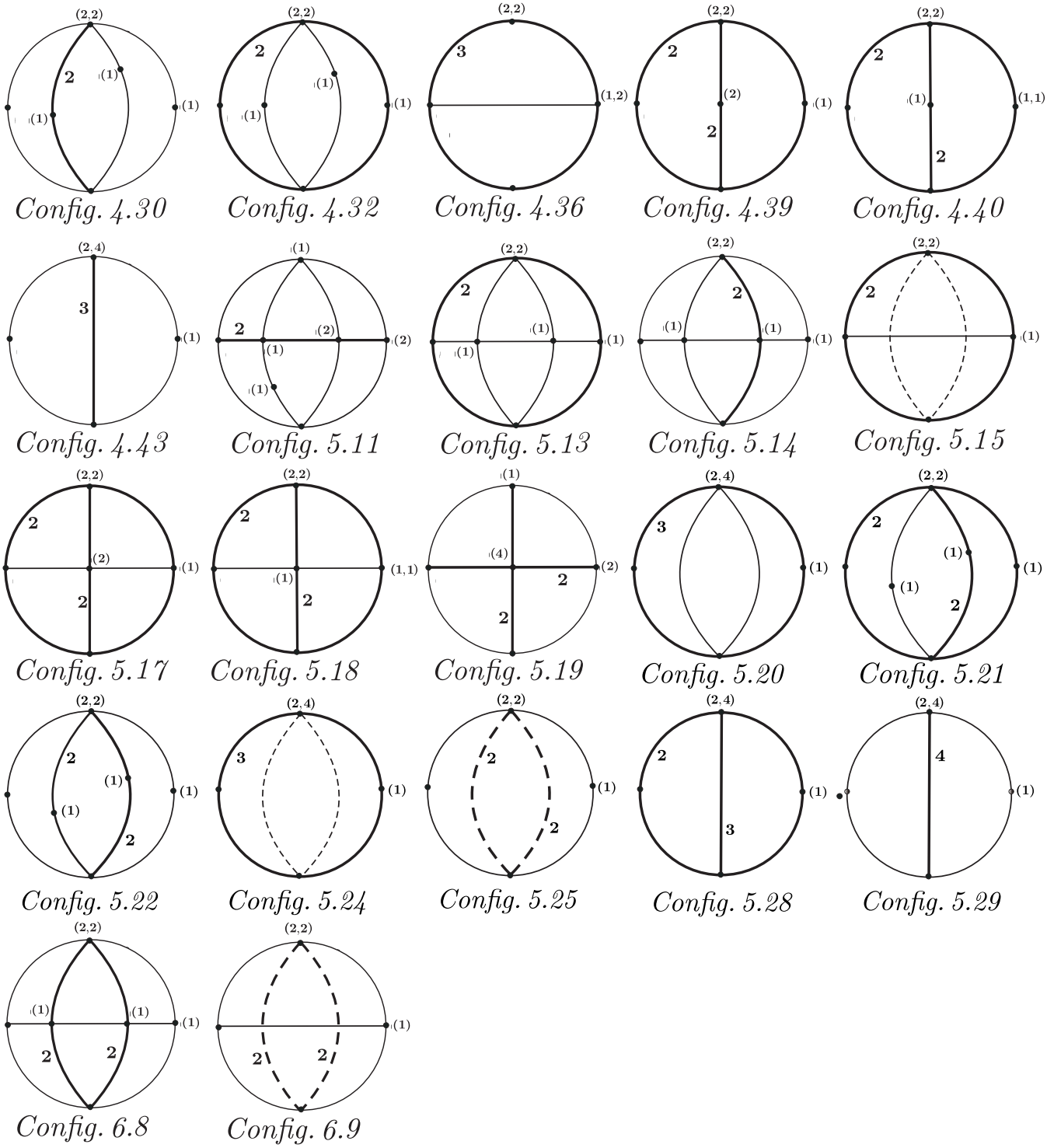

Figure 3 *(continued)*: The configurations of quadratic systems in $\mathbf{QSL^{2p}}$ (case $\eta = 0 \neq \widetilde{M}$)

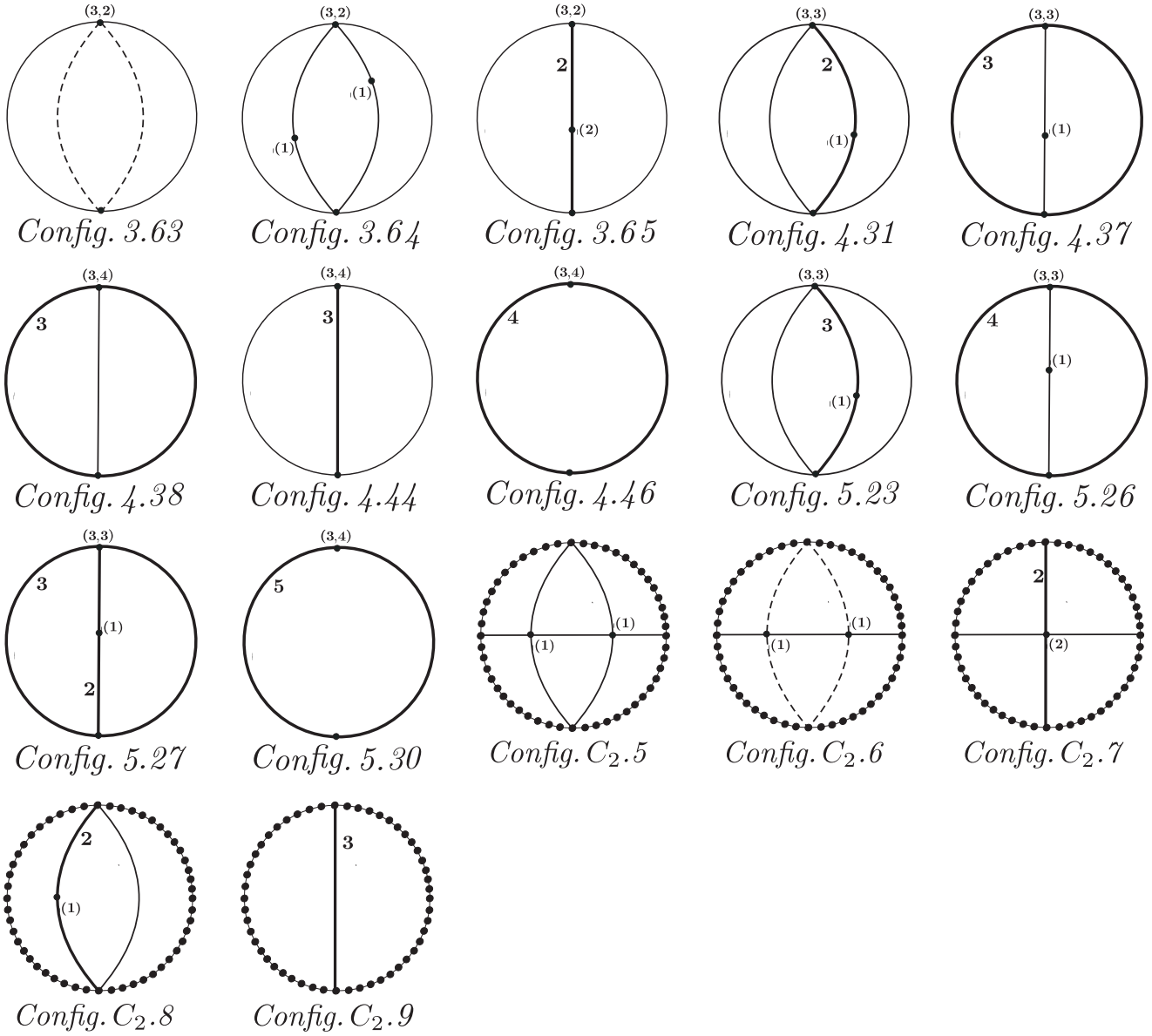

Figure 4. The configurations of quadratic systems in $\mathbf{QSL^{2p}}$ (case $\eta = \widetilde{M} = 0$)

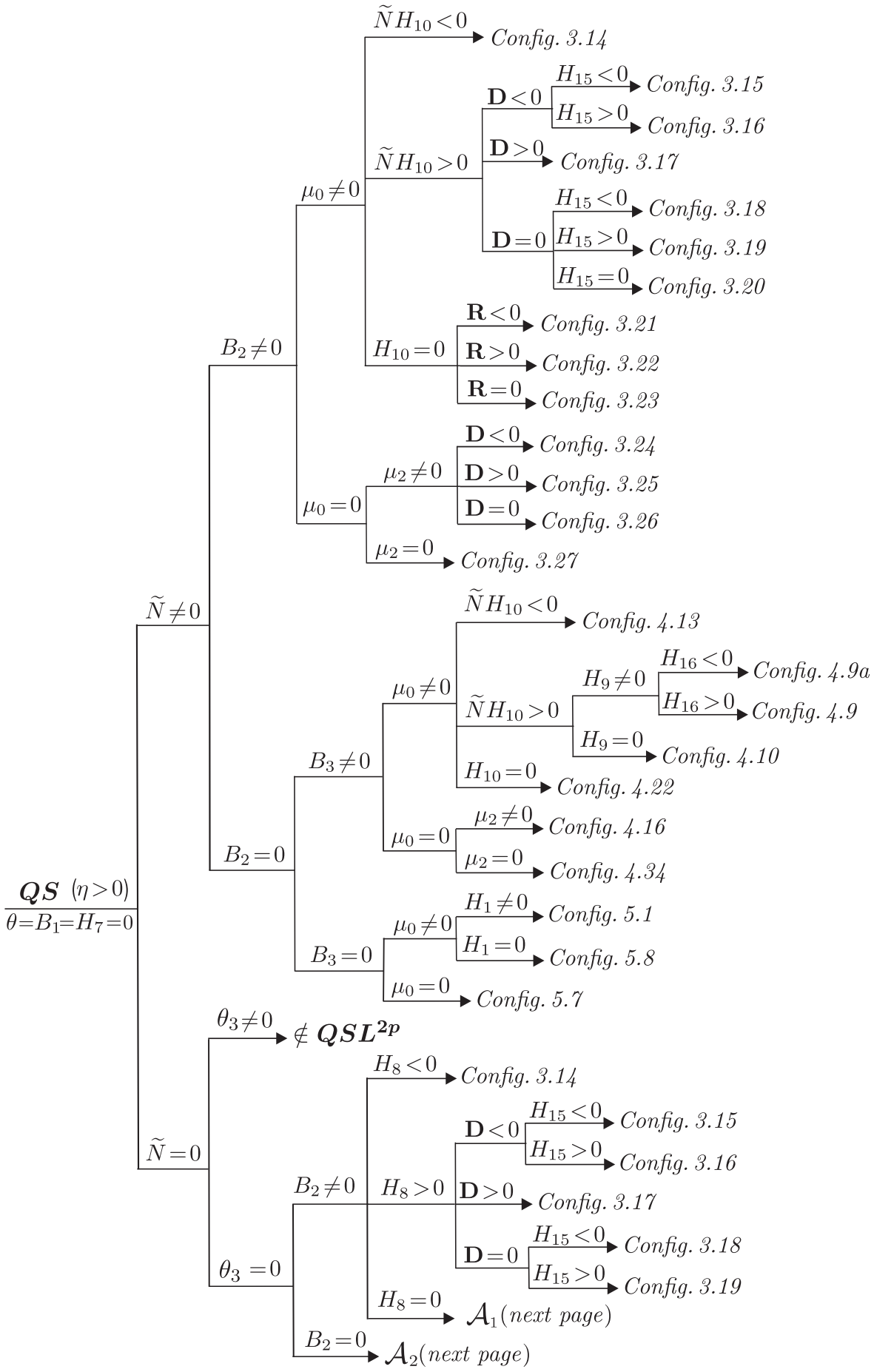

Diagram 1. The invariant criteria for configurations of systems in $\mathbf{QSL^{2p}}$ (case $\eta > 0$)

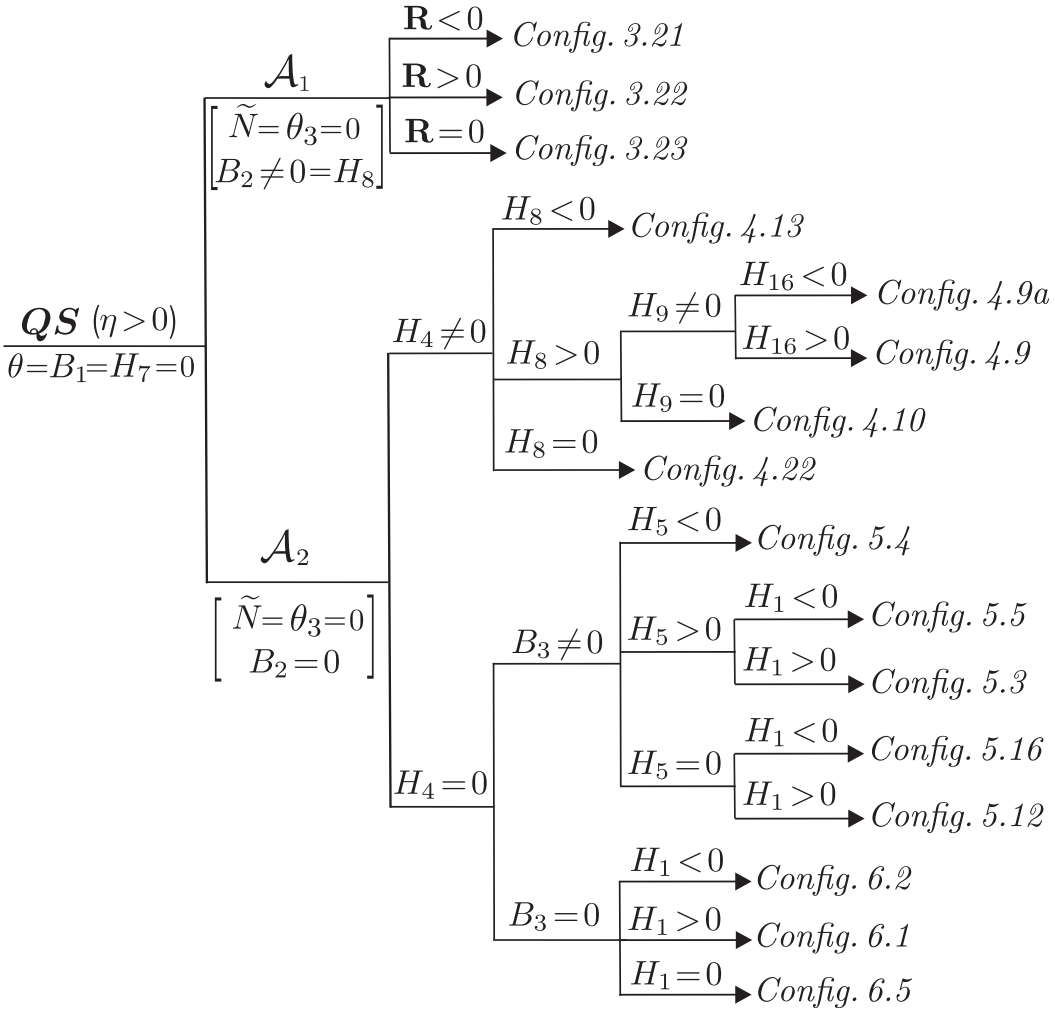

Diagram 1 *(continued)*: The invariant criteria for configurations of systems in $\mathbf{QSL^{2p}}$ (case $\eta > 0$)

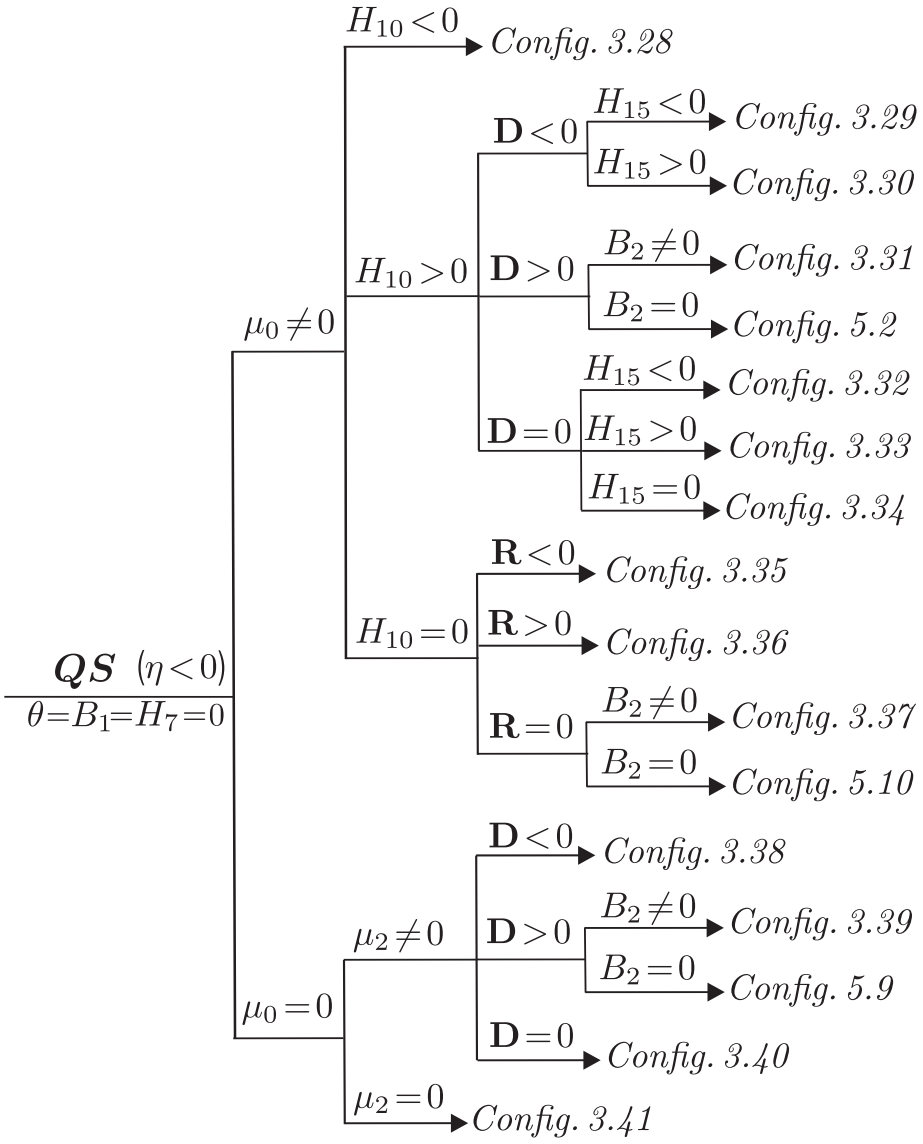

Diagram 2. The invariant criteria for configurations of systems in $\mathbf{QSL^{2p}}$ (case $\eta < 0$)

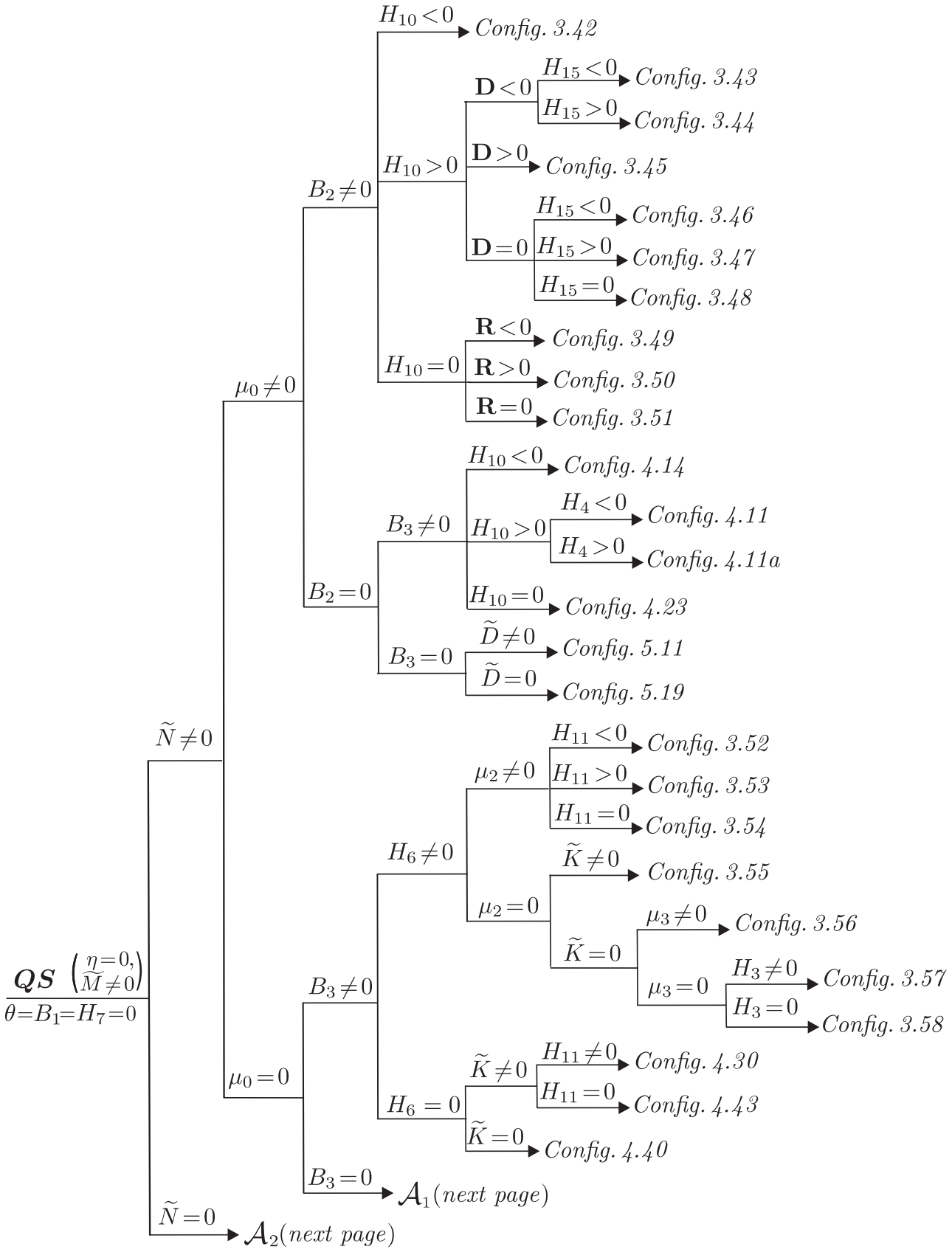

Diagram 3. The invariant criteria for configurations of systems in $\mathbf{QSL^{2p}}$ (case $\eta = 0 \neq \widetilde{M}$)

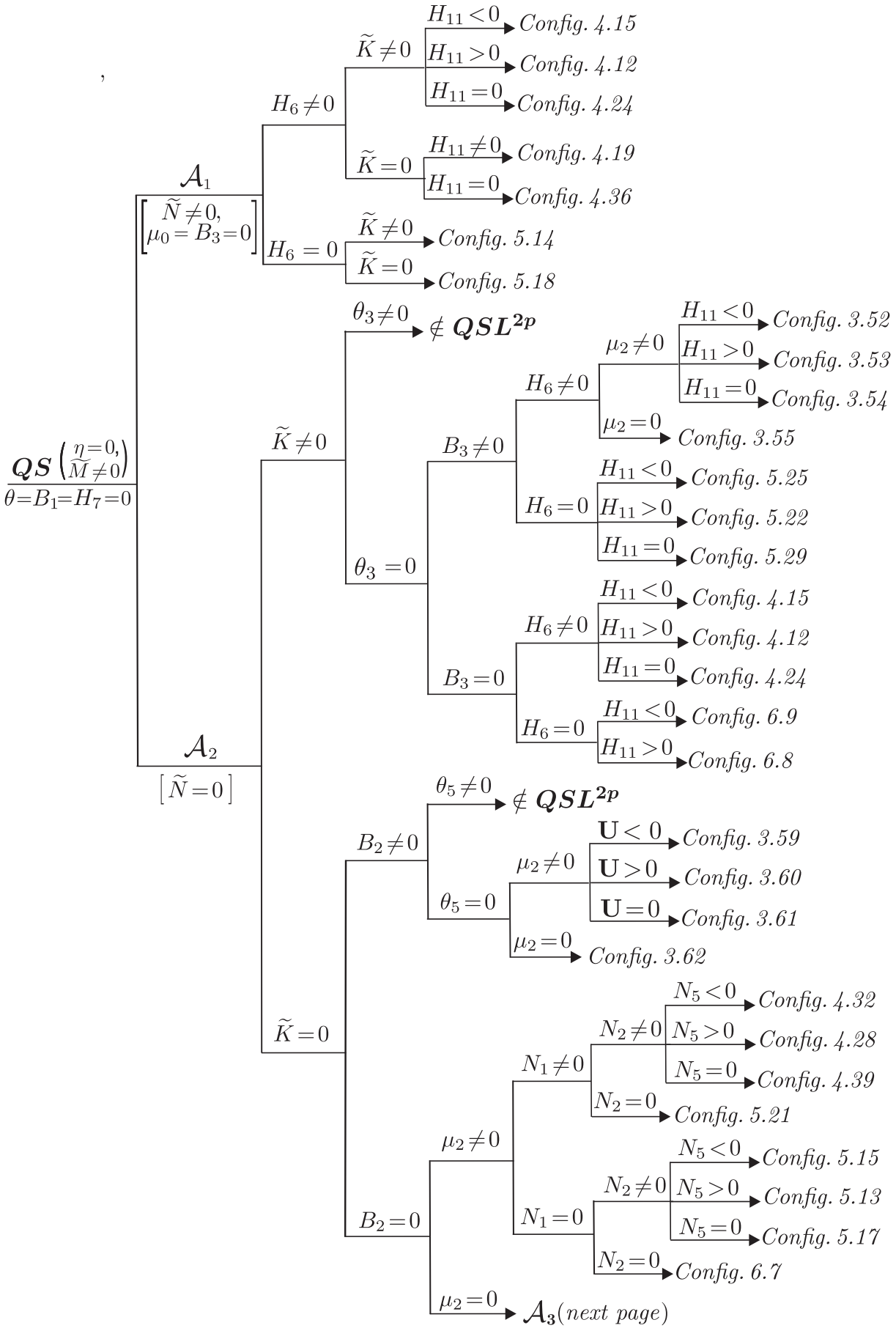

Diagram 3 *(continued)*: The invariant criteria for configurations of systems in $\mathbf{QSL^{2p}}$ (case $\eta = 0 \neq \widetilde{M}$)

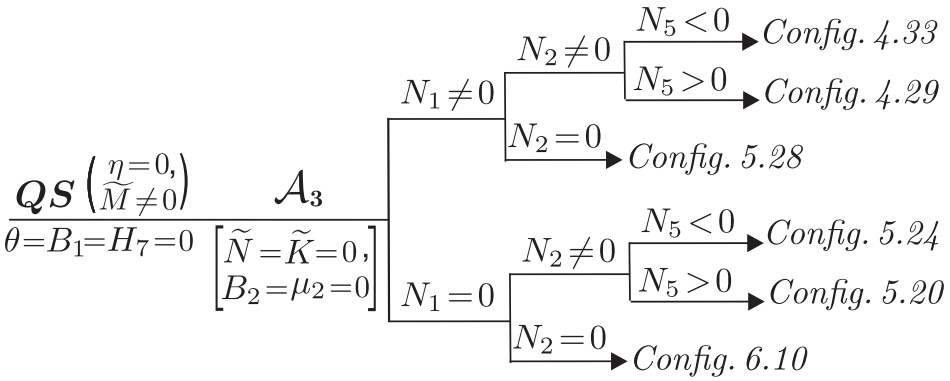

Diagram 3 *(continued)*: The invariant criteria for configurations of systems in $\mathbf{QSL^{2p}}$ (case $\eta = 0 \neq \widetilde{M}$)

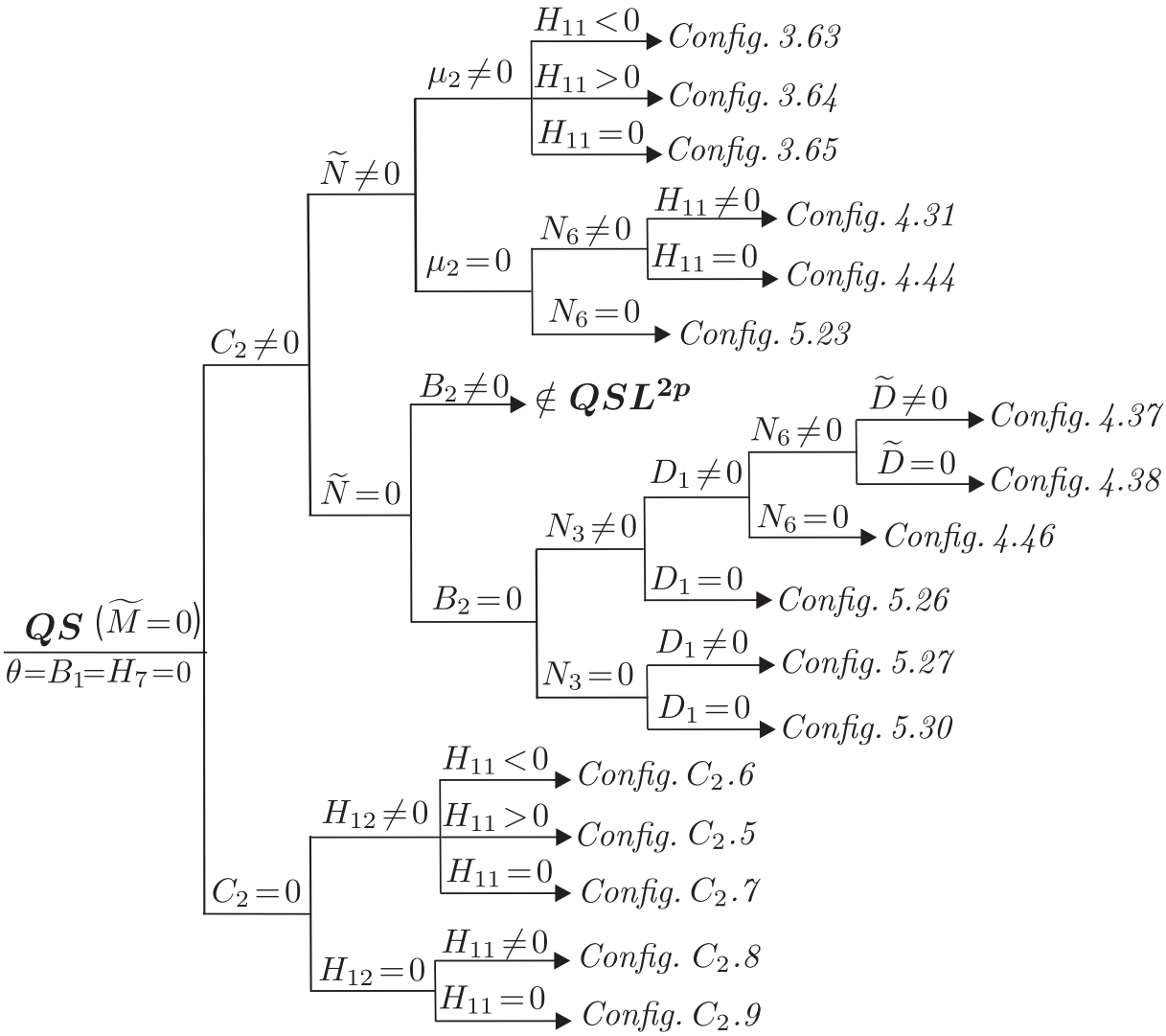

Diagram 4. The invariant criteria for configurations of systems in $\mathbf{QSL^{2p}}$ (case $\eta = 0 = \widetilde{M}$)

4. Phase portraits of the Riccati systems

Theorem 4.1. *If a quadratic system* (S) *belongs to the class of Riccati systems* $\boldsymbol{QS}_{Ric}$*, then system* (S) *possesses one of the following phase portraits if and only if the corresponding conditions hold respectively:*

- ***(i)*** *For* $\eta > 0$ *a non-degenerate (respectively, degenerate) system* (S) *possesses one of the phase portraits Ric. 1–Ric. 27 (respectively, Ric.* D_1*–Ric.* D_3 *) given in Figure 5 (respectively, Figure 6) if and only if one of the sets of conditions given in Diagram 5 holds, correspondingly.*

- ***(ii)*** *For* $\eta < 0$ *a non-degenerate (respectively, degenerate) system* (S) *possesses one of the phase portraits Ric. 28–Ric. 35 (respectively, Ric.* D_4*, Ric. 28d and Ric. 35d) if and only if one of the sets of conditions given in Diagram 6 holds, correspondingly. The phase portraits Ric. 28–Ric. 35 (respectively, Ric.* D_4*) are given in Figure 5 (respectively, Figure 6), whereas Ric. 28d and Ric. 35d are topologically equivalent to Ric. 28 and Ric. 35, correspondingly.*

- ***(iii)*** *For* $\eta = 0$ *and* $\widetilde{M} \neq 0$ *a non-degenerate (respectively, degenerate) system* (S) *possesses one of the phase portraits Ric. 36–Ric. 76 (respectively, Ric.* D_5*–Ric.* D_{18} *and Ric. 53d) if and only if one of the sets of conditions given in Diagram 7 holds, correspondingly. The phase portraits Ric. 36–Ric. 76 (respectively, Ric.* D_5*–Ric.* D_{18}*) are given in Figure 5 (respectively, Figure 6), whereas Ric. 53d is topologically equivalent to Ric. 53.*

- ***(iv)*** *For* $\eta = \widetilde{M} = 0$ *a non-degenerate (respectively, degenerate) system* (S) *possesses one of the phase portraits Ric. 28 and Ric. 77–Ric. 93 (respectively, Ric.* D_{19}*–Ric.* D_{26} *and Ric. 28d) if and only if one of the sets of conditions given in Diagram 8 holds, correspondingly. The phase portraits Ric. 28 and Ric. 77–Ric. 93 (respectively, Ric.* D_{19}*–Ric.* D_{26}*) are given in Figure 5 (respectively, Figure 6), whereas Ric. 28d is topologically equivalent to Ric. 28.*

Proof of Theorem 4.1: First of all we prove the following lemma.

Lemma 4.2. *Consider an arbitrary quadratic system* (2) *and assume that its phase portrait possesses a separatrix connection between two singularities* p_1 *and* p_2 *at least one of them finite. Suppose that this connection is not part of an invariant straight line. Then inside the region* R *bordered by this separatrix and the segment* $\overline{p_1p_2}$ *necessarily there exists either one singularity or at least one of the points* p_1 *or* p_2 *is a non-elemental singularity which is* $\alpha-$ *(or* $\omega-$*) limit for orbits that reach the singular point inside the region* R*.*

Proof: According to [Artés *et al.*, 2018, Lemma 3.4] (see also [Ye *et al.*, 1986]) if a straight line in a quadratic system passes through two finite singularities p_1 and p_2 then either this straight line is invariant or the trajectories of the flow crossing the segment $\overline{p_1p_2}$ do it in the opposite direction as the trajectories that cross the half lines $\overline{\infty p_1}$ and $\overline{p_2\infty}$.

On the other hand by Lemma [Artés *et al.*, 2018, Lemma 3.5] (see also [Ye *et al.*, 1986]) the straight line connecting one finite singular point and a couple of infinite singular points in a quadratic system is either formed by trajectories or it is a line with exactly one contact point. This contact point is the finite singularity. For the latter case the flow goes in different directions on each half line.

An orbit passing through a point inside R can neither have its $\alpha-$ nor $\omega-$limit inside the closure $\overline{R}$ of R. Thus the orbits must come from outside $\overline{R}$ and proceed by going out of it, forcing then the existence of at least one contact point on the segment $\overline{p_1p_2}$ which contradicts Lemma 3.4 (or Lemma 3.5) from [Artés *et al.*, 2018]. ∎

In the following we will prove only the case (i) of Theorem 4.1, i.e. the condition $\eta > 0$ holds. The rest of the cases are proved in [Artés *et al.*, 2023].

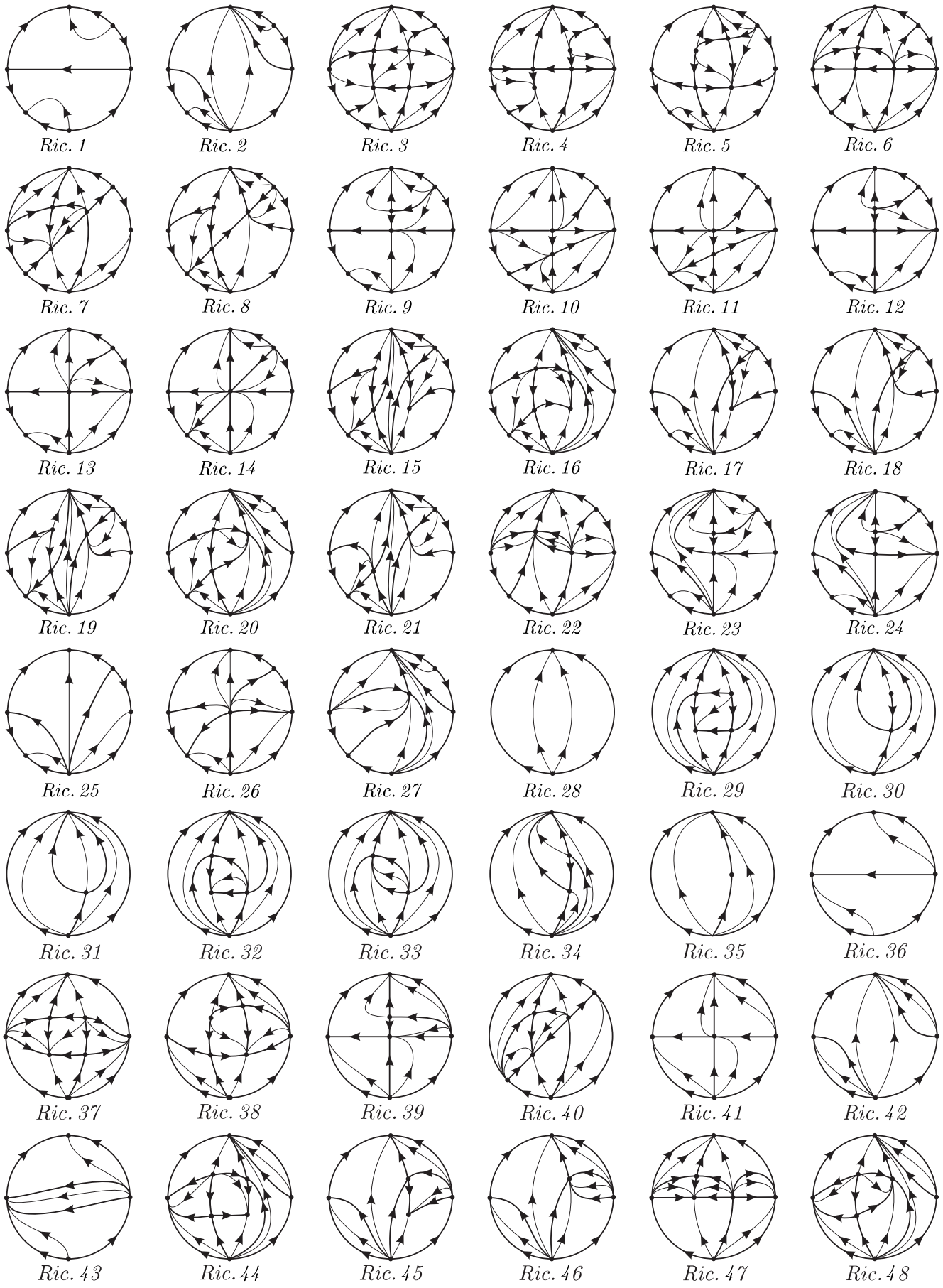

Figure 5. The phase portraits of Riccati quadratic systems

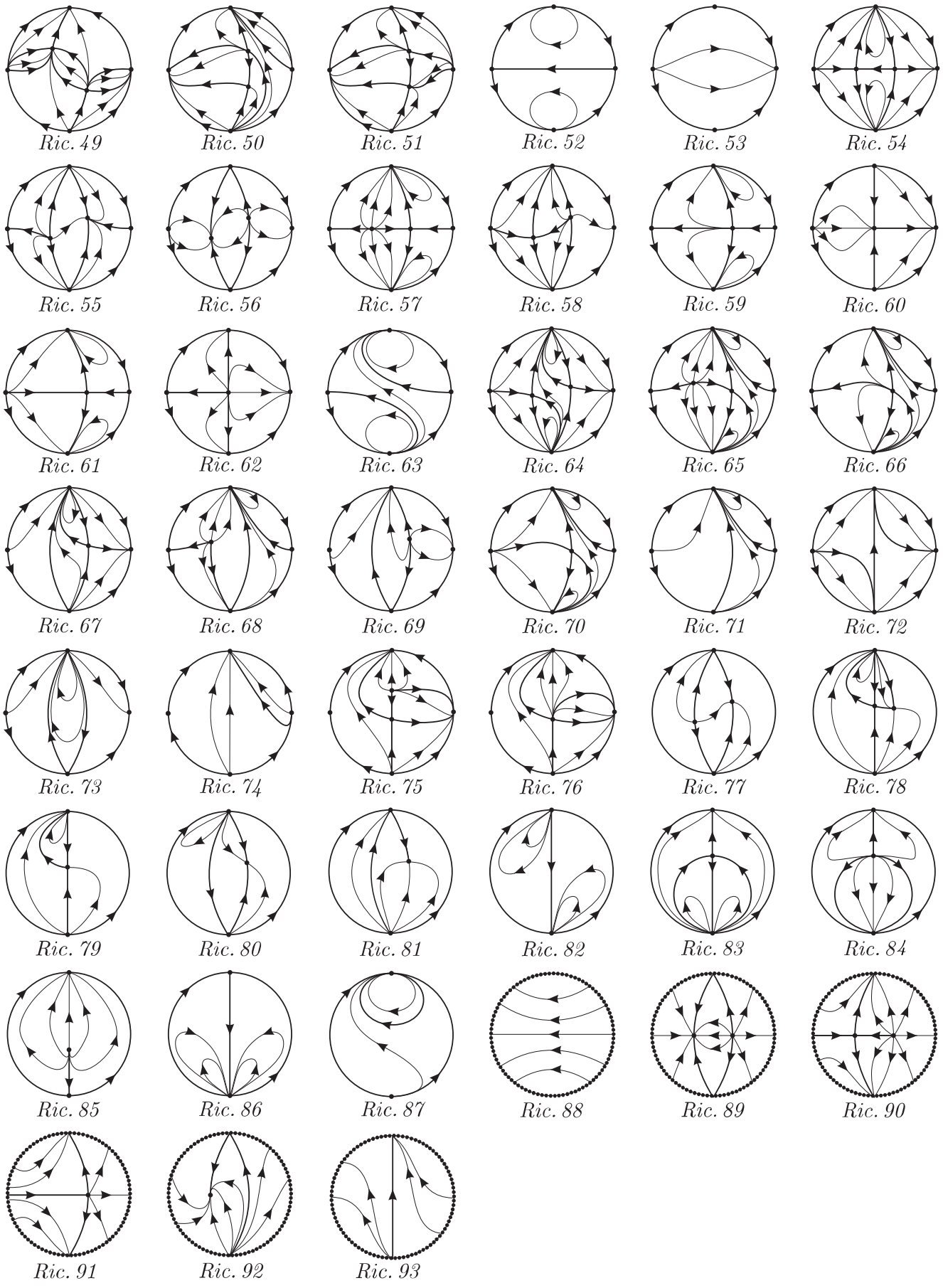

Figure 5 *(continuation)*: The phase portraits of Riccati quadratic systems

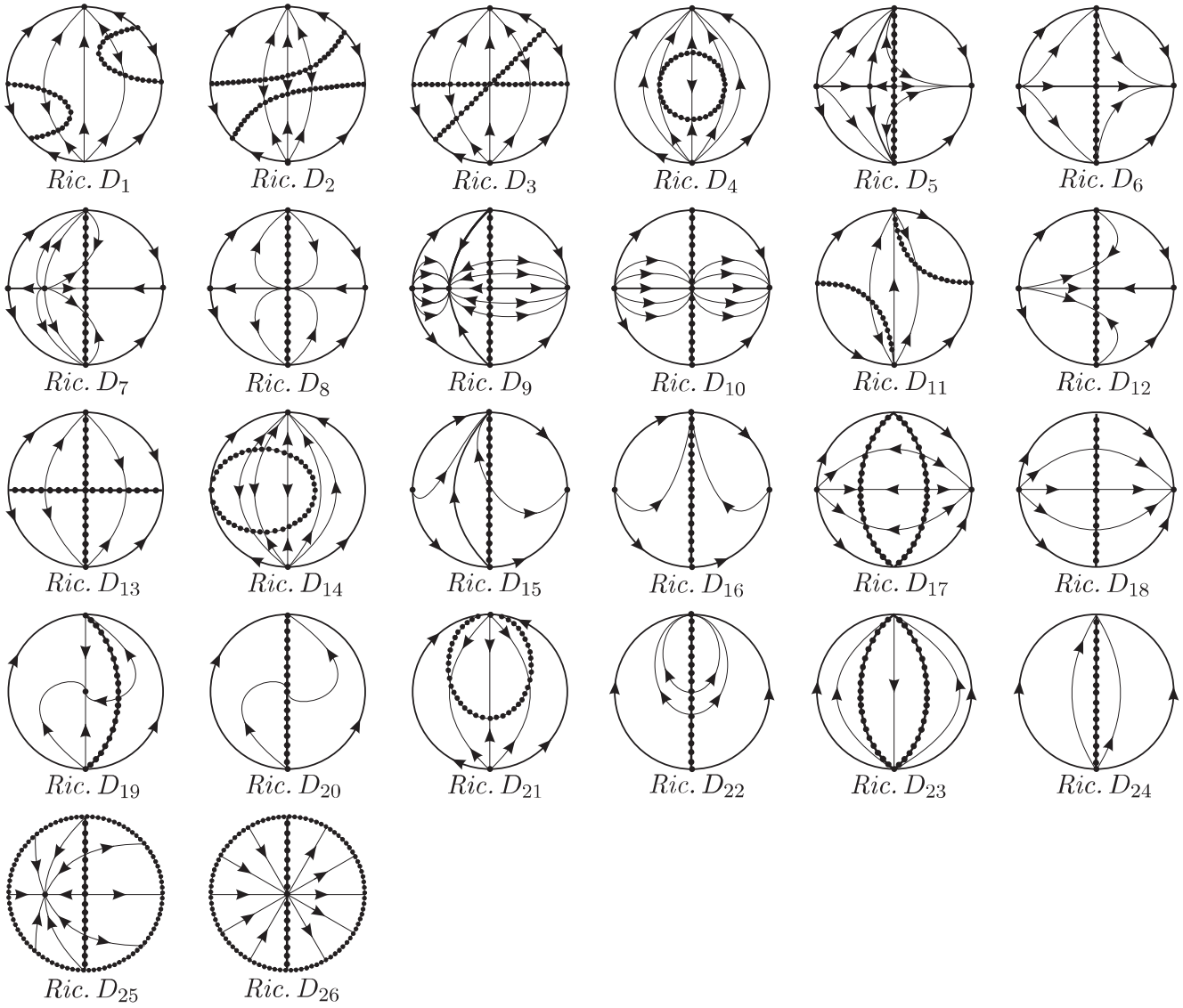

Figure 6. The phase portraits of Riccati degenerate quadratic systems

Corollary 4.3. *If the phase portrait of a quadratic system possesses a separatrix connection between two singularities p_1 and p_2 at least one of them being finite and the region R is defined like in previous lemma and does not contain the required elements imposed by Lemma 4.2 then the region R is empty and the separatrix connection is part of an invariant straight line.*

According to the Diagram 1 we examine two subcases: $\widetilde{N} \neq 0$ and $\widetilde{N} = 0$.

4.1. The subcase $\widetilde{N} \neq 0$

Since $\eta > 0$, according to [Sibirskii, 1998] (see also [Schlomiuk & Vulpe, 2005]) we consider the following canonical form:

$$\begin{aligned} \dot{x} =& a + cx + dy + gx^2 + (h-1)xy, \\ \dot{y} =& b + ex + fy + (g-1)xy + hy^2, \end{aligned} \tag{7}$$

for which by Lemma 3.7 the conditions $\theta = B_1 = H_7 = 0$ have to be fulfilled.

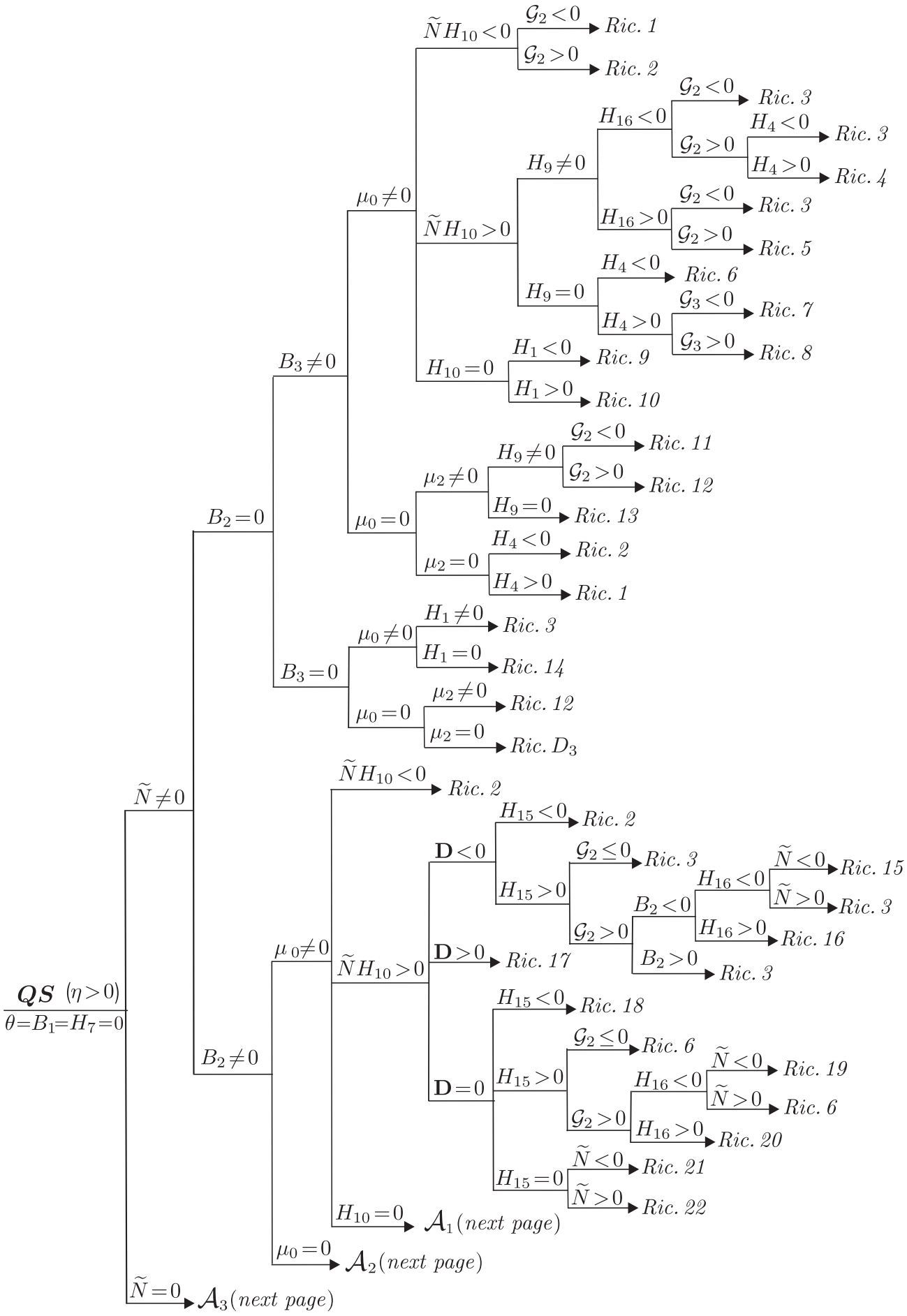

Diagram 5. The invariant criteria for phase portraits of systems in $\mathbf{QS}_{Ric}$ (case $\eta > 0$).

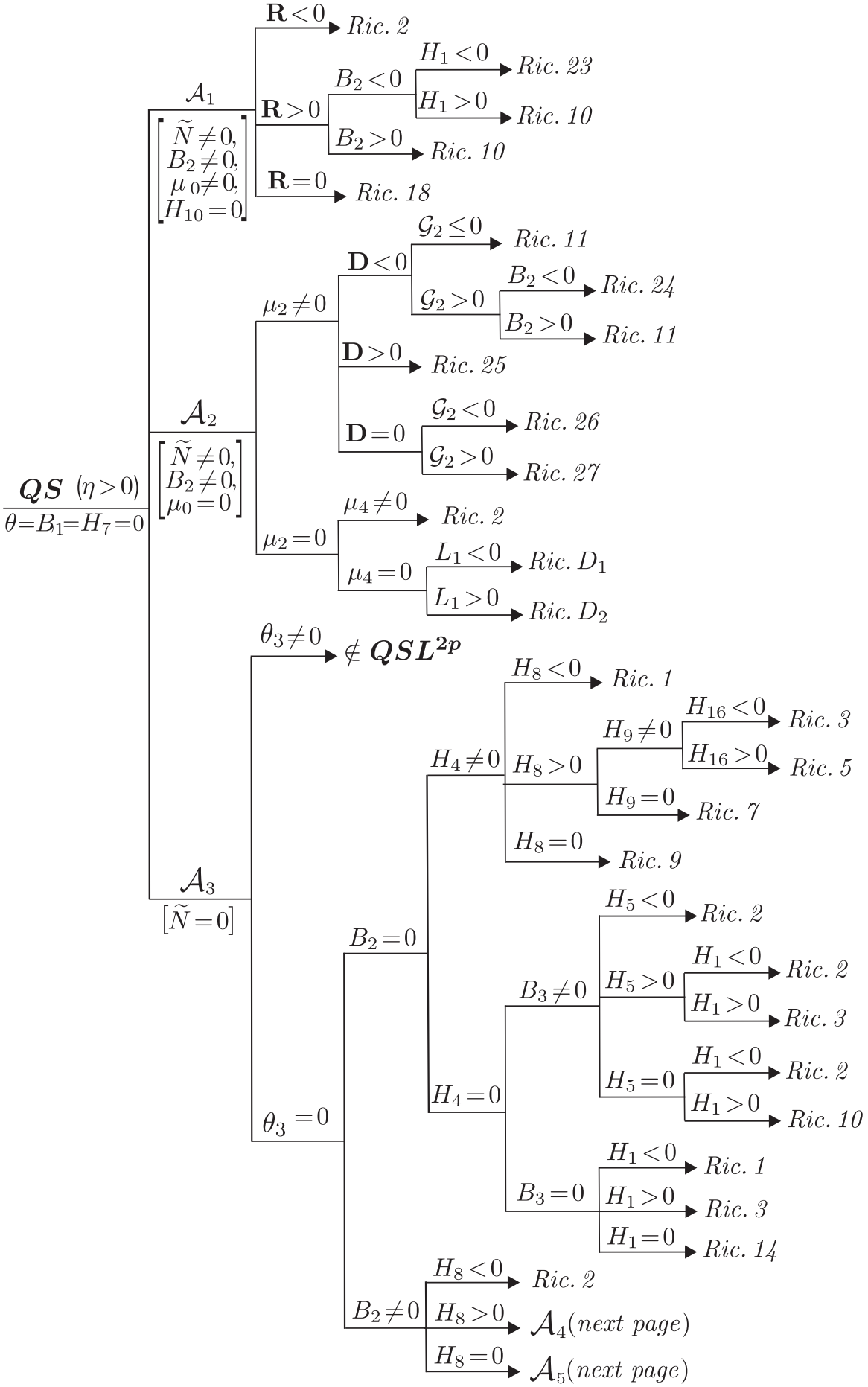

Diagram 5 *(continuation)*: The invariant criteria for phase portraits of systems in $\mathbf{QS}_{Ric}$ (case $\eta > 0$).

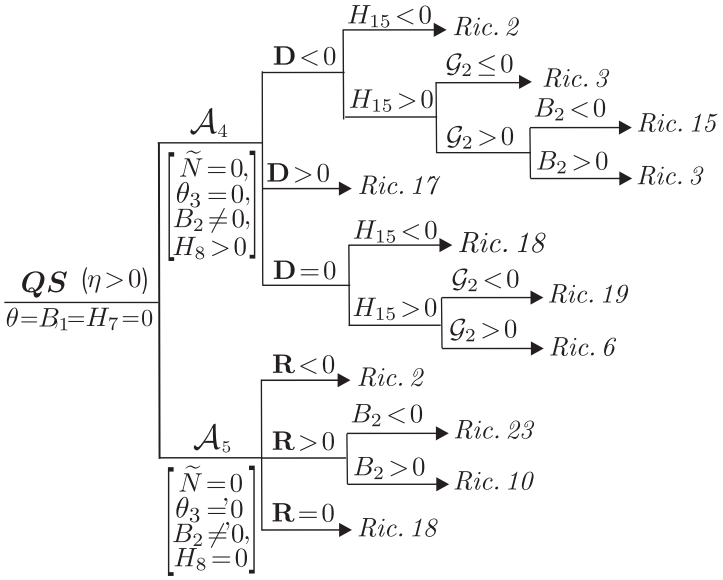

Diagram 5 *(continuation)*: The invariant criteria for phase portraits of systems in $\mathbf{QS}_{Ric}$ (case $\eta > 0$).

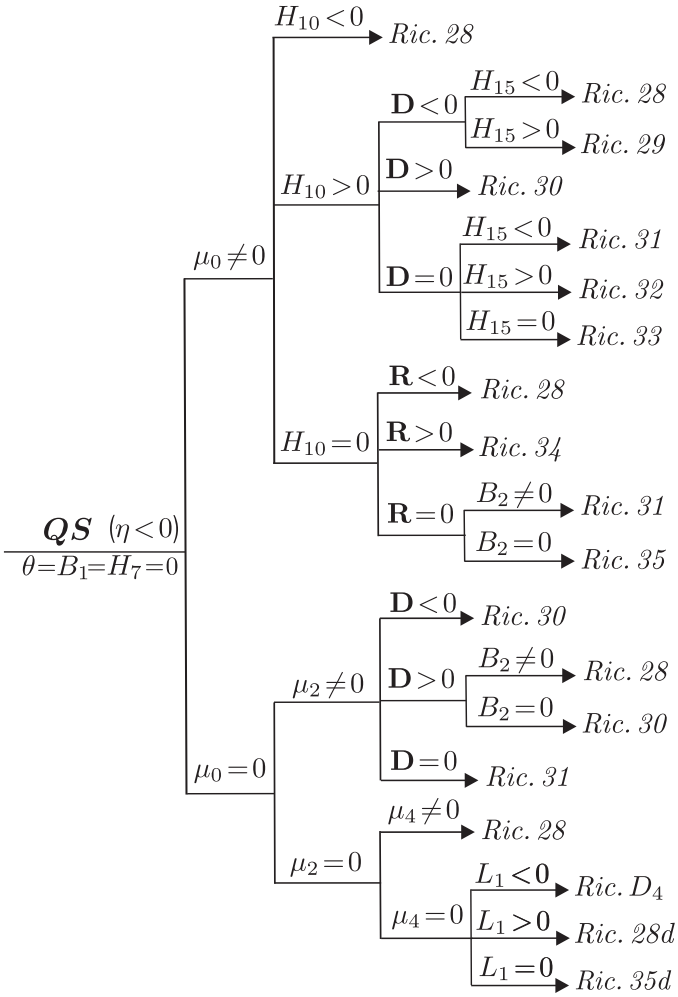

Diagram 6. The invariant criteria for phase portraits of systems in $\mathbf{QS}_{Ric}$ (case $\eta < 0$).

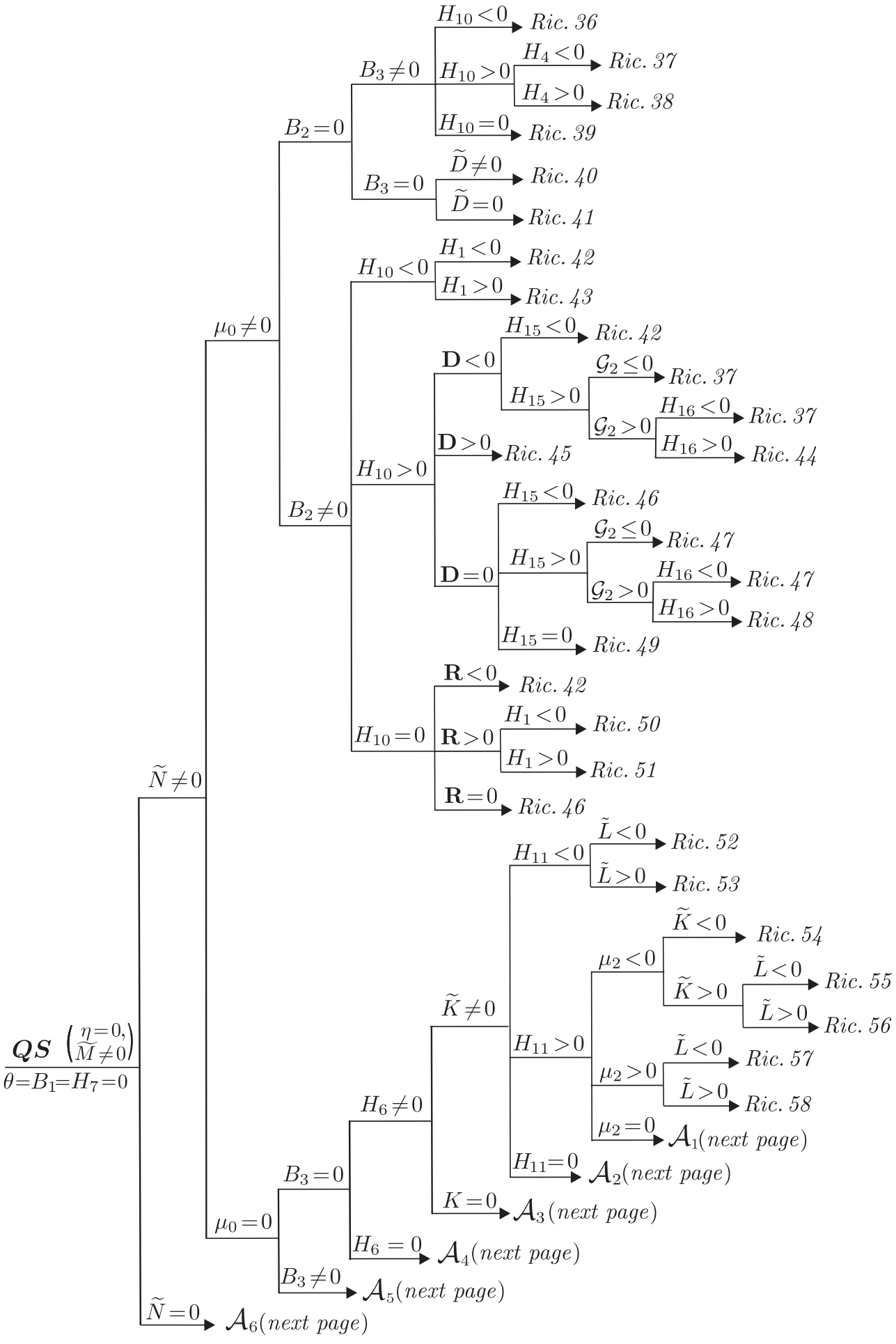

Diagram 7. The invariant criteria for phase portraits of systems in $\mathbf{QS}_{Ric}$ (case $\eta = 0 \neq \widetilde{M}$).

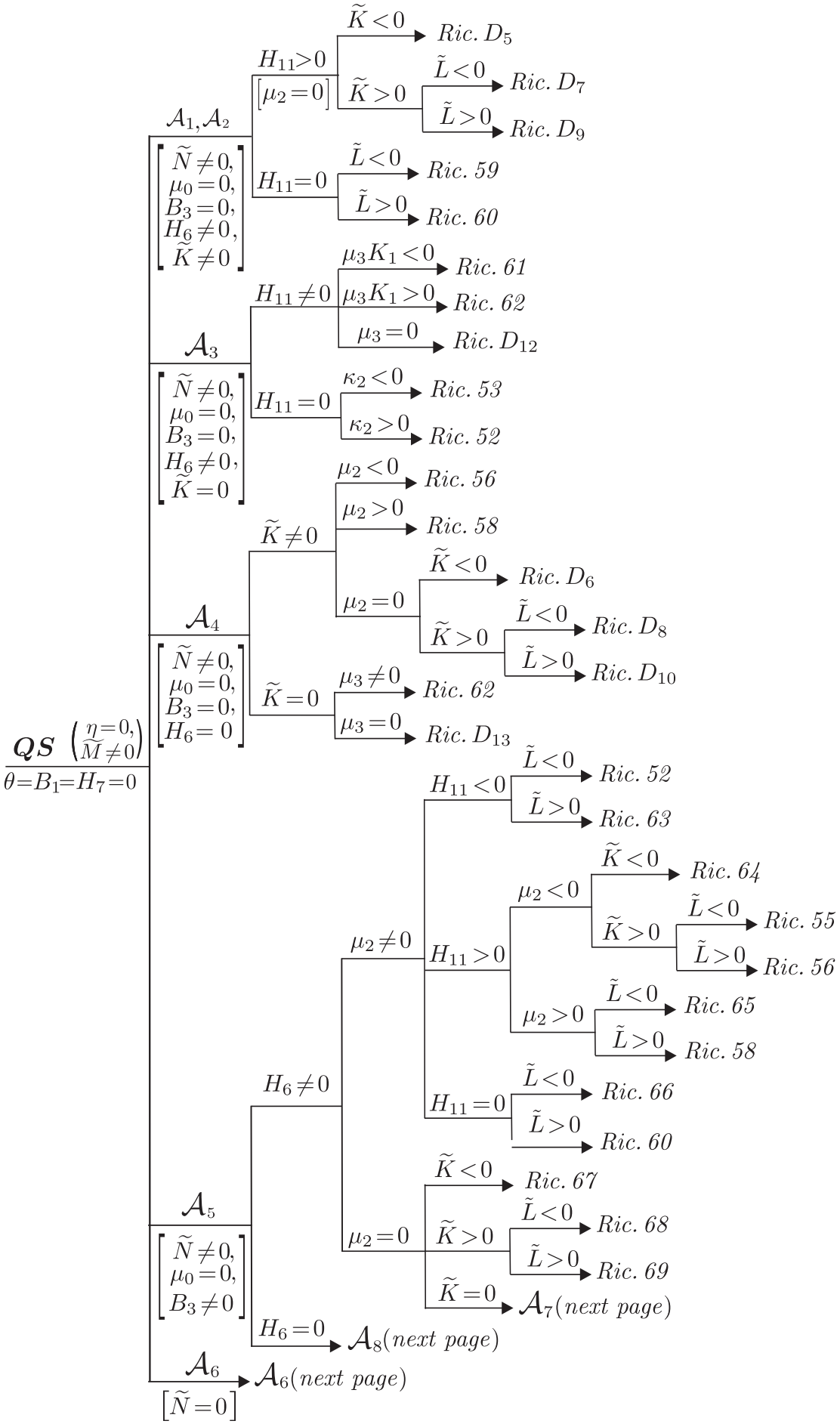

Diagram 7 *(continuation)*: The invariant criteria for phase portraits of systems in $\mathbf{QS}_{Ric}$ (case $\eta = 0 \neq \widetilde{M}$).

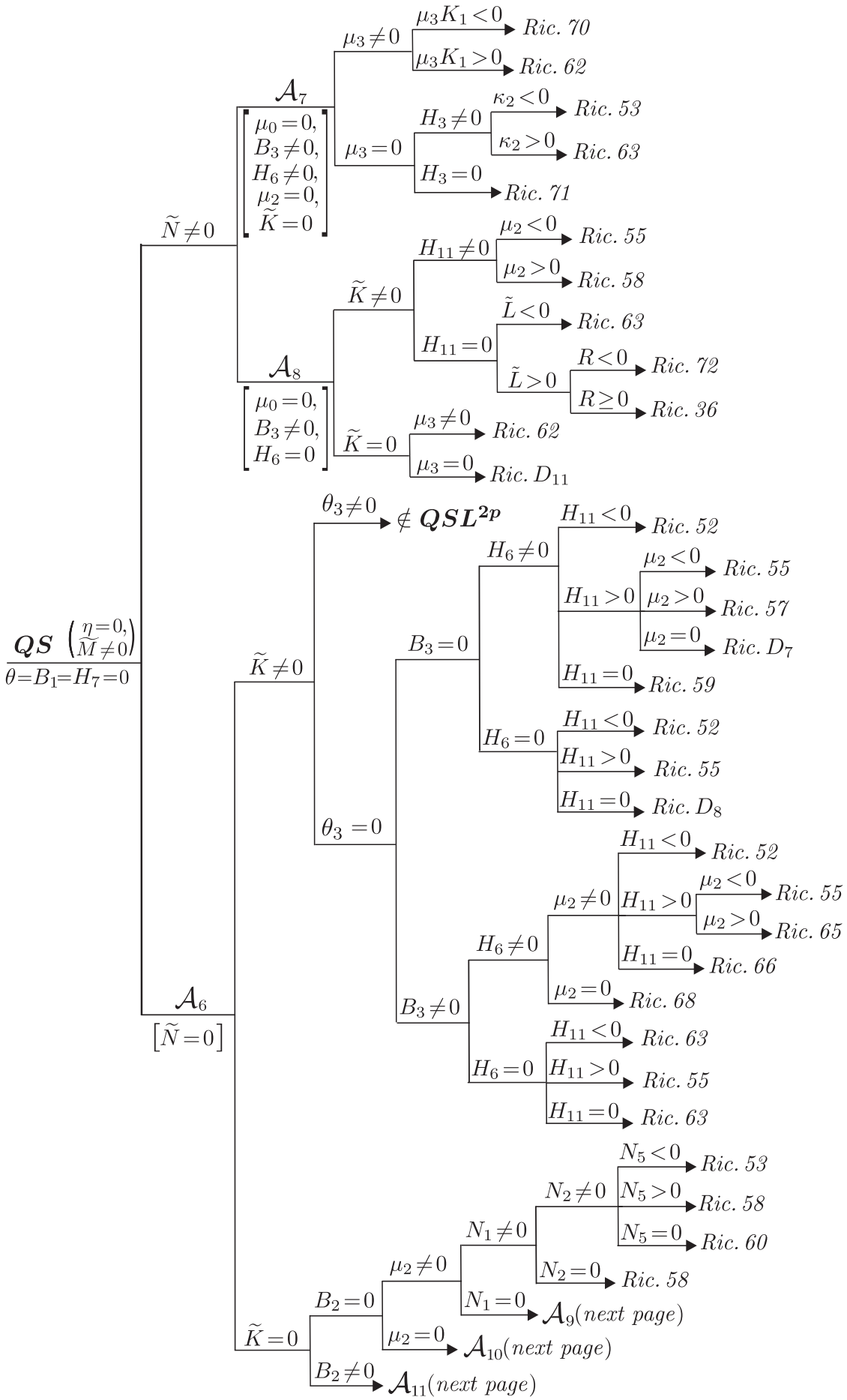

Diagram 7 *(continuation)*: The invariant criteria for phase portraits of systems in $\mathbf{QS}_{Ric}$ (case $\eta = 0 \neq \widetilde{M}$).

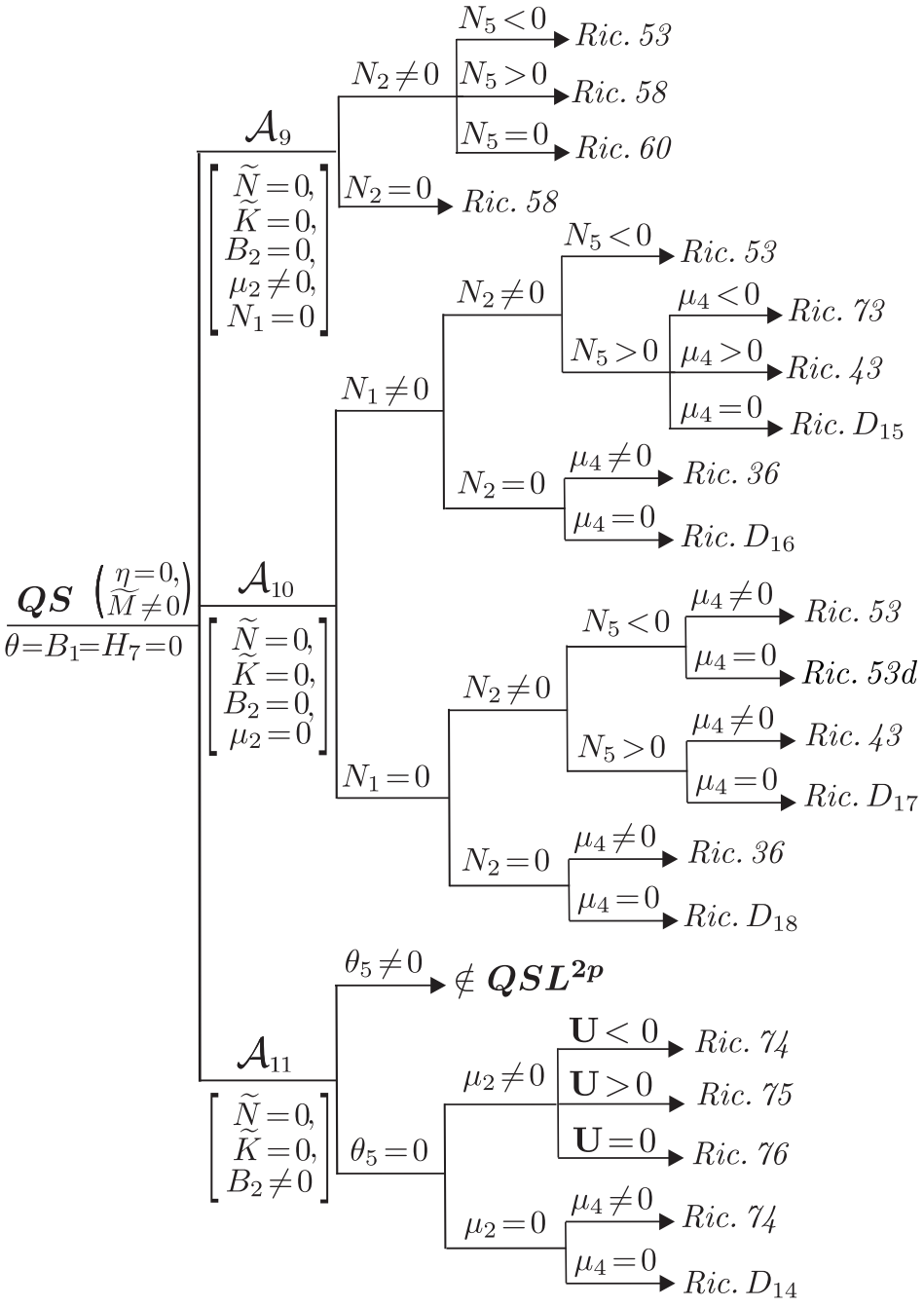

Diagram 7 *(continuation)*: The invariant criteria for phase portraits of systems in $\mathbf{QS}_{Ric}$ (case $\eta = 0 \neq \widetilde{M}$).

As it was shown in [Bujac *et al.*, 2022] forcing the conditions $\theta = B_1 = H_7 = 0$ we arrive to the family of systems (11) (from [Bujac *et al.*, 2022]), i.e. we obtain the following family of a Riccati systems:

$$\begin{aligned} \dot{x} =& a + cx + gx^2, \\ \dot{y} =& b + ex + fy + (g-1)xy + y^2. \end{aligned} \tag{8}$$

We observe that for these systems $\mu_0 = g^2 \geq 0$ and since $\eta > 0$ considering [Artés *et al.*, 2015] (see Diagram 1 on the page 36) we have the next remark.

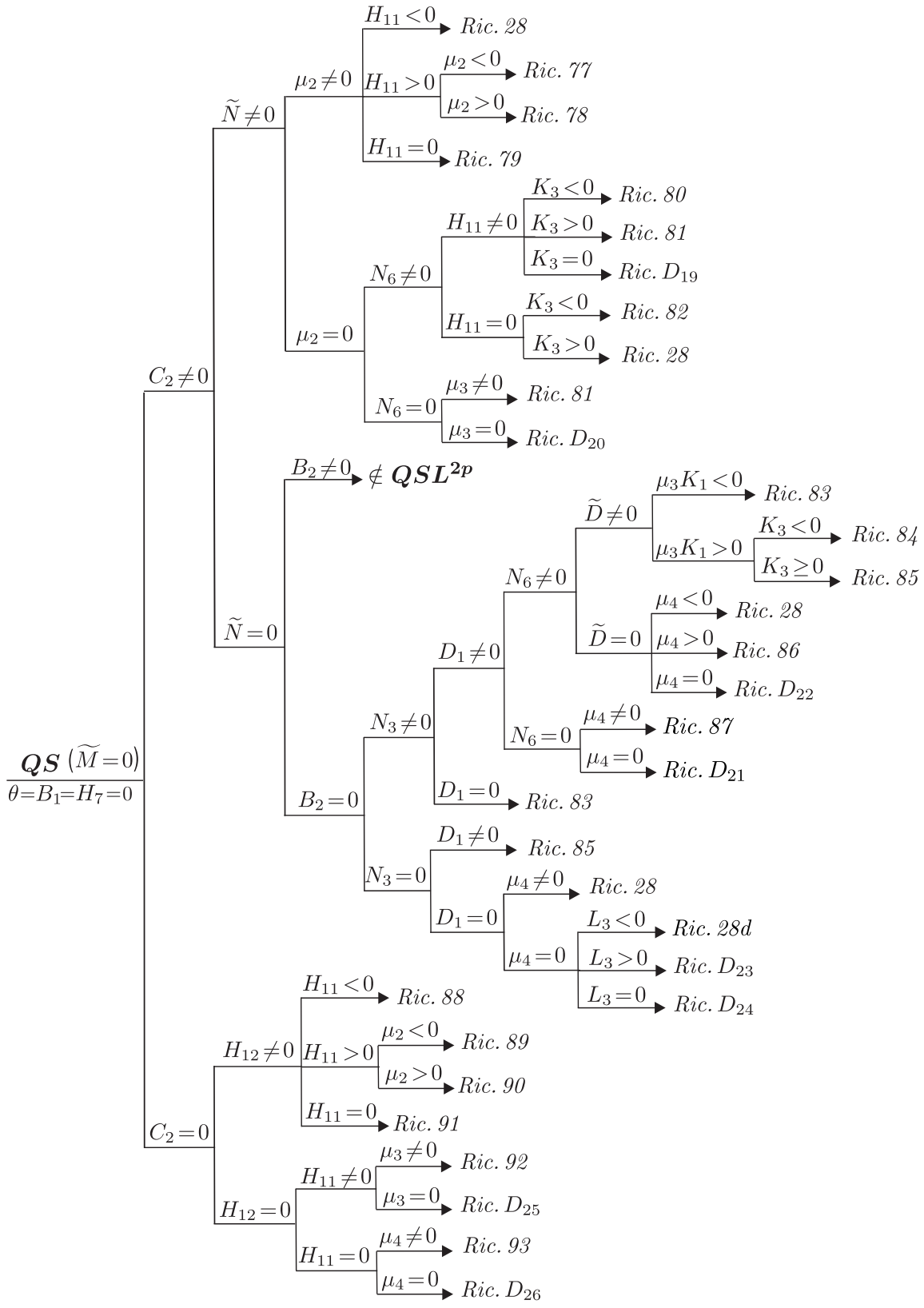

Diagram 8. The invariant criteria for phase portraits of systems in $\mathbf{QS}_{Ric}$ (case $\eta = 0 = \widetilde{M}$).

Remark 4.4. In the case $\mu_0 \neq 0$ (then $\mu_0 > 0$) systems (8) possess at infinity one saddle and two nodes, all elemental.

Since by Lemma 3.1 the condition $B_2 = 0$ is necessary for the existence of invariant lines at least in two directions, we consider two possibilities: $B_2 = 0$ and $B_2 \neq 0$. Even if in the Diagram 1 the case $B_2 = 0$ follows after $B_2 \neq 0$ we begin here with $B_2 = 0$. Our motivation is because in the case $B_2 = 0$ the systems belong to a higher codimension subfamilies and these subfamilies form an skeleton from which the systems with $B_2 \neq 0$ will bifurcate.

4.1(A). The possibility $B_2 = 0$.

According to Diagram 1 we examine two cases: $B_3 \neq 0$ and $B_3 = 0$.

The case $B_3 \neq 0$. Then by Lemma 3.1 we could not have invariant lines in three directions and we examine the corresponding cases provided by Diagram 1. Following this diagram we consider each one of the configurations of invariant lines in order to determine how many topological phase portraits could be obtained from each one of the configurations.

1: $\mu_0 \neq 0, \widetilde{N} H_{10} < 0 \Rightarrow$ *Config. 4.13.* Since we are in the class of quadratic systems possessing invariant lines of total multiplicity 4 we shall use the classification given in [Schlomiuk & Vulpe, 2008d]. According to this classification the configuration *Config. 4.13* leads to the two phase portraits: *Portrait 4.13(a)* and *Portrait 4.13(b)*. However we have detected an inexactitude concerning these two phase portraits. More exactly we have the next remark.

Remark 4.5. In Table 2 [Schlomiuk & Vulpe, 2008d, page 55] it is claimed that in the case $\widetilde{N} \neq 0$ we have *Portrait 4.13(a)* if $\mathcal{G}_2 < 0$ and *Portrait 4.13(b)* if $\mathcal{G}_2 > 0$. On the other hand in the proof of the Main Theorem (see page 68) we find an opposite affirmation, i.e. we have *Portrait 4.13(a)* if $\mathcal{G}_2 > 0$ and *Portrait 4.13(b)* if $\mathcal{G}_2 < 0$. This is correct and in Table 2 the conditions $\mathcal{G}_2 < 0$ and $\mathcal{G}_2 > 0$ from the 3rd column and 1st and 2nd lines, respectively, must be interchanged.

We denote the phase portraits *Portrait 4.13(b)* and *Portrait 4.13(a)* by *Ric. 1* and *Ric. 2* .

For each branch of the Diagrams 1 to 4 for the configurations of the family $\mathbf{QSL^{2p}}$ leading to a specific configuration we find the phase portraits of the systems having that configuration of invariant lines and complete these diagrams by adding the branch of these various phase portraits. Many of these phase portraits have been encountered before in the papers on $\mathbf{QSL}_{\geq 3}$. Since this paper is the first one that has the complete topological classification of Riccati systems, we denote a phase portrait of the Riccati family by *Ric. i* starting with the two phase portraits *Ric. 1* and *Ric. 2* just introduced here above and of course taking care not to repeat anyone of these phase portraits in this list.

Thus considering Remark 4.5 we get *Ric. 1* if $\mathcal{G}_2 < 0$ and *Ric. 2* if $\mathcal{G}_2 > 0$.

2: $\mu_0 \neq 0, \widetilde{N} H_{10} > 0, H_9 \neq 0$ and either (i) $H_{16} < 0 \Rightarrow$ *Config. 4.9a* or (ii) $H_{16} > 0 \Rightarrow$ *Config. 4.9.* We examine these two cases together because in the paper [Schlomiuk & Vulpe, 2008d] (as well as in [Schlomiuk & Vulpe, 2008]) the configuration *Config. 4.9a* is omitted. This mistake was corrected in [Bujac *et al.*, 2022] (see Remark 6.2 and Lemma 6.1) where a new invariant polynomial H_{16} was defined. This invariant distinguishes these two configurations as it is indicated above. To be more precise we present here jointly one result from [Bujac *et al.*, 2022] (see Lemma 6.1) and one result from [Schlomiuk & Vulpe, 2008d] (see Table 2).

Lemma 4.6. *Assume that for an arbitrary quadratic system* (2) *the conditions* $\eta > 0$, $\theta = H_7 = B_2 = 0$, $\mu_0 B_3 H_4 H_9 \neq 0$ *and* $\widetilde{N} H_{10} > 0$ *hold. Then the configuration of the invariant lines of this system corresponds to Config. 4.9a if* $H_{16} < 0$ *and to Config. 4.9 if* $H_{16} > 0$. *Moreover the phase portrait of this system corresponds to one of the portraits given below if and only if the corresponding set of the conditions hold:*

$$\begin{array}{lcl} \textit{Portrait 4.9(a)} & \Leftrightarrow & \mathcal{G}_2 > 0,\ H_4 > 0,\ \mathcal{G}_3 < 0; \\ \textit{Portrait 4.9(b)} & \Leftrightarrow & \textit{either}\ \ \mathcal{G}_2 > 0,\ H_4 < 0 \\ & & \textit{or}\ \ \mathcal{G}_2 < 0; \\ \textit{Portrait 4.9(c)} & \Leftrightarrow & \mathcal{G}_2 > 0,\ H_4 > 0,\ \mathcal{G}_3 > 0. \end{array}$$

Next we would like to distinguish which of these three phase portraits is generated by the configuration *Config. 4.9a* and which by *Config. 4.9*.

Assume that for an arbitrary quadratic system (2) the conditions provided by Lemma 4.6 hold. Then as it was shown in [Bujac *et al.*, 2022] (see the proof of Lemma 6.1), this system could be brought via an affine transformation and time rescaling to the 2-parameter family of systems

$$\dot{x} = x^2 - 1, \quad \dot{y} = y(y + ax + b). \tag{9}$$

For these systems we calculate

$$\begin{aligned} H_4 =& -48a\big[(a-2)^2 - b^2\big], \\ H_{16} =& 180(b^2 - a^2)\big[(a-2)^2 - b^2\big]^2, \\ \mathcal{G}_2 =& 13824(a-1)(b^2 - a^2), \\ \mathcal{G}_3 =& 288a(a-1)\big[(a-2)^2 - b^2\big]. \end{aligned}$$

Considering these expressions it is not too difficult to prove the following implications:

- The conditions $H_{16} < 0$, $\mathcal{G}_2 > 0$ and $H_4 > 0$ imply $\mathcal{G}_3 > 0$.
- The conditions $H_{16} > 0$ and $\mathcal{G}_2 > 0$ imply $H_4 > 0$ and $\mathcal{G}_3 < 0$.

Therefore taking into account Lemma 4.6 we can state the next remark.

Remark 4.7. **(i)** The configuration *Config. 4.9a* (i.e. $H_{16} < 0$) leads to the phase portrait *Portrait 4.9(b)* if and only if either $\mathcal{G}_2 < 0$, or $\mathcal{G}_2 > 0$ and $H_4 < 0$; and it leads to the phase portrait *Portrait 4.9(c)* if and only if $\mathcal{G}_2 > 0$ and $H_4 > 0$.

(ii) The configuration *Config. 4.9* (i.e. $H_{16} > 0$) leads to the phase portrait *Portrait 4.9(b)* if and only if $\mathcal{G}_2 < 0$ and to the phase portrait *Portrait 4.9(a)* if and only if $\mathcal{G}_2 > 0$.

We denote *Portrait 4.9(b)*, *Portrait 4.9(c)* and *Portrait 4.9(a)* by *Ric. 3*, *Ric. 4* and *Ric. 5*, respectively.

3: $\mu_0 \neq 0, \widetilde{N} H_{10} > 0, H_9 = 0 \ \Rightarrow$ *Config. 4.10*. Considering [Schlomiuk & Vulpe, 2008d] (see Table 2) and taking into account the condition $\widetilde{N} \neq 0$ we obtain that *Config. 4.10* leads to one of the three possible phase portraits, determined by the invariant polynomials H_4 and $\mathcal{G}_3$. More exactly we have the following classification of the corresponding phase portraits:

$$\begin{array}{lcl} \textit{Portrait 4.10(a)} & \Leftrightarrow & H_4 > 0,\ \mathcal{G}_3 > 0; \\ \textit{Portrait 4.10(b)} & \Leftrightarrow & H_4 < 0; \\ \textit{Portrait 4.10(c)} & \Leftrightarrow & H_4 > 0,\ \mathcal{G}_3 < 0. \end{array}$$

We denote *Portrait 4.10(b)*, *Portrait 4.10(c)* and *Portrait 4.10(a)* by *Ric. 6*, *Ric. 7* and *Ric. 8*, respectively.

4: $\mu_0 \neq 0, H_{10} = 0 \Rightarrow$ *Config. 4.22*. Since $\widetilde{N} \neq 0$ according to [Schlomiuk & Vulpe, 2008d] we get *Portrait 4.22(a)* if $H_1 > 0$ and *Portrait 4.22(b)* if $H_1 < 0$. We denote here *Portrait 4.22(b)* by *Ric. 9* and *Portrait 4.22(a)* by *Ric. 10*.

5: $\mu_0 = 0, \mu_2 \neq 0, H_9 \neq 0 \Rightarrow$ *Config. 4.16*. By [Schlomiuk & Vulpe, 2008d] we get *Portrait 4.16(a)* if $\mathcal{G}_2 > 0$ and *Portrait 4.16(b)* if $\mathcal{G}_2 < 0$. We denote *Portrait 4.16(b)* and *Portrait 4.16(a)* by *Ric. 11*, and *Ric. 12*, respectively.

6: $\mu_0 = 0, \mu_2 \neq 0, H_9 = 0 \Rightarrow$ *Config. 4.17*. According to [Schlomiuk & Vulpe, 2008d, Table 2] this configuration leads to a unique phase portrait which we denote by *Ric. 13*.

7: $\mu_0 = 0, \mu_2 = 0 \Rightarrow$ *Config. 4.34*. In this case according to [Schlomiuk & Vulpe, 2008d] (see page 56, Table 2) we could have only two phase portraits: *Portrait 4.34(a)* and *Portrait 4.34(b)*. Moreover it is claimed that the first phase portrait is defined by the condition $H_4 < 0$ and the second one by the condition $H_4 > 0$.

However we have detected an error in the above paper. More precisely the next remark holds.

Remark 4.8. In the article [Schlomiuk & Vulpe, 2008d] in Table 3(a) on page 57 there appear

the phase portraits *Portrait 4.34(a)* with *Portrait 4.34(b)*. In the proof for the invariant conditions for these two phase portraits each one of them appeared with the correct conditions. However in the Table these conditions were interchanged. More exactly, in the case $H_4 > 0$ (respectively $H_4 < 0$) we must have a phase portrait with a separatrix connection (respectively without separatrix connection).

Considering this remark we deduce that in the case $H_4 < 0$ the phase portrait corresponds to *Ric. 2* (which is equivalent to *Portrait 4.34(b)*), whereas in the case $H_4 > 0$ the phase portrait corresponds to *Ric. 1* (which is equivalent to *Portrait 4.34(a)*).

The case $B_3 = 0$. Then by Lemma 3.1 we could have invariant lines in three directions. Moreover according to Diagram 1 the systems in this class possess invariant lines of total multiplicity five. So we shall apply the classification of this family of systems given in [Schlomiuk & Vulpe, 2004]. According to Diagram 1 we have to consider the next 3 possibilities.

1: $\mu_0 \neq 0, H_1 \neq 0 \Rightarrow$ *Config. 5.1.* According to [Schlomiuk & Vulpe, 2008b] (see Diagram 3) this configuration leads to the unique phase portrait given by *Picture 5.1* which is topologically equivalent to *Ric. 3*.

2: $\mu_0 \neq 0, H_1 = 0 \Rightarrow$ *Config. 5.8* By [Schlomiuk & Vulpe, 2008b] we arrive at the unique phase portrait given by *Picture 5.8* which we denote by *Ric. 14*.

3: $\mu_0 = 0 \Rightarrow$ *Config. 5.7.* According to [Schlomiuk & Vulpe, 2008b] we get the unique phase portrait given by *Picture 5.7* ($\simeq$ *Ric. 12*)

4.1(B). The possibility $B_2 \neq 0$.

By Lemma 3.1 systems (8) could possess invariant lines only in the direction $x = 0$ and we examine the corresponding cases provided by Diagram 1.

1: $\mu_0 \neq 0, \widetilde{N} H_{10} < 0$. According to Diagram 1 these conditions lead to *Config. 3.14*. We observe that due to the condition $\mu_0 \neq 0$ by Remark 4.4 at infinity there are one saddle and two nodes.

On the other hand, according to [Sotomayor & Paterlini, 1983] for quadratic systems we have the next lemma.

Lemma 4.9. *If two affine separatrices of a pair of opposite infinite saddles connect, then this separatrix connection is an invariant straight line.*

Therefore by $B_2 \neq 0$ we could not have a separatrix connection and this leads to the unique phase portrait which is topological equivalent to the one given by *Ric. 2*.

Remark 4.10. We point out that some of the phase portraits that we will obtain for the systems with $B_2 \neq 0$ are topologically equivalent to some already obtained for the case $B_2 = 0$. This happens even if the systems with $B_2 \neq 0$ belong to the class $\mathbf{QSL}_3$, whereas the systems with $B_2 = 0$ belong to the class $\mathbf{QSL}_{\geq 4}$. The affine equivalence relation is finer than the topological one. This means that a topological equivalence class is a union of distinct affine equivalence classes. This is basically what occurs here it is then not at all surprising that two portraits from distinct affine equivalence classes are united into a unique larger topological equivalence class

2: $\mu_0 \neq 0, \widetilde{N} H_{10} > 0, \mathbf{D} < 0, H_{15} < 0 \Rightarrow$ *Config. 3.15*. We observe that the phase plane is divided by two parallel real invariant lines in three regions. And for the affine separatrices of the opposite infinite saddles there exists the unique possibility to go to the infinite node located at the intersections of invariant lines (in the corresponding direction). As a result we arrive at the unique phase portrait *Ric. 2*.

3: $\mu_0 \neq 0, \widetilde{N} H_{10} > 0, \mathbf{D} < 0, H_{15} > 0 \Rightarrow$ *Config. 3.16*. This family has four finite singularities: two saddles and two nodes and three elemental infinite singularities: two nodes and one saddle (see Remark 4.4). Similarly to the case of *Config. 3.15* the phase plane of this family is divided by two parallel real invariant lines in three regions. The finite

singularities are located on these lines, more exactly a saddle and a node on each line. Clearly the singular point at infinity common to the two lines is a node. So in each one of the three regions there are two separatrices which may either connect or not.

If there is no separatrix connection, then systems (8) belong to family 10 of the structurally stable quadratic systems modulo limit cycles [Artés *et al.*, 1998]. From the 16 possible phase portraits of this family it is easy to see that only three of them are compatible with the existence of two real parallel invariant lines. More exactly we have the phase portraits presented in Figure 7 as $\mathbb{S}^2_{10,14}$, $\mathbb{S}^2_{10,15}$ and $\mathbb{S}^2_{10,16}$.

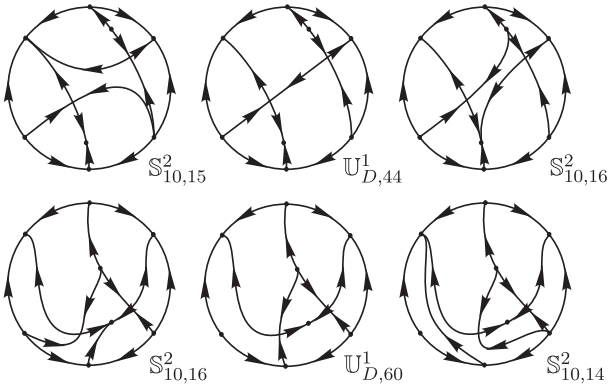

Figure 7. Potential phase portraits generated by *Config. 3.16*

In the case when they have a connection of separatrices then according to [Artés *et al.*, 2018] they must be either the phase portrait $\mathbb{U}^1_{D,44}$ or $\mathbb{U}^1_{D,60}$ (see Figure 7), which bifurcate in the previously mentioned structurally stable systems.

According to [Artés *et al.*, 2018, Lemma 3.5] (see also [Ye *et al.*, 1986]) these two phase portraits force (in this family) the existence of another invariant line which contradicts the condition $B_2 \neq 0$ (see Lemma 3.1).

So *Config. 3.16* leads to three topologically distinct phase portraits: two of them, corresponding to $\mathbb{S}^2_{10,15}$ and $\mathbb{S}^2_{10,14}$ are new and we denote them by *Ric. 15* and *Ric. 16*, respectively. The remaining one which corresponds to $\mathbb{S}^2_{10,16}$ is topologically equivalent to *Ric. 3*.

In order to construct the affine invariant conditions for distinguishing each one of the detected phase portraits we determine first the corresponding canonical form of the Riccati systems possessing *Config. 3.16*.

As it was shown in [Bujac *et al.*, 2022] if for a system (8) the conditions

$$\eta > 0,\ \widetilde{N} \neq 0,\ \mu_0 \neq 0,\ \widetilde{N}H_{10} > 0,\ \mathbf{D} < 0,\ H_{15} > 0$$

hold, then this system possess *Config. 3.16* and via an affine transformation and time rescaling it could be brought to the canonical form (37) from [Bujac *et al.*, 2022], i.e. it belongs to the family of systems

$$\dot{x} = g(x^2-1),\ \dot{y} = b + ex + (g-1)xy + y^2. \tag{10}$$

For these systems calculations yield

$$\begin{aligned}
B_2 =& -648\big[e^2 + b(g-1)^2\big]\times \\
&\big[e^2+(b+g)(1+g)^2\big]x^4 \equiv -648x^4\Phi_1\Phi_2, \\
\mathbf{D} =& -768g^6\big[(g-1)^2 - 4(b+e)\big]\times \\
&\big[(g-1)^2 - 4(b-e)\big] \equiv -768g^6V_1V_2, \\
H_{15} =& 256g^4(1-4b-2g+g^2) \equiv \\
&128(V_1+V_2), \\
\widetilde{N} =& (g^2-1)x^2,\ \ \mu_0 = g^2
\end{aligned} \tag{11}$$

and we observe that the conditions $\mathbf{D} < 0$ and $H_{15} > 0$ imply $V_1 > 0$ and $V_2 > 0$ which in addition with $\mu_0 \neq 0$ guarantee the existence of four finite real distinct singularities. We prove the following lemma.

Lemma 4.11. *For the* 3*-parameter family of systems* (10) *we may assume without loosing the generality that the conditions* $g > 0$ *and* $e > 0$ *hold.*

Proof: Applying the linear transformation $x_1 = -x$, $y_1 = -x+y$ to systems (10) we arrive at the systems

$$\begin{aligned}
\dot{x}_1 =& g_1(x_1^2 - 1), \\
\dot{y}_1 =& b_1 + e_1x_1 + (g_1-1)x_1y_1 + y_1^2
\end{aligned} \tag{12}$$

which have exactly the form (10) but with new parameters

$$g_1 = -g,\ b_1 = b+g,\ e_1 = -e.$$

Thus we may assume in systems (10) $g > 0$. Then keeping the sign of this parameter via the rescaling $(x, y, t) \to (-x, -y, -t)$ we change the sign of the parameter e and this completes the proof of Lemma 4.11. ∎

Next we fix the parameter $g = g_0$ obtaining a family of two parameters b and e. We point out, that due to the conditions (11) the condition $g_0(g_0^2 - 1) \neq 0$ has to hold. However considering Lemma 4.11 it is clear that we could choose $g_0 \in (0, 1) \cup (1, \infty)$ and clearly these two intervals are distinguished by the invariant polynomial $\widetilde{N}$. More exactly we could choose $g_0 \in (0, 1)$ if $\widetilde{N} < 0$ and $g_0 \in (1, \infty)$ if $\widetilde{N} > 0$.

In order to construct the bifurcation diagram for (10) with fixed $g = g_0$, additionally to the invariant polynomials $\mathbf{D}$ and B_2 we consider here two other invariant polynomials: $\mathcal{G}_2$ and H_{16}. For systems (10) we calculate

$$\begin{aligned}\mathcal{G}_2 =& 13824g^2\big[2b(1+g^2)+2e^2+g(g-1)^2\big],\\ H_{16} =& -180g^6\big[4b+(1+g)^2\big]\times\\ &\big[16b^2+16bg-8e^2+(g^2-1)^2\big].\end{aligned}$$

In what follows we investigate the locations in the plane (e, b) and their geometry of the following curves, depending on the parameter g_0:

$$\begin{aligned}
&V_1(b,e,g_0)=0 \Rightarrow\ b=-e+(g_0-1)^2/4; && (\mathcal{V}_1)\\
&V_2(b,e,g_0)=0 \Rightarrow\ b=e+(g_0-1)^2/4; && (\mathcal{V}_2)\\
&\Phi_1(b,e,g_0)=0 \Rightarrow\ b=-\frac{e^2}{(g_0-1)^2}; && (\mathcal{F}_1)\\
&\Phi_2(b,e,g_0)=0 \Rightarrow\ b=-\frac{e^2}{(g_0+1)^2}-g_0; && (\mathcal{F}_2)\\
&\mathcal{G}_2(b,e,g_0)=0 \Rightarrow\ b=-\frac{e^2}{g_0^2+1}-\frac{(g_0-1)^2g_0}{2\,(g_0^2+1)}; && (\mathcal{G}')\\
&H_{16}(b,e,g_0)=0 \Rightarrow \begin{cases} b=-(g_0+1)^2/4; & (\mathcal{H}')\\ 16b^2+16bg_0-8e^2+\\ \quad(g_0^2-1)^2=0. & (\mathcal{H}'')\end{cases}
\end{aligned} \tag{13}$$

Remark 4.12. We observe that for any value of the parameter $g_0 \neq 0, \pm 1$ the curves $(\mathcal{V}_1)$, $(\mathcal{V}_2)$ and $(\mathcal{H}')$ are lines; $(\mathcal{F}_1)$ and $(\mathcal{F}_2)$ are parabolas and the curve $(\mathcal{H}'')$) is a hyperbola.

It is not too difficult to determine that in the domain $\widehat{\mathcal{D}}$ defined by the condition $0 < e \leq -b + (g_0 - 1)^2/4$ (where we have $V_1 \geq 0$ and $V_2 > 0$) there are located only the following four points of intersection of some of the above defined curves:

$E_1\Big(\frac{1}{2}(g_0-1)^2,\ -\frac{1}{4}(g_0-1)^2\Big)$:
intersection of $(\mathcal{V}_1)$, $(\mathcal{F}_1)$, $(\mathcal{G}')$, $(\mathcal{H}'')$;

$E_2\Big(\frac{1}{2}(g_0+1)^2, \frac{1}{4}(1+6g_0+g_0^2)\Big)$:
intersection of $(\mathcal{V}_1)$, $(\mathcal{F}_2)$, $(\mathcal{G}')$, $(\mathcal{H}'')$;

$E_3\Big(\frac{1}{2}(g_0^2-1),\ -\frac{1}{4}(g_0+1)^2\Big)$:
intersection of $(\mathcal{H}')$, $(\mathcal{H}'')$, $(\mathcal{F}_1)$, $(\mathcal{F}_2)$;

$E_4\Big(\frac{1}{2}(g_0^2+1),\ -\frac{1}{4}(g_0+1)^2\Big)$:
intersection of $(\mathcal{V}_1)$, $(\mathcal{H}')$.

We point out that the point E_3 is located in the domain $\widehat{\mathcal{D}}$ for $g_0^2 - 1 > 0$ (i.e. $\widetilde{N} > 0$). In this case the corresponding symmetric point with respect to the axis $e = 0$ is $E_3'\Big(-\frac{1}{2}(g_0^2-1),\ -\frac{1}{4}(g_0+1)^2\Big)$. So in the case $\widetilde{N} < 0$ the point E_3' is located in the domain $\widehat{\mathcal{D}}$. However this does not affect the number and the positions of the intersection points E_i depending on the parameter g_0.

We point out several properties of the curves $(\mathcal{V}_1)$, $(\mathcal{F}_1)$, $(\mathcal{F}_2)$, $(\mathcal{H}')$ and $(\mathcal{H}'')$ as well as of their intersection points.

Lemma 4.13. *For any value of the parameter $g_0 > 0$, $g_0 \neq 1$ the following properties hold:*

(*i*) *The four points E_j $(j = 1, 2, 3, 4)$ are distinct, i.e. $E_j \neq E_k$, $j, k \in \{1, 2, 3, 4\}$, $j \neq k$.*

(*ii*) *The parabolas $(\mathcal{F}_1)$ and $(\mathcal{F}_2)$ are located entirely in the domain $b - (g_0 - 1)^2/4 \leq e \leq -b + (g_0 - 1)^2/4$ and each one of them has a tangent point with the line $(\mathcal{V}_1)$.*

(*iii*) *For $g_0 > 0$ the hyperbola $(\mathcal{H}'')$ is reducible into two intersecting straight lines for two distinct values of g_0: $g_0' \in (0, 1)$ and $g_0'' \in (1, \infty)$.*

Proof: The statement (*i*) follows directly from the comparison of the coordinates of the points

$E_j(e_j, b_j)$ $(j = 1, 2, 3, 4)$. We have

$$e_1 - e_2 = -2g_0, \quad e_1 - e_3 = 1 - g_0, \quad e_1 - e_4 = -g_0,$$
$$e_2 - e_3 = g_0 + 1, \quad e_2 - e_4 = g_0, \quad e_3 - e_4 = -1$$

and evidently due to the conditions $\mu_0 \widetilde{N} \neq 0$ (i.e. $g_0(g_0^2-1) \neq 0$) we have $e_j - e_k \neq 0$, $j, k \in \{1, 2, 3, 4\}$, $j \neq k$. In other words all four mentioned points of intersections are distinct for any value of the parameter g_0 holding the condition $g_0(g_0^2 - 1) \neq 0$.

(ii) Consider now the curves $(\mathcal{F}_1)$ (i.e. $b = -e^2/(g_0 - 1)^2$) and $(\mathcal{F}_2)$ (i.e. $b = -e^2/(g_0 + 1)^2 - g_0$) and taking into account (11) we calculate:

$$\begin{aligned} V_{1,2}(b, e, g_0)\Big|_{(\mathcal{F}_1)} &= \big[(g_0 - 1)^2 - 4(b \pm e)\big]\Big|_{(\mathcal{F}_1)} \\ &= \frac{\big[(g_0 - 1)^2 \mp 2e\big]^2}{(g_0 - 1)^2}; \\ V_{1,2}(b, e, g_0)\Big|_{(\mathcal{F}_2)} &= \big[(g_0 - 1)^2 - 4(b \pm e)\big]\Big|_{(\mathcal{F}_2)} \\ &= \frac{\big[(g_0 + 1)^2 \mp 2e\big]^2}{(g_0 + 1)^2}. \end{aligned}$$

So we obtain that on the parabolas $(\mathcal{F}_1)$ and $(\mathcal{F}_2)$ we have $V_1 \geq 0$ and $V_2 \geq 0$, i.e. these curves are entirely located on the domain $b - (g_0 - 1)^2/4 \leq e \leq -b + (g_0 - 1)^2/4$. Moreover since the curve $(\mathcal{F}_1)$ (respectively $(\mathcal{F}_2)$) for $e > 0$ has the unique point of intersection E_1 (respectively E_2) with the line $(\mathcal{V}_1)$ we deduce that this point is a tangent point of the parabola $(\mathcal{F}_1)$ (respectively $(\mathcal{F}_2)$) with the line $(\mathcal{V}_1)$. This completes the proof of statement (ii) of the lemma.

(iii) Calculating the discriminant $\bar{\Delta}$ of the conic $(\mathcal{H}'')$ (which is a hyperbola) we obtain:

$$\bar{\Delta} = -128\left(g_0^2 - 2g_0 - 1\right)\left(g_0^2 + 2g_0 - 1\right).$$

Therefore for $g_0 > 0$ we have two values $g_0' = \sqrt{2} - 1$ and $g_0'' = \sqrt{2} + 1$ of this parameter for which $\bar{\Delta} = 0$ and hence the hyperbola $(\mathcal{H}'')$ is reducible. We observe that $g_0' \in (0, 1)$ and $g_0'' \in (1, \infty)$. Lemma 4.13 is proved. ∎

Remark 4.14. We point out that the values $g_0 = g_0'$, $g_0 = g_0''$ for which the hyperbola $(\mathcal{H}'')$ becomes reducible are not bifurcation points for the phase portraits. Moreover we could have one of the following possibilities:

- when $(\mathcal{H}'')$ does not intersect the axis $e = 0$ then the same branch of the hyperbola passes through both points E_1 and E_2 (as it is shown in Figure 8);
- when $(\mathcal{H}'')$ intersects the axis $e = 0$ then one branch of the hyperbola passes through E_1 and another one through E_2 (as it is shown in Figure 9);
- when $(\mathcal{H}'')$ is reducible then both its components (i.e. straight lines) intersect at the axis $e = 0$, one line passing through E_1 and another one through E_2.

Considering the fact that the invariant polynomial H_{16} contains as components the line $(\mathcal{H}')$ and the hyperbola $(\mathcal{H}'')$, it is clear that the sign of H_{16} is always negative (respectively positive) in the domains $(\mathcal{A})$ (respectively $(\mathcal{B})$) independently of the position of the branches of the hyperbola (see Figures 8 and 9) or if it splits into two intersecting straight lines..

Taking into account Remarks 4.12 and 4.14 as well as Lemma 4.13 we conclude that in order to detect the affine invariant conditions for the realization of each one of the phase portraits *Ric. 3*, *Ric. 15* and *Ric. 16* it is sufficient to examine the bifurcation diagram in the space (e, b) of the systems (10) with $g = g_0 > 0$ taking only two values of the parameter g_0: one from the interval $(0, 1)$ and another from $(1, \infty)$.

In Figure 8 we have the bifurcation diagram for systems (10) with $g > 1$. As it can be observed directly from this diagram the next remark follows.

Remark 4.15. Assume that for a system (10) the conditions $\mu_0 \neq 0$ and $\widetilde{N} > 0$ hold. Then under one of the conditions listed below we have on its right side the corresponding phase portrait:

$\mathcal{G}_2 \leq 0$	$\Rightarrow$	*Ric. 3*;
$\mathcal{G}_2 > 0,\ B_2 > 0$	$\Rightarrow$	*Ric. 3*;
$\mathcal{G}_2 > 0,\ B_2 < 0,\ H_{16} < 0$	$\Rightarrow$	*Ric. 3*;
$\mathcal{G}_2 > 0,\ B_2 < 0,\ H_{16} > 0$	$\Rightarrow$	*Ric. 16*.

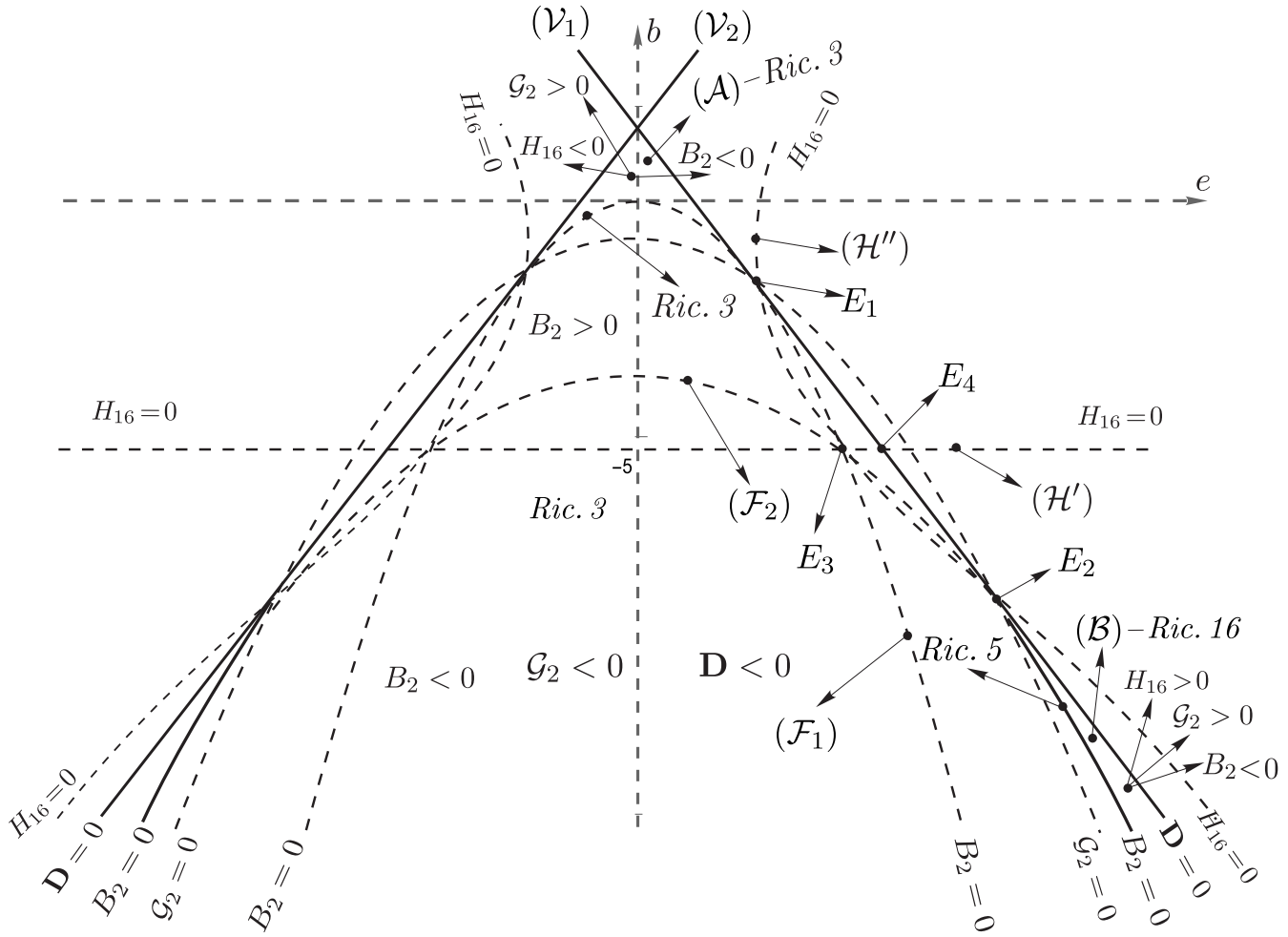

Figure 8. Bifurcation diagram for systems (10) with $g > 1$

In the case $\widetilde{N} < 0$ we take a value of the parameter $g_0 \in (0, 1)$ and we arrive at the bifurcation diagram represented in Figure 9. As it can be detected directly from this diagram the next remark follows.

Remark 4.16. Assume that for a system (10) the conditions $\mu_0 \neq 0$ and $\widetilde{N} < 0$ hold. Then the phase portrait of this system corresponds to the one of the indicated below if the corresponding conditions hold, respectively:

$\mathcal{G}_2 \leq 0 \quad \Rightarrow \quad$ *Ric. 3*;
$\mathcal{G}_2 > 0,\ B_2 > 0 \quad \Rightarrow \quad$ *Ric. 3*;
$\mathcal{G}_2 > 0,\ B_2 < 0,\ H_{16} < 0 \quad \Rightarrow \quad$ *Ric. 15*;
$\mathcal{G}_2 > 0,\ B_2 < 0,\ H_{16} > 0 \quad \Rightarrow \quad$ *Ric. 16*.

We observe that the conditions provided by Remarks 4.15 and 4.16 could be joined and we arrive at the next lemma.

Lemma 4.17. *Assume that for a system* (10) *the condition* $\mu_0 \widetilde{N} \neq 0$ *holds. Then under the conditions given below on the left we obtain the corresponding phase portrait on the right.*

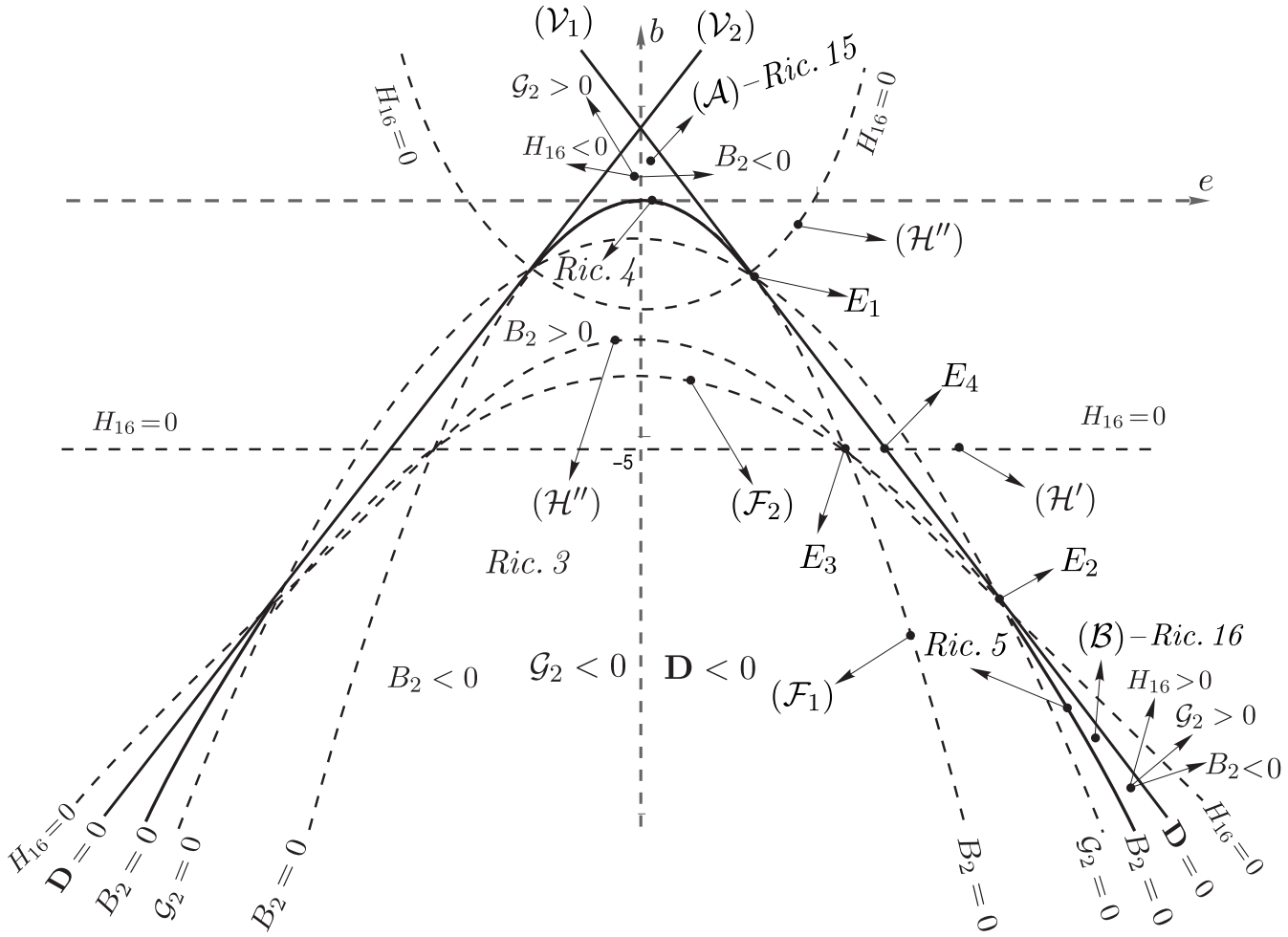

Figure 9. Bifurcation diagram for systems (10) with $0 < g < 1$

$\mathcal{G}_2 \le 0$	$\Rightarrow$	*Ric. 3;*
$\mathcal{G}_2 > 0,\ B_2 > 0$	$\Rightarrow$	*Ric. 3;*
$\mathcal{G}_2 > 0,\ B_2 < 0,\ H_{16} < 0,\ \widetilde{N} < 0$	$\Rightarrow$	*Ric. 15;*
$\mathcal{G}_2 > 0,\ B_2 < 0,\ H_{16} < 0,\ \widetilde{N} > 0$	$\Rightarrow$	*Ric. 3;*
$\mathcal{G}_2 > 0,\ B_2 < 0,\ H_{16} > 0$	$\Rightarrow$	*Ric. 16.*

4: $\mu_0 \neq 0, \widetilde{N} H_{10} > 0, \mathbf{D} > 0 \Rightarrow$ *Config. 3.17.* Considering this configuration it is easy to detect that it leads to the three potential topologically distinct phase portraits: $\mathbb{S}^2_{9,1}$, $\mathbb{U}^1_{I,18}$ and $\mathbb{I}_{9,1}$ (see Figure 10).

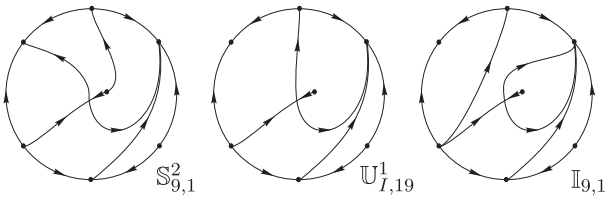

Figure 10. Potential phase portraits generated by *Config. 3.17*

These phase portraits are given in [Artés *et al.*, 2018, Figure 5.133] where it is shown that the last two are not realizable. Thus there remains only the phase portrait $\mathbb{S}^2_{9,1}$ which we denote by *Ric. 17*.

5: $\mu_0 \neq 0, \widetilde{N} H_{10} > 0, \mathbf{D} = 0, H_{15} < 0 \Rightarrow$ *Config. 3.18*. We observe that this configuration is obtained from *Config. 3.17* by coalescing the two singularities (a node and a saddle) on the invariant line. As a consequence by continuity we obtain the unique phase portrait which we denote by *Ric. 18*.

6: $\mu_0 \neq 0, \widetilde{N} H_{10} > 0, \mathbf{D} = 0, H_{15} > 0 \Rightarrow$ *Config. 3.19*. It is evident that this configuration could be obtained from *Config. 3.16* by coalescing the two singularities (a node and a saddle) on one of the invariant lines. We recall that *Config. 3.16* leads to the phase portraits *Ric. 3*, *Ric. 15* and *Ric. 16*. From *Ric. 3* as well as from *Ric. 15* (due to the symmetry that they have) only one phase portrait is possible to obtain from each of them and they are respectively *Ric. 6* and a new phase portrait which we denote by *Ric. 19*.

However in *Ric. 16* we have 2 possibilities to produce the coalescence, but from [Artés *et al.*, 2018] if follows that only one is realizable ($\mathbb{U}^1_{A,52}$) which is denoted here by *Ric. 20*.

We point out that the conditions for distinguishing these three phase portraits can be obtained from Lemma 4.17 and Figures 8 and 9 because the bifurcation surface $\mathbf{D} = 0$ borders the generic regions where *Config. 3.16* is given.

On the other hand for systems (10) for $\mathbf{D} = 0$ (we can take $V_1 = 0$ due to $e > 0$) we have $b = \frac{1}{4}\left[(g-1)^2 - 4e\right]$ and this gives us

$$B_2 = -\frac{81}{2}\left[(g-1)^2 + 2e\right]^2\left[(g-1)^2 - 2e\right]^2 x^4 < 0.$$

Therefore considering Lemma 4.17 and Figures 8 and 9 the next lemma follows.

Lemma 4.18. *Assume that for a system* (10) *the conditions* $\mu_0 \widetilde{N} \neq 0$ *and* $\mathbf{D} = 0$ *hold. Then under the conditions given below on the left we obtain the corresponding phase portrait on the right.*

$$\begin{array}{lcl}
\mathcal{G}_2 \leq 0 & \Rightarrow & \textit{Ric. 6;} \\
\mathcal{G}_2 > 0,\ H_{16} < 0,\ \widetilde{N} < 0 & \Rightarrow & \textit{Ric. 19;} \\
\mathcal{G}_2 > 0,\ H_{16} < 0,\ \widetilde{N} > 0 & \Rightarrow & \textit{Ric. 6;} \\
\mathcal{G}_2 > 0,\ H_{16} > 0 & \Rightarrow & \textit{Ric. 20.}
\end{array}$$

7: $\mu_0 \neq 0, \widetilde{N} H_{10} > 0, \mathbf{D} = 0, H_{15} = 0 \Rightarrow$ *Config. 3.20*. We observe that this configuration could be obtained from *Config. 3.19* by coalescing the elemental singularities (a node and a saddle). Then from *Ric. 19* and *Ric. 6* we produce new phase portraits which we denote respectively by *Ric. 21* and *Ric. 22*. These pictures are topologically equivalent to the phase portraits given in Table 9 on page 37 in [Artés *et al.*, 2020b] under the names AA^{snsn}_{19} and AA^{snsn}_{20} (see Remark 4.19 below).

However it is not possible to do the same from *Ric. 20* (as from *Ric. 19* and *Ric. 6*) because as we have shown earlier for *Config. 3.19* only one of the couples of elemental singularities from *Ric. 16* can coalesce. As a result we arrive at two topologically distinct phase portraits in the case of *Config. 3.20*.

We determine that the conditions $\mathbf{D} = H_{16} = 0$ define the point of intersection of the lines $\mathcal{V}_1$ and $\mathcal{V}_2$ on both diagrams in Figures 8 and 9. We observe that in the interior of the region $(\mathcal{A})$ in Figure 8 corresponding to the condition $\widetilde{N} > 0$ we have *Ric. 3* and on the line $\mathcal{V}_1$ (border of $(\mathcal{A})$) we have *Ric. 6*. Therefore as it was mentioned above we get *Ric. 22* at the point of intersection of the lines $\mathcal{V}_1$ and $\mathcal{V}_2$.

Similarly if $\widetilde{N} < 0$ considering Figure 9 we have respectively *Ric. 15*, *Ric. 19* and *Ric. 21*.

Thus we get *Ric. 21* for $\widetilde{N} < 0$ and *Ric. 22* for $\widetilde{N} > 0$.

Remark 4.19. A final enumeration of phase portraits determined in the article [Artés *et al.*, 2020b] is given in Table 9. However there exists a gap in this enumeration namely the notation $\mathbb{U}^2_{AA,32}$ is skipped. So in the last three cases from the Table 9 it must be $\mathbb{U}^2_{AA,32}$, $\mathbb{U}^2_{AA,33}$ and $\mathbb{U}^2_{AA,34}$ instead of the notations $\mathbb{U}^2_{AA,33}$, $\mathbb{U}^2_{AA,34}$ and $\mathbb{U}^2_{AA,35}$, respectively.

8: $\mu_0 \neq 0, H_{10} = 0, \mathbf{R} < 0 \Rightarrow$ *Config. 3.21*. Since we do not have real finite singularities and

there is an invariant (double) straight line it is clear that we get a unique phase portrait which is topologically equivalent to *Ric. 2*.

9: $\mu_0 \neq 0, H_{10} = 0, \mathbf{R} > 0 \Rightarrow$ *Config. 3.22*. We have two saddle-nodes on the double invariant line. It is clear that a perturbation of this configuration could lead to *Config. 3.16* whose singularities are saddles and nodes in a convex quadrilateral. Then when we pass from *Config. 3.16* to *Config. 3.22* the parabolic sectors of the saddle–nodes must be on the opposite sides of the semi-planes defined by the double invariant line. Therefore there are two possibilities: (a) the separatrices (with zero eigenvalue) of the saddle-nodes have the same stability (seen from their respective saddle-node) as the separatrix of the infinite saddle (seen from the infinite saddle) or (b) they have opposite stabilities(see Figure 11)

In the first case both separatrices (finite and infinite) in every semi-plane must come/go from/to the infinite node $N_3[0:1:0]$. However this phase portrait (see Figure 11 (a_1)) is impossible because by a perturbation, it leads to the phase portrait $\mathbb{I}_{10,20}$ from [Artés *et al.*, 2018] (see Figure 11 (a_2)) which was proved to be impossible in [Artés *et al.*, 1998].

In the case (b) we have three generic potential phase portraits (b_1)–(b_3) given in Figure 11 and two that have a separatrix connection. The cases (b_1) and (b_2) are realizable whereas (b_3) is impossible because a perturbation of it may lead to the phase portrait (a_2) ($\simeq \mathbb{I}_{10,20}$ from [Artés *et al.*, 1998]) which is impossible as it is mentioned above. Moreover the phase portrait (b_1) is topologically equivalent to *Ric. 10* whereas (b_2) is new and we denote it by *Ric. 23*.

Next we claim that if there is any separatrix connection then either this connection is part of an invariant straight line or the phase portrait is impossible. Indeed there are two potential ways to produce a separatrix connection. One leads to a phase portrait topologically equivalent to *Ric. 9* and by Lemma 3.5 of [Artés *et al.*, 2018], this separatrix connection must be part of an invariant straight line which contradicts $B_2 \neq 0$. We observe

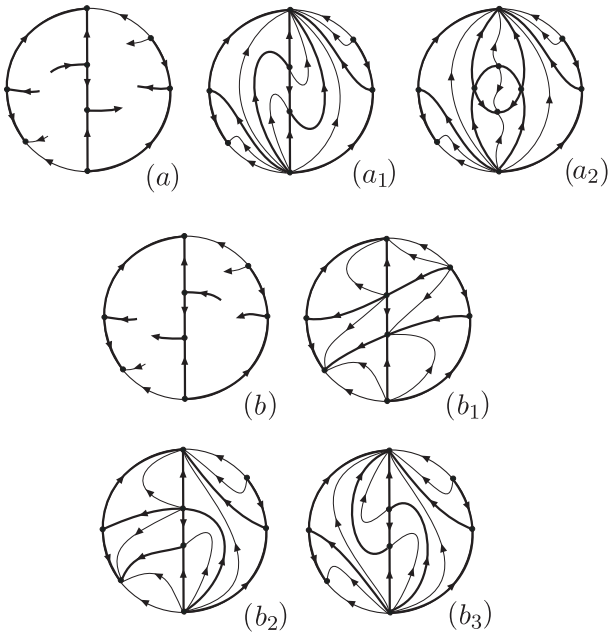

Figure 11. Generic potential phase portraits generated by *Config. 3.22*

that *Ric. 9* may bifurcate in *Ric. 10* or *Ric. 23*. The phase portrait with the second potential connection would bifurcate into *Ric. 23* or the phase portrait (b_3) of Figure 11. Since the latter has already been proved to be impossible we deduce that the connection is also impossible.

As it was shown in [Bujac *et al.*, 2022] if for a system (8) the conditions

$$\eta > 0,\ \widetilde{N} \neq 0,\ \mu_0 \neq 0,\ H_{10} = 0, \mathbf{R} > 0$$

hold then this system possesses *Config. 3.22* and via an affine transformation and time rescaling it could be brought to the canonical form (39) from [Bujac *et al.*, 2022], i.e. it belongs to the family of systems

$$\dot{x} = gx^2, \quad \dot{y} = b + ex + (g-1)xy + y^2.$$

For these systems we have $\mu_0 = g^2,\ \mathbf{R} = -16bg^4x^2$ and due to $\mu_0 \neq 0$ the condition $\mathbf{R} > 0$ implies $b < 0$. Then we may assume $b = -1$ due to the rescaling $(x, y, t) \mapsto (\sqrt{-b}\,x, \sqrt{-b}\,y, t/\sqrt{-b})$. Then we arrive at the 2-parameter family of systems

$$\dot{x} = gx^2, \quad \dot{y} = -1 + ex + (g-1)xy + y^2 \qquad (14)$$

for which we may assume $g > 0$ and $e \geq 0$ because this can be achieved via the transformation $(x, y, t) \to \xi(-x, y - x, t)$, where $\xi = -\text{sign}\,(e)$ (see also the proof of Lemma 4.11).

Next we construct the bifurcation diagram in the space (e, g) of systems (14) (see Figure 12).

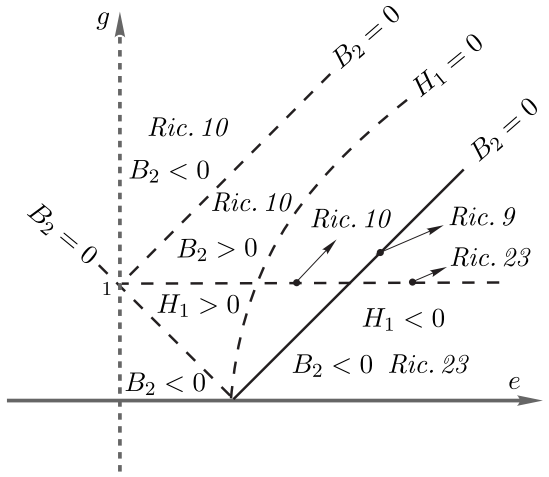

Figure 12. Bifurcation diagram of systems (14) for $g \neq 0$

The following Remark follows directly from this diagram.

Remark 4.20. The phase portraits of systems (14) with $\mu_0 \widetilde{N} \neq 0$ correspond to the ones indicated below if the corresponding conditions on the left hold, respectively:

$B_2 > 0 \quad \Rightarrow \quad$ *Ric. 10*;
$B_2 < 0,\ H_1 < 0 \quad \Rightarrow \quad$ *Ric. 23*;
$B_2 < 0,\ H_1 > 0 \quad \Rightarrow \quad$ *Ric. 10.*

10: $\mu_0 \neq 0, H_{10} = 0, \mathbf{R} = 0 \Rightarrow$ *Config.3.23.* It is not so difficult to determine that the unique finite singularity of multiplicity four is a nilpotent saddle-node. More precisely two separatrices of this singular point form the invariant line $x = 0$ and the third one lies on one of the semi-planes divided by invariant line. As a result we arrive at the unique phase portrait which is equivalent to *Ric. 18.*

11: $\mu_0 = 0, \mu_2 \neq 0, \mathbf{D} < 0 \Rightarrow$ *Config. 3.24.* According to [Bujac *et al.*, 2022] a system (8) possessing this configuration could be brought via an affine transformation and time rescaling to the canonical form (41) from [Bujac *et al.*, 2022], i.e. we consider the family of systems

$$\dot{x} = a + x, \quad \dot{y} = b - xy + y^2. \tag{15}$$

We observe that for $B_2 = -648b(1 - a + b)x^4 = 0$ the above systems gain an invariant straight line: $y = 0$ if $b = 0$ and $y = x + 1$ if $b = a - 1$. In the case $B_2 = 0$ we obtain *Config. 4.16* and as it was shown earlier (see page 36, p. **5:**) this configuration generates two phase portraits: *Ric. 11* if $\mathcal{G}_2 < 0$ and *Ric. 12* if $\mathcal{G}_2 > 0$.

Since *Ric. 11* contains no separatrix connection it is clear that after breaking the non-vertical invariant line then we get the same phase portrait *Ric. 11.*

On the other hand *Ric. 12* contains a separatrix connection (which is part of the invariant line) and after breaking this connection we get either *Ric. 11* or *Ric. 24.* In order to determine the conditions for distinguishing these two phase portraits we construct the bifurcation diagram in the parameter space (a, b) of systems (15) (see Figure 13). The next remark follows directly from this diagram.

Remark 4.21. A phase portrait of systems (15) with $\mathbf{D} < 0$ under one of the conditions indicated below on the left side is the portrait indicated on the right side.

$\mathcal{G}_2 \leq 0 \quad \Rightarrow \quad$ *Ric. 11*;
$\mathcal{G}_2 > 0, B_2 < 0 \quad \Rightarrow \quad$ *Ric. 24*;
$\mathcal{G}_2 > 0, B_2 > 0 \quad \Rightarrow \quad$ *Ric. 11.*

12: $\mu_0 = 0, \mu_2 \neq 0, \mathbf{D} > 0 \Rightarrow$ *Config. 3.25.* According to this configuration we do not have real finite singularities and moreover at infinity we have the node $N_3[0 : 1 : 0]$ and two double singularities which are saddle-nodes. We observe that we could not have the two finite separatrices of the infinite saddle-nodes on the same semi-plane with respect to invariant line because on the other semi-plane there would be two sources of orbits and two sinks without any separatrix. However this contradicts Lemma 4.7 from [Artés *et al.*, 1998]. As a result we arrive at a single phase portrait which we denote by *Ric. 25.*

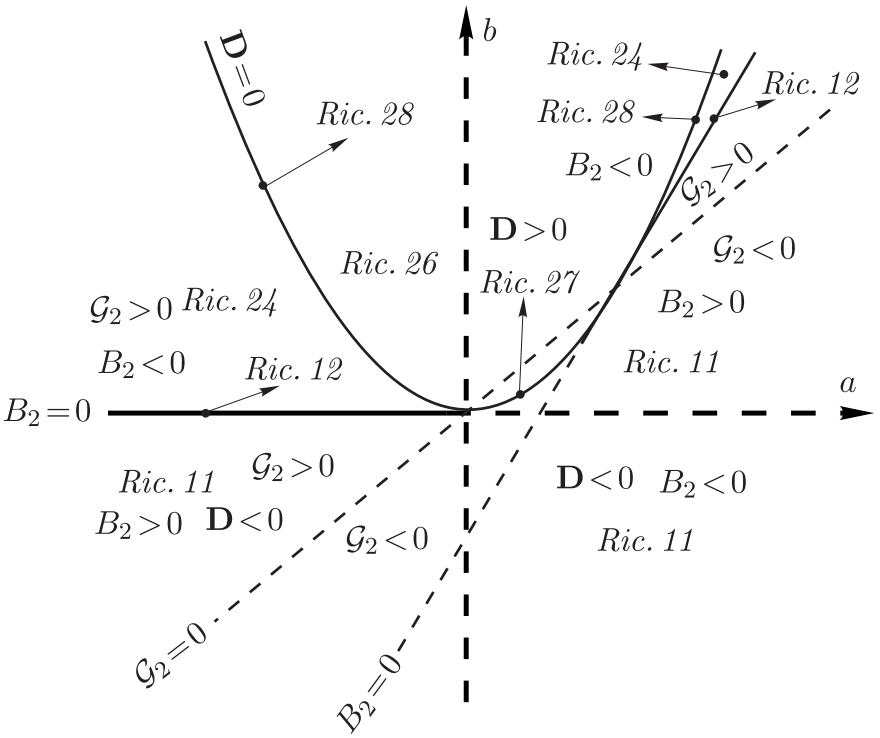

Figure 13. Bifurcation diagram of systems (15).

13: $\mu_0 = 0, \mu_2 \neq 0, \mathbf{D} = 0 \Rightarrow$ *Config. 3.26.* This configuration is related with *Config. 3.24* which generates two phase portraits *Ric. 11* and *Ric. 24*. So if we force the coalescence of the two elemental finite singular points along the invariant line in *Ric. 11* we obtain a new phase portrait which we denote by *Ric. 26*. If we do the the same for *Ric. 24* we obtain again a new phase portrait which we denote by *Ric. 27*.

We point out that this information can be obtained from the bifurcation diagram in Figure 13 consideing the parabola $\mathbf{D} = -48(a^2 - 4b) = 0$. So we observe that we get the phase portrait *Ric. 26* if $\mathcal{G}_2 < 0$ and *Ric. 27* if $\mathcal{G}_2 > 0$.

14: $\mu_0 = 0, \mu_2 = 0 \Rightarrow$ *Config. 3.27.* In this family we have no finite real singular points and the line at infinity is triple. Moreover we have two triple semi-elemental singularities which are a saddle and a node in the vicinity of which the behavior of the trajectories is the same as around elemental singularities. Therefore as in the case of the configuration *Config. 3.14* we arrive at the same phase portrait *Ric. 2.*

4.2. The subcase $\widetilde{N} = 0$

According to Lemma 3.7 in this case a quadratic system with $\theta_3 \neq 0$ could not belong to the class $\mathbf{QSL^{2p}}$ and hence, it could neither belong to the family $\mathbf{QS}_{Ric}$.

On the other hand according to [Bujac *et al.*, 2022] for $\theta_3 = 0$ this system could be brought via an affine transformation and time rescaling to the form (14) (from [Bujac *et al.*, 2022]), i.e. we arrive at the subfamily of the Riccati systems

$$\dot{x} = a + x^2, \quad \dot{y} = b + ex + y^2. \tag{16}$$

We observe that for these systems $\mu_0 = 1 > 0$ and since $\eta > 0$ we conclude that Remark 4.4 also holds for the above systems. So systems (16) possess at infinity one saddle and two nodes, all elemental.

According to Diagram 1 we examine again two possibilities: $B_2 = 0$ and $B_2 \neq 0$.

4.2(A). The possibility $B_2 = 0$.

Following Diagram 1 we examine the next cases considering the topological classifications of systems in the families $\boldsymbol{QSL_{\geq 4}}$ given in the articles [Schlomiuk & Vulpe, 2008b] and [Schlomiuk & Vulpe, 2008d].

1: $H_4 \neq 0, H_8 < 0 \Rightarrow$ *Config. 4.13.* Since the condition $\widetilde{N} = 0$ holds, according to [Schlomiuk & Vulpe, 2008d] (see Table 2) we get the unique phase portrait *Portrait 4.13(b)* which is topologically equivalent to *Ric. 1.*

2: $H_4 \neq 0, H_8 > 0, H_9 \neq 0$ and either (i) $H_{16} < 0 \Rightarrow$ *Config. 4.9a* or (ii) $H_{16} > 0 \Rightarrow$ *Config. 4.9.* We examine these two cases together due to the inexactitude in [Schlomiuk & Vulpe, 2008d] (as well as in [Schlomiuk & Vulpe, 2008]) concerning the configuration *Config. 4.9* (see Lemma 4.6). As it was shown earlier in the case $\widetilde{N} \neq 0$ (see Remark 4.7) we distinguished which of the phase portraits *Portrait 4.9(a)*, *Portrait 4.9(b)* and *Portrait 4.9(c)* are generated by *Config. 4.9a* and which by *Config.4.9.*

Then we have to do the same in the case $\widetilde{N} = 0$. First of all we give here the next lemma which is analogous to Lemma 4.6 and whose proof follows directly from [Bujac *et al.*, 2022] (see Lemma 6.2) and from [Schlomiuk & Vulpe, 2008d] (see Table 2).

Lemma 4.22. *Assume that for an arbitrary quadratic system the conditions $\eta > 0$, $\theta = H_7 = B_2 = 0$, $\mu_0 B_3 H_4 H_9 \neq 0$, $\widetilde{N} = 0$ and $H_8 > 0$ hold. Then the configuration of the invariant lines of this system corresponds to Config. 4.9a if $H_{16} < 0$ and to Config. 4.9 if $H_{16} > 0$. Moreover the phase portrait of this system corresponds to one of the portraits given below if and only if the corresponding set of the conditions hold, respectively:*

$$\begin{aligned}
&\textit{Portrait 4.9(a)} \Leftrightarrow \quad \mathcal{G}_2 > 0,\ H_4 > 0,\ \mathcal{G}_3 < 0;\\
&\textit{Portrait 4.9(b)} \Leftrightarrow \quad \textit{either}\ \ \mathcal{G}_2 > 0,\ H_4 < 0\\
&\qquad\qquad\qquad\quad\ \ \textit{or}\ \ \mathcal{G}_2 < 0;\\
&\textit{Portrait 4.9(c)} \Leftrightarrow \quad \mathcal{G}_2 > 0,\ H_4 > 0,\ \mathcal{G}_3 > 0.
\end{aligned}$$

Next we would like to distinguish which of these three phase portraits is generated by the configuration *Config. 4.9a* and which by *Config. 4.9.*

Assume that for an arbitrary quadratic system (2) the conditions provided by Lemma 4.22 hold. Then as it was shown in [Bujac *et al.*, 2022] (see the proof of Lemma 6.2), this system could be brought via an affine transformation and time rescaling to the 1-parameter family of systems

$$\dot{x} = x^2 - 1, \quad \dot{y} = -1 - e^2/4 + ex + y^2. \tag{17}$$

For these systems we calculate

$$\begin{aligned}
H_4 =& 96e^2, \quad H_{16} = 180(-2+e)e^4(2+e),\\
\mathcal{G}_2 =& 13824(-2+e)(2+e), \quad \mathcal{G}_3 = -576e^2.
\end{aligned}$$

Since for the above systems the condition $H_4 \neq 0$ holds we obtain $H_4 > 0$, $\mathcal{G}_3 < 0$ and $\operatorname{sign}(\mathcal{G}_2) = \operatorname{sign}(H_{16})$. Therefore considering Lemma 4.22 we evidently arrive at the next remark.

Remark 4.23. If for a quadratic system the conditions provided by Lemma 4.22 hold then this system possesses the phase portrait *Portrait 4.9(b)* (i.e. *Ric. 3*) if $H_{16} < 0$ and *Portrait 4.9(a)* (i.e. *Ric. 5*) if $H_{16} > 0$.

Observation 4.1. *According to the above remark we conclude that in the case $\widetilde{N} = 0$ the phase portrait Portrait 4.9(c) is not realizable.*

3: $H_4 \neq 0, H_8 > 0, H_9 = 0 \Rightarrow$ *Config. 4.10.* According to [Schlomiuk & Vulpe, 2008d] (see Table 2) due to the condition $\widetilde{N} = 0$ we get the unique phase portrait *Portrait 4.10(c)* ($\simeq$ *Ric. 7*).

4: $H_4 \neq 0, H_8 = 0 \Rightarrow$ *Config. 4.22.* By [Schlomiuk & Vulpe, 2008d, Table 2] $\Rightarrow$ *Portrait 4.22(b)* ($\simeq$ *Ric. 9*).

5: $H_4 = 0, B_3 \neq 0, H_5 < 0 \Rightarrow$ *Config. 5.4.* By [Schlomiuk & Vulpe, 2008b, Diagram 3] $\Rightarrow$ *Picture 5.4* ($\simeq$ *Ric. 2*).

6: $H_4 = 0, B_3 \neq 0, H_5 > 0, H_1 < 0 \Rightarrow$ *Config. 5.5.* By [Schlomiuk & Vulpe, 2008b, Diagram 3] $\Rightarrow$ *Picture 5.5* ($\simeq$ *Ric. 2*).

7: $H_4 = 0, B_3 \neq 0, H_5 > 0, H_1 > 0 \Rightarrow$ *Config. 5.3.* By [Schlomiuk & Vulpe, 2008b, Diagram 3] $\Rightarrow$ *Picture 5.3* ($\simeq$ *Ric. 3*).

8: $H_4 = 0, B_3 \neq 0, H_5 = 0, H_1 < 0 \Rightarrow$ *Config. 5.16.* By [Schlomiuk & Vulpe, 2008b, Diagram 3] $\Rightarrow$ *Picture 5.16* ($\simeq$ *Ric. 2*).

9: $H_4 = 0, B_3 \neq 0, H_5 = 0, H_1 > 0 \Rightarrow$ *Config. 5.12.* By [Schlomiuk & Vulpe, 2008b, Diagram 3] $\Rightarrow$ *Picture 5.12* ($\simeq$ *Ric. 10*).

10: $H_4 = 0, B_3 = 0, H_1 < 0 \Rightarrow$ *Config. 6.2.* By [Schlomiuk & Vulpe, 2008b, Diagram 1] $\Rightarrow$ *Picture 6.2* ($\simeq$ *Ric. 1*).

11: $H_4 = 0, B_3 = 0, H_1 > 0 \Rightarrow$ *Config. 6.1.* By [Schlomiuk & Vulpe, 2008b, Diagram 1] $\Rightarrow$ *Picture 6.1* ($\simeq$ *Ric. 3*).

12: $H_4 = 0, B_3 = 0, H_1 = 0 \Rightarrow$ *Config. 6.5.* By [Schlomiuk & Vulpe, 2008b, Diagram 1] $\Rightarrow$ *Picture 6.5* ($\simeq$ *Ric. 14*).

4.2(B). The possibility $B_2 \neq 0$.

By Lemma 3.1 systems (16) could possess invariant lines only in the direction $x = 0$.

In what follows we consider one by one all the configurations provided by Diagram 1 and we determine the corresponding phase portraits.

1: $H_8 < 0 \Rightarrow$ *Config. 3.14.* As it was shown in the case $\widetilde{N} \neq 0$ this configuration leads to the unique phase portrait *Ric. 2.*

2: $H_8 > 0, \mathbf{D} < 0, H_{15} < 0 \Rightarrow$ *Config. 3.15.* We have exactly the same situation as in the previous case and so we arrive at the same phase portrait *Ric. 2.*

3: $H_8 > 0, \mathbf{D} < 0, H_{15} > 0 \Rightarrow$ *Config. 3.16.* Since for systems (16) we have

$$H_8 = -3456ae^2, \quad H_{15} = 1024ab,$$
$$B_2 = -648e^2(-4a + 4b + e^2)x^4$$

the conditions $B_2 \neq 0$, $H_8 > 0$ and $H_{15} > 0$ imply $e \neq 0$, $a < 0$ and $b < 0$. Therefore via the rescaling $(x, y, t) \mapsto (\sqrt{-a}\,x, \sqrt{-a}\,y, t/\sqrt{-a})$ we may assume $a = -1$ and we get the 2-parameter family of systems

$$\dot{x} = x^2 - 1, \quad \dot{y} = b + ex + y^2. \tag{18}$$

For these systems we calculate

$$H_{15} = -1024b > 0, \ B_2 = -648e^2(4+4b+e^2)x^4 \neq 0,$$
$$\mathbf{D} = -12288(b-e)(b+e) < 0, \ \mathcal{G}_2 = 27648(2b+e^2).$$

Taking into account the curves defined by the equations $B_2 = 0$, $\mathbf{D} = 0$ and $\mathcal{G}_2 = 0$ we arrive at the bifurcation diagram for the phase portraits of systems (18) with the conditions $H_{15} > 0$ and $\mathbf{D} < 0$ (see Figure 14).

From this diagram it follows that under the provided conditions we get the phase portrait *Ric. 3* if $\mathcal{G}_2 \leq 0$. If $\mathcal{G}_2 > 0$ then we obtain *Ric. 15* for $B_2 < 0$ and *Ric. 3* for $B_2 > 0$.

4: $H_8 > 0, \mathbf{D} > 0 \Rightarrow$ *Config. 3.17.* It was proved earlier (see page 42) that this configuration leads to the unique phase portrait *Ric. 17.*

5: $H_8 > 0, \mathbf{D} = 0, H_{15} < 0 \Rightarrow$ *Config. 3.18.* As it was shown earlier (see page 43) *Config. 3.18* leads to the unique phase portrait *Ric. 18.*

6: $H_8 > 0, \mathbf{D} = 0, H_{15} > 0 \Rightarrow$ *Config. 3.19.* We examined this configuration earlier (see page 43) and have shown that this configuration could only lead to the two phase porraits: *Ric. 19* and *Ric. 6.* More exactly, by coalescing the two singularities (a node and a saddle) on one of the invariant lines (i.e. when $\mathbf{D} \to 0$) from *Ric. 15* we obtain *Ric. 19*, whereas from *Ric. 3* we obtain *Ric. 6.*

Therefore considering diagram in Figure 14 we conclude that the phase portrait corresponds to *Ric. 19* for $\mathcal{G}_2 < 0$ and *Ric. 6* for $\mathcal{G}_2 > 0$.

7: $H_8 = 0, \mathbf{R} < 0 \Rightarrow$ *Config. 3.21.* This configurations was investigated earlier in the case $\widetilde{N} \neq 0$ where it was shown the existence of the unique phase portrait *Ric. 2* which is also realizable for $\widetilde{N} = 0$.

8: $H_8 = 0, \mathbf{R} > 0 \Rightarrow$ *Config. 3.22.* The condition $H_8 = -3456ae^2 = 0$ due to $B_2 \neq 0$ (i.e. $e \neq 0$) gives us $a = 0$ for systems (16) and then $\mathbf{R} = -16bx^2 > 0$ implies $b < 0$. Then we may assume $b = -1$ due to the rescaling $(x, y, t) \mapsto (\sqrt{-b}\,x, \sqrt{-b}\,y, t/\sqrt{-b})$ and we observe that in this case we get a subfamily of systems (14) defined by the condition $g = 1$.

So from the bifurcation diagram of systems (14) given in Figure 12, for systems (16) we obtain *Ric. 23* if $B_2 < 0$ and *Ric. 10* if $B_2 > 0$.

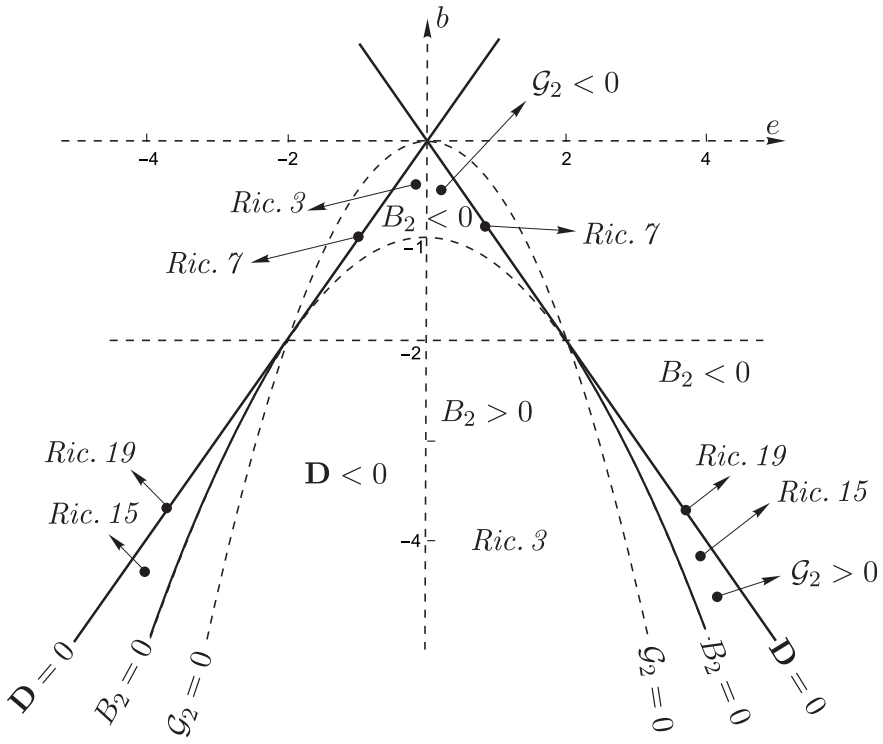

Figure 14. Bifurcation diagram for systems (18) with $b < 0$ and $b^2 - e^2 > 0$

9: $H_8 = 0, \mathbf{R} = 0 \Rightarrow$ *Config. 3.23*. As in the generic case $\widetilde{N} \neq 0$ examined before we get the unique phase portrait *Ric. 18*.

Acknowledgments. The work of the first and second authors is partially supported by the Agencia Estatal de Investigación grant PID2019-104658GB-I00, the H2020 European Research Council grant MSCA-RISE-2017-777911 and the AGAUR (Generalitat de Catalunya) grant 2021-SGR 00113. The second author also is partially supported by the Acadèmia de Ciències i Arts de Barcelona. The work of the third and the fourth authors are partially supported by the grants: NSERC Grants No. RN000355 and No. RN001102; the fourth author is also partially supported by the NARD grant No. 21.70105.31 ȘD.

References

J.C. Artés, B. Grunbaum and J. Llibre [1998] On the number of invariant straight lines for polynomial differential systems, Pacific J. of Math. 184, 207–230.

J.C. Artés, R. Kooij & J. Llibre [1998b] "Structurally stable quadratic vector fields," Memoires Amer. Math. Soc., **134 (639)**, 108 pp.

J.C. Artés, J. Llibre, D. Schlomiuk and N. Vulpe [2015] From topological to geometric equivalence in the classification of singularities at infinity for quadratic vector fields, Rocky Mountain J. of Math. **45**, 29–113.

J.C. Artés, J. Llibre, D. Schlomiuk and N. Vulpe [2023] Riccati quadratic differential systems, Preprint **1**, 82 pp.

J. C. Artés, J. Llibre, D. Schlomiuk and N. I. Vulpe [2020] Global topological configurations of singularities for the whole family of quadratic differential systems, Qual. Theory Dyn. Syst. 19 no. 1, Paper No. 51, 32 pp.

J. C. Artés, J. Llibre and A. C. Rezende [2018] *Structurally unstable quadratic vector fields of codimension one*, Birkhäuser/Springer, Cham, vi+267 pp.

J.C. Artés, J. Llibre and A.C. Rezende [2018b] *Structurally unstable quadratic vector fields of codimension one*, Birkh¨auser/Springer, Cham, vi+267 pp.

J. C. Artés, R. Oliveira and A. C. Rezende [2020b] Structurally unstable quadratic fields of codimension two: families possessing either a cusp point or two finite saddle nodes, J. Dynam. Differential Equations, DOI: https://doi.org/10.1007/s10884-020-09871-2, 43 pp.

J.C. Artés, J. Llibre, D. Schlomiuk and N. Vulpe [2021] *Geometric configurations of singularities of planar polynomial differential systems* [*A global classification in the quadratic case*]. Birkhäuser/Springer, Cham, ©2021. xii+699 pp. ISBN: 978-3-030-50569-1; 978-3-030-50570-7

V.A. Baltag and N.I. Vulpe [1997] Total multiplicity of all finite critical points of the polynomial differential system, Differ. Equ. Dyn. Syst. **5**, 455–471.

C. Bujac, D. Schlomiuk and N. Vulpe [2022] On families $\mathbf{QSL}_{\geq 2}$ of quadratic systems with invariant lines of total multiplicity at least 2, Qual. Theory Dyn. Syst. 21, no. 4, Paper No. 133, 68 pp.

J.H. Grace and A. Young [1941] *The algebra of invariants*, New York, Stechert.

M. Jungers [2017] Historical perspectives of the Riccati equations, ScienceDirect, www.sciencedirect.com, IFAC PapersOnLine 50-1, 9535–9546.

J. Llibre, D. Schlomiuk [2004] The geometry of quadratic differential systems with a weak focus of third order, Canad. J. Math. 56, no. 2, 310—343.

J. Llibre, B.D. Lopes, P.R. da Silva [2021] Bifurcations of the Riccati Quadratic Polynomial Differential Systems, International Journal of Bifurcation and Chaos, Vol. 31, No. 6, 2150094 (13 pages).

P.J. Olver [1999] *Classical Invariant Theory*, London Mathematical Society student texts: **44**, Cambridge University Press.

D. Schlomiuk and N. Vulpe [2004] Planar Quadratic Vector Fields with invariant lines of total Multiplicity at least Five, Qual. Theory Dyn. Syst., **5**, no. 1, 135–194.

D. Schlomiuk and N.I. Vulpe [2005] Geometry of quadratic differential systems in the neighborhood of infinity, J. Differential Equations, **215**, no. 2, 357–400.

D. Schlomiuk and N. Vulpe [2008] Planar quadratic differential systems with invariant straight lines of total multiplicity four, Nonlinear Anal., **68**, no. 4, 681–715.

D. Schlomiuk and N. Vulpe [2008b] Integrals and phase portraits of planar quadratic differential systems with invariant lines of at least five total multiplicity, Rocky Mountain J. Math., **38**, no. 6, 2015–2075.

D. Schlomiuk and N. Vulpe [2008c] The full study of planar quadratic differential systems possessing a line of singularities at infinity, J. Dynam. Differential Equations, **20**, no. 4, 737–775.

D. Schlomiuk and N. Vulpe [2008d] Integrals and phase portraits of planar quadratic differential systems with invariant lines of total multiplicity four, Bul. Acad. Ştiinţe Repub. Mold. Mat., **1 (56)**, 27–83.

D. Schlomiuk and N. Vulpe [2012] *Global topological classification of Lotka–Volterra quadratic differential systems.* Electron. J. Differential Equations, **2012**, No. 64, 69 pp.

D. Schlomiuk, X. Zhang [2018] Quadratic differential systems with complex conjugate invariant lines meeting at a finite point, J. Differential Equations 265, no. 8, 3650–3684.

K.S. Sibirskii [1998] *Introduction to the algebraic theory of invariants of differential equations*, Translated from Russian, Nonlinear Science: Theory and Applications, Manchester, University Press, Manchester.

J. Sotomayor and R. Paterlini [1983] Quadratic vector fields with finitely many periodic orbits, in Geometric dynamics, Lecture Notes in Mathematics, vol. 1007, Springer, Berlin, pp. 753–766.

Y. Q. Ye et al. [1986] *Theory of limit cycles*, translated by Y. L. Chi, Translations of Mathematical Monographs, vol. 66, American Mathematical Society, Providence, RI, xi+435 pp.